

Tesis Doctoral
Programa oficial de doctorado en
automática, robótica y telemática (RD.1393/2007)

Contribución al control económico con criterios cambiantes



Autor: Mario Pereira Martín
Directores: Daniel Limón Marruedo
Teodoro Álamo Cantarero
David Muñoz de la Peña Sequedo

Ingeniería de Sistemas y Automática
Escuela Técnica Superior de Ingeniería
Universidad de Sevilla

Sevilla, 2015



Tesis Doctoral
Programa oficial de doctorado en automática, robótica y
telemática (RD.1393/2007)

Contribución al control económico con criterios cambiantes

Autor:

Mario Pereira Martín

Directores:

Daniel Limón Marruedo

Profesor Titular

Teodoro Álamo Cantarero

Catedrático

David Muñoz de la Peña Sequedo

Profesor Titular

Ingeniería de Sistemas y Automática
Escuela Técnica Superior de Ingeniería
Universidad de Sevilla

2015

A mi familia y ,especialmente, a mi mujer
A mis profesores
To my family and ,especially, to my wife
To my advisors

Agradecimientos

This Thesis is the result of four years of studies and work in the department of Systems and Automation Engineering of the University of Seville. First of all, I would like to thank my advisors, Prof. Daniel Limon Marruedo, Prof. Teodoro Alamo Cantarero and Prof. David Muñoz de la Peña Sequedo, for their teachings, their great help during the development of this thesis, their support, encouragement and their dedication. They make me love the research profession. The things that I learnt from them, the opportunities they gave me and behaviour with me has been invaluable. They are great teachers and researchers and I will always be in debt with them always. Thanks also to Dr. Ignacio Alvarado and all the researchers of the group of *Estimation, prediction, optimization and control* for all their help during the years of development of this thesis.

A special thanks goes to Prof. Carlos Bordons Alba and his research group for the opportunity of realizing this thesis and its friendly environment during the development of this thesis. Thanks also to Dr. Luis Valverde Isorna for the work done together and his help in my fight with microgrids and hydrogen based systems.

Another special thanks goes to Prof. Colin Jones, for his hospitality and for receiving me at his research group as one of them, at the Automatic Control Laboratory (LA), at the *École polytechnique fédérale de Lausanne*, Switzerland. The time he dedicated to me and his teaching have been very important. I can not forget all his research group which demonstrated a great hospitality. Thanks also to Phd. Sanket Diwale and Dr. Lymperopoulos Ioannis for all their great help during my host, and why not, the good time spent together flying kites.

These years have been an adventure. Many thanks go to my friends, partners and other teachers of the department of Systems and Automation Engineering of the University of Seville for all their help.

I would really like to thank my father and my brother, for being always supporting me and encouraging me during this period. And finally, I would like to dedicate this thesis to my wife and to my mother for her patience, dedication and love and for stay there when I need.

*Mario Pereira Martin
Sevilla, 2015*

Resumen

Esta tesis se centra en el problema del diseño de controladores predictivos basados en modelo (MPC) para procesos caracterizados por trayectorias periódicas permitiéndose que puedan cambiar repentinamente. La formulación tradicional para MPC, normalmente denominada formulación para regulación, garantiza el seguimiento asintótico de puntos de equilibrio. Cuando se formula el control predictivo para resolver el problema de seguimiento de referencias, la metodología de diseño estabilizante puede no ser apropiada, debido a la posible pérdida de factibilidad del controlador ante cambios en la referencia. Recientemente se ha propuesto una nueva formulación (Ferramosca et al., 2009; Limon et al., 2008) que soluciona este problema y que se caracteriza por el uso de una referencia artificial la cual es tomada como variable de decisión del problema.

Uno de los principales objetivos de los controladores predictivos en la industria de procesos es garantizar una operación segura a la vez que se maximizan los beneficios. La gestión económica de una planta se resuelve tradicionalmente a través de estructuras de control jerárquicas multicapa donde la capa inferior soluciona la regulación de la planta mediante la utilización de mecanismos de realimentación implementados con controladores rápidos, normalmente controladores PID. Mientras que la capa superior, sin embargo, se compone de un controlador avanzado multivariable que calcula los puntos de operación necesarios para el control de la capa inferior. En el problema económico, este controlador avanzado lo compone normalmente un optimizador en tiempo real que proporciona los puntos de equilibrio óptimos desde un punto de vista económico y un controlador predictivo que proporciona los puntos de operación necesarios para el control de bajo nivel. Una de las desventajas de este sistema reside en que la operación más beneficiosa de una planta desde un punto de vista económico no suele ocurrir en un punto de equilibrio, sino mas bien por ciclos. Además, esta el hecho de que los transitorios entre posibles puntos de equilibrio del sistema no optimizan el beneficio económico de la planta y que las diferencias entre los modelos usados por el optimizador en tiempo real y el controlador predictivo pueden desembocar en una pérdida de factibilidad del problema.

Es logico pensar que debido al caracter periódico de muchos sistemas, fundamentalmente por factores como las demandas, precios o simplemente por el caracter repetitivo de ciertos procesos industriales, el funcionamiento óptimo de estos sistemas desde un punto de vista

económico tendrá un fuerte carácter periódico. Un ejemplo de este hecho lo podemos encontrar en los sistemas eléctricos que dependen de una demanda externa que tiende a repetirse cada cierto periodo de tiempo, hecho observable en microredes de potencia.

Teniendo en cuenta todos los aspectos previos, esta tesis propone el desarrollo de nuevas técnicas de control de procesos industriales donde la solución óptima desde un punto de vista económico se encuentra en el seguimiento de trayectorias no estacionarias. Estas formulaciones garantizan la estabilidad del sistema en bucle cerrado, la convergencia a una trayectoria óptima o a la más cercana a ésta que pueda ser alcanzada por el sistema, además de la satisfacción de las restricciones y la convergencia a una nueva trayectoria óptima en el caso de que la función de coste económica cambie de improviso.

Principalmente se presentan tres nuevas formulaciones: Una formulación MPC para el seguimiento de señales periódicas que regula el sistema controlado a la curva referencia periódica, cuando esta es alcanzable. En el caso que no fuese alcanzable, entonces converge a la trayectoria periódica alcanzable más cercana. Este controlador satisface un conjunto de restricciones en entradas y estados y garantiza la estabilidad y factibilidad recursiva incluso cuando los parámetros de la función de coste presentan cambios repentinos. En este caso, la formulación se centra en la mejor manera de seguir la trayectoria económica óptima y no en el desarrollo del optimizador en tiempo real.

El siguiente paso es la formulación de un controlador económico que regule el sistema en bucle cerrado a la mejor trayectoria económica y periódica que minimiza una función de coste económico. La función de coste económica podría cambiar repentinamente alguno sus parámetros económicos. Este controlador satisfará el conjunto de restricciones operacionales del sistema además de garantizar la estabilidad y la factibilidad recursiva del sistema controlado. La factibilidad se mantendrá incluso cuando la función de coste económico cambie evitando la necesidad del rediseño del controlador.

Este controlador se ha utilizado para controlar a una micro-red de potencia no aislada con un sistema de almacenamiento basado en hidrógeno compuesto por una pila de combustible tipo PEM, un electrolizador y un depósito para el almacenamiento de hidrógeno basado en hidruros metálicos. Para la gestión eficiente de esta microred se propuso una nueva función de coste económico que tiene en cuenta la compra/venta de energía a un proveedor eléctrico, una fuente de energía producida por paneles solares, una demanda de energía interna y finalmente dos sistemas de almacenamiento, un juego de baterías de PB-ácido y el comentado sistema de almacenamiento de hidrógeno. La gestión económica de este tipo de sistemas energéticos están tomando mucha relevancia en la comunidad científica por lo que se ha considerado que la aplicación del controlador económico previo propone una solución muy novedosa e interesante a este tipo de problemas de control dado todas las características que permite garantizar.

La formulación final y más importante presentada en esta tesis se centra en la proposición de una nueva solución al problema de controlar sistemas inciertos de gran escala. A pesar de la robustez inherente presentada por los controladores anteriores, el buen funcionamiento de dichos controladores se ve muy afectado por las incertidumbres presentadas por ciertos sistemas de control. Si estas incertidumbres no son muy grandes, los controladores previos podrían mantener todas sus buenas características, sin embargo se hace necesario la presentación de una formulación que permita trabajar con situaciones que presenten incertidumbres desconocidas y acotadas. Existen muchas formulaciones que podrían

usarse para mejorar las formulaciones anteriores sin embargo se presenta una nueva formulación que permite evitar una de las desventajas computacionales mas grandes de la mayoría de ellas, el calculo del conjunto invariante positivo robusto mínimo, el cual consume una cantidad enorme de tiempo volviendo imposible el control de ciertos sistemas inciertos de gran tamaño con garantías.

Con objeto de demostrar todas las nuevas ventajas de esta formulación se ha propuesto la aplicación de este controlador a un sistema de gran escala que no es otro que una sección de la red de distribución de aguas de Barcelona compuesta por sesenta y una entradas entre valvulas y bombas y diecisiete tanques de almacenamiento de agua. Este sistema es controlado garantizando todos las ventajas previas y sin la necesidad de realizar el cálculo del tedioso conjunto invariante robusto mínimo.

Abstract

This thesis deals with the problem of designing Model based Predictive Control (MPC) for process characterized by periodic trajectories allowing sudden changes. The traditional MPC formulation, usually called MPC for regulation, guarantees the asymptotic tracking of set-points. When the predictive controller is formulated to resolve the problem of tracking references, the stabilizing design methodology may not be a good option, because of the controller can lose the feasibility if the reference suddenly changes. Recently a new formulation was proposed by (Ferramosca et al., 2009; Limon et al., 2008) to overcome this problem which is characterized by the use of an artificial reference considered as decision variable.

The main goal of an advanced control system in the process industries is to ensure a safe operation of the plant while the economic profits are maximized. The economic problem in a plant is traditionally solved using a multi-layer hierarchical control structure where the low level control layer deals with the regulation of the plant usually done by control loop feedback mechanisms commonly used in industrial control systems such as Proportional Integral Derivative Regulator (PID). The upper layer control is usually a high level control composed by a multi-variable advanced controller which function is the calculation of the set points of the low level controls in order to move or keep the system at the desired operation point. This advanced controlled is usually composed by a Real Time Optimizer (RTO) which calculates the economically optimal equilibrium points and a predictive controller which provides the operational points of the low level controls. One of the disadvantage of this approach is that the most profitable operation of the plant may not happen at an equilibrium set-point and it may be a periodic cycle. In addition, the transient trajectory of the closed-loop system between equilibrium points does not optimize the economic profit of the plant and the mismatches between the static model used in the RTO and the dynamic model used in the MPC may lead to a loss of feasibility of the problem.

The periodic nature of a lot of systems, essentially by issues as the demands, prices or simply by the repetitive character of certain industrial process, make us think that the optimal operation of these systems has a strong periodic feature from an economic point of view. An example of this fact, can be found in electric systems which depend on an exogenous demand which it is repeated in time, such as power microgrids.

Taking into account the previous issues, this thesis proposes the development of new control techniques of industrial process where the optimal solution from an economic point of view is presented by non steady state trajectories. These formulations guarantee the stability of the closed-loop system, the convergence to the optimal trajectory, or the nearest to this one that can be reached by the system, the constraint satisfaction and convergence to a new optimal trajectory if the parameters of the economic cost function changes.

We presents three new formulations. The first formulation is designed for tracking periodic signals which regulate the closed loop system to the periodic reference when it is reachable. If it is unreachable, then it converges to the nearest reachable periodic trajectory. This approach satisfies a set of input and state constraints and guarantees stability and recursive feasibility even when the parameters of the economic profit present sudden changes. In this case the formulation is focused on the best way to track the optimal economic trajectory and not in the development of the real time optimizer.

The following step is the formulation of an economic approach which regulates the closed-loop system to the best periodic and economic trajectory which minimizes an economic cost function. This economic cost function might change suddenly some of its economic parameters. This controller satisfies the set of operational constraints while guaranteeing the stability and recursive feasibility of the closed loop system. Feasibility is maintained even when the economic parameters change avoiding the necessity of the typical online re-design of the controller.

This approach was applied to a non-isolated micro-grid with an hydrogen based storage system composed by a Polymer (or Proton) Electrolyte Membrane (PEM) fuel cell, a electrolyzer and an metal hidride based storage system. For the management of this micro-grid is proposed a new economic cost function which take into account the energy selling/buying to/from the electric utility, a source of energy produced by solar panels, an internal energy demand and finally, two storage systems, a cluster of Pb-acid based batteries and the previous hydrogen storage system. The economic management of this type of energy systems are taken a lot of relevant in the research community therefore it is considered that the application of the previous formulation proposes an interesting and novel solution for this control problems due to all the features which can be guaranteed.

The final and most important formulation presented in this thesis is focused on proposing an new solution for the problem of controlling uncertain large scale systems. Instead of the inherited robustness shown by the previous controllers, the good performance of the previous controller are very affected by the uncertainties presented by some control systems. If this uncertainties are not very strong, the previous controller might hold all its good features, however it is necessary to present a formulation which let us work with situations which presents a set of unknown and bounded uncertainties. There are a lot of approaches which let us improve the previous formulations, however we propose a new one which avoid one of the biggest computational disadvantages of most of them, the computation of the minimal robust positive invariant set which can consume a huge amount of time making impossible the control of certain large scale systems with guarantees.

In order to demonstrate all the new advantages of the new robust approach, it was proposed the application of this controller to a large scale system, that is a section of the Barcelona's drinking water network composed by 61 control inputs between valves and

pumps, and 17 water storage tanks. This system is controlled guaranteeing all the previous issues and without the necessity of computing the tedious minimal robust invariant set.

Short Contents

<i>Resumen</i>	V
<i>Abstract</i>	IX
<i>Short Contents</i>	XIII
<i>Notation</i>	XIX
1. Introduction	1
1.1. Motivation	1
1.2. Model predictive control	2
1.3. Set-point tracking model predictive control	5
1.4. Economic MPC	6
1.5. Robust MPC	8
1.6. Model predictive controller for tracking periodic signals	9
1.7. Objectives of this thesis	10
1.8. Thesis outline	11
1.9. List of publications	12
2. Model predictive controller for tracking periodic signals	15
2.1. Problem formulation	17
2.2. Proposed controller	19
2.3. Stability analysis	21
2.4. Some properties of the proposed controller	28
2.5. Example	29
3. Economic MPC for changing periodic operation	39
3.1. Problem formulation	40
3.2. Economic MPC for changing periodic operation	43
3.3. Application to a four tank plant	52
3.4. Application to a drinking water network	60
4. Periodic economic control of a non-isolated micro-Grid	69

4.1.	Control of a non-isolated microgrid	70
4.2.	Economic cost function	76
4.3.	Simulation results	81
5.	Robust model predictive controller for tracking periodic signals	87
5.1.	Problem formulation	88
5.2.	Controller formulation	89
5.3.	Robust stability of the controlled system	92
5.4.	Application to a ball and plate system	98
6.	Application to a large-scale DWN of robust MPC for tracking periodic references	107
6.1.	Application to a drinking water network	109
7.	Conclusions and future lines	125
7.1.	Future work	127
	Appendix A. Data about DWN example	129
	<i>List of Figures</i>	137
	<i>List of Tables</i>	141
	<i>List of Codes</i>	143
	<i>Bibliography</i>	145
	<i>Glossary</i>	153

Contents

<i>Resumen</i>	V
<i>Abstract</i>	IX
<i>Short Contents</i>	XIII
<i>Notation</i>	XIX
1. Introduction	1
1.1. Motivation	1
1.2. Model predictive control	2
1.2.1. Basic scheme of predictive control	2
1.2.2. Stability and recursive feasibility of nominal MPC	3
1.3. Set-point tracking model predictive control	5
1.4. Economic MPC	6
1.5. Robust MPC	8
1.6. Model predictive controller for tracking periodic signals	9
1.7. Objectives of this thesis	10
1.8. Thesis outline	11
1.9. List of publications	12
1.9.1. Journal papers	12
1.9.2. International conference papers	13
1.9.3. National conference papers	14
2. Model predictive controller for tracking periodic signals	15
2.1. Problem formulation	17
2.2. Proposed controller	19
2.3. Stability analysis	21
2.3.1. Technical Lemmata	24
2.4. Some properties of the proposed controller	28
2.5. Example	29
3. Economic MPC for changing periodic operation	39

3.1.	Problem formulation	40
3.1.1.	Economically optimal periodic operation	41
3.2.	Economic MPC for changing periodic operation	43
3.2.1.	Lyapunov asymptotic stability of a periodic trajectory	44
3.2.2.	Stabilizing design of the proposed controller	46
	Technical lemmata	48
3.3.	Application to a four tank plant	52
3.4.	Application to a drinking water network	60
4.	Periodic economic control of a non-isolated micro-Grid	69
4.1.	Control of a non-isolated microgrid	70
4.1.1.	Simulation model	73
4.1.2.	Controller design model	75
4.2.	Economic cost function	76
4.2.1.	Sold energy cost h_{mg}	77
4.2.2.	Purchased or wasted energy h_{sp}	78
4.2.3.	Degradation cost of equipments	79
	Battery cost h_b	79
	Hydrogen cost h_{fc}, h_{ez}, h_{mh}	79
	Metal hydride tank h_{mh} :	80
4.2.4.	Operation costs f_{op}	80
4.3.	Simulation results	81
4.3.1.	First scenario: convergence.	81
4.3.2.	Second scenario: changing the economic cost	84
5.	Robust model predictive controller for tracking periodic signals	87
5.1.	Problem formulation	88
5.2.	Controller formulation	89
5.3.	Robust stability of the controlled system	92
5.4.	Application to a ball and plate system	98
6.	Application to a large-scale DWN of robust MPC for tracking periodic references	107
6.1.	Application to a drinking water network	109
6.1.1.	Proposed robust MPC controller	113
6.1.2.	Recursive feasibility	116
6.1.3.	Simulation results	118
7.	Conclusions and future lines	125
7.1.	Future work	127
	Appendix A. Data about DWN example	129
	<i>List of Figures</i>	137
	<i>List of Tables</i>	141
	<i>List of Codes</i>	143

<i>Bibliography</i>	145
<i>Glossary</i>	153

Notation

\mathbf{z}	sequence of T vectors of a trajectory $\{z(0), \dots, z(T-1)\}$
$\mathbf{z}(\theta)$	sequence of T vectors of a trajectory $\{z(0; \theta), \dots, z(T-1; \theta)\}$ which depend on the external parameter θ
$\mathbf{z}_N(\theta)$	sequence of N vectors of a trajectory ($N \neq T$) which depend on the external parameter θ
$\mathbb{I}_{[a,b]}$	set of integer numbers contained in the interval $[a,b]$, that is $\mathbb{I}_{[a,b]} = \{a, a+1, \dots, b\}$
\mathbb{I}_b	set of integer numbers contained in the interval $[0,b]$, that is $\mathbb{I}_b = \{0, 1, \dots, b\}$
\mathbb{R}	set of real numbers
\mathbb{Z}^+	set of positive real numbers
$z^o(i;k)$	the optimal solution for a certain optimization problem $\min_{z \in Z} F(z)$ where k is the initial time and i indicates the i -th predicted state
$F(x_0, \dots, x_i; y_0, \dots, y_i)$	Function F which depends on the parameters x_0, \dots, x_i and the variables y_0, \dots, y_i
$A \oplus B$	Minkowski sum of two sets $A \subset \mathbb{R}^n$ and $B \subset \mathbb{R}^n$ defined by $A \oplus B = \{a+b : a \in A, b \in B\}$
$A \ominus B$	Pontryagin set subtraction of two sets $A \subset \mathbb{R}^n$ and $B \subset \mathbb{R}^n$ defined by $A \ominus B = \{a : a \oplus B \subseteq A\}$
$\bigoplus_{i=a}^b X(i)$	For a given sequence of sets $X(i) \subset \mathbb{R}^n$, $\bigoplus_{i=a}^b X(i) = X(a) \oplus X(a+1) \oplus \dots \oplus X(b)$
$\ x\ _P$	Weighted Euclidean norm of vector x defined by $\sqrt{x^t P x}$ for a given symmetric matrix $P > 0$

1 Introduction

Predictive control is the only advance control technique to have had a significant and widespread impact on industrial process control

J.M. MACIEJOWSKI, 2002

This chapter describes the motivation and objectives of the research work shown in this thesis. In addition, an overview of the state of the art in this field is presented.

1.1 Motivation

In recent years, the research community has focused its interest in developing new control techniques which allow the introduction of important issues in the operation of process industries such as the necessity of production in a safe, clean and competitive way while satisfying the requirements imposed by the market with respect to both demand and quality. These requirements are affected by social and cultural habits and the necessity of strict safety controls on the quality and variety of the products. In addition, the actual boom of renewable energies and the importance of minimizing the environment impact and resource consumption contributes to the desire for a most efficient production fulfilling the requisites and limits imposed on the products. Thus, it is desirable to develop control techniques to address these issues.

The main objective of an advanced control system is to operate a plant in a safe and efficient way which means operating the plant minimizing a cost function while it is guaranteed the stability and the operation limits. The most successful control technique satisfying these issues is model based predictive control.

In industry, the processes are usually operated in a given operation point in order to maximize their efficiency. However, the optimal operation point is affected by certain time varying economic parameters. Thus, in these cases it does not exist a unique operation point, but a sequence of operation points along the time. An important typology of process

are those which present a periodic behaviour along time. This type of processes are very common in industry such as batch-processes, management of renewable energy systems or infrastructures in which forecast demand plays an important role. The main contribution of this thesis is the development and application of model predictive control focused to improve the management of this type of constrained process in an economic way taking into account the changing character of the economic parameters.

1.2 Model predictive control

Model predictive control (MPC) is one of most successful techniques of advanced control in the process industry (Camacho and Bordons (1999); Rawlings and Mayne (2009)) because it allows the control of constrained systems, minimizing a criteria and guaranteeing stability and convergence (Mayne et al. (2000); Mayne (2014)); in addition of its conceptual simplicity and its ability to manage easily and effectively complex systems with many inputs and outputs. MPC provides a finite sequence of control actions by solving online a constrained, discrete-time optimal control problem. The computation of this optimization problem is very arduous but it is perfectly acceptable if the computation time of the optimization problems is lower than the sampling time.

Nowadays sufficient conditions that guarantee closed-loop stability using a Lyapunov-based approach are well known in the MPC community (Mayne et al. (2000)), although they are seldom used in industry because in general they are not necessary.

1.2.1 Basic scheme of predictive control

Systems with large ranges of operation are characterized by complex dynamics usually defined by systems with coupled algebraic, ordinary differential or partial differential equations. Another important aspect related with these plants is the existence of constraints which limits the range of the process control variables (manipulable variables) or process measurable variable (process variables). Predictive control is composed by the following ingredients:

- *Prediction model*: A set of differential-algebraic equations which describe the dynamic behaviour of a control system. Depending on these equations, the models can be classified on linear/nonlinear, deterministic/uncertain or discrete/continuous. For a given sequence of control actions, the prediction model is used to estimate the future trajectory of the system along a given prediction horizon.
- *Cost function*: This mathematic function shows the criteria to optimize. Usually is a positive definite function which defines the cost of the closed-loop system trajectory along the prediction horizon denoted as N . This cost function is often composed by two terms: a *stage cost* usually denoted as $\ell(\cdot)$ which defines the cost of the system at a certain state and input in every step and the *terminal cost* function which penalizes the terminal state, that is, the system state predicted at the end of the prediction horizon. This can be considered as a cost-to-go function and it is denoted as $V_f(\cdot)$.

- *Constraints*: A set of equations which define the region where the state and input of the system must be confined at each sampling time. This region is the so called *admissible region*. These constraints are imposed by physical limits of the system or due to safety reasons and they are posed as a set of inequalities. The constraints on the states and control inputs of the system are denoted as $x(i) \in \mathcal{X}$, $u(i) \in \mathcal{U}$ for all instant i . Typically a constraint in the state at instant N is added because of stability reasons. This constraint is called *terminal constraint* and can be expressed as $x(N) \in \mathcal{X}_f$ where $\mathcal{X}_f \subseteq \mathcal{X}$ is called *terminal region* (Mayne et al. (2000)).

Ideally, the horizon in the optimal control problem should be infinite in order to consider the cost of the whole trajectory of the closed-loop. However this is impossible to solve in practice, except in certain simple cases, such as unconstrained Linear Quadratic Regulator (LQR) for linear systems. To avoid these disadvantages, a finite horizon is used which implies that the resulting controller may loose important properties of infinite-horizon controllers, such as closed-loop stability. The classical scheme of the finite horizon optimization problem of a standard model predictive controller denoted as $\mathbb{P}_N(x)$ can be posed as follows

$$\min_{\mathbf{u}} \quad \sum_{i=0}^{N-1} \ell(x(i), u(i)) + V_f(x(N)) \quad (1.1)$$

$$st \quad x(0) = x \quad (1.2)$$

$$x(i+1) = Ax(i) + Bu(i) \quad \forall i \in \mathbb{I}_{N-1} \quad (1.3)$$

$$u(i) \in \mathcal{U} \quad \forall i \in \mathbb{I}_{N-1} \quad (1.4)$$

$$x(i) \in \mathcal{X} \quad \forall i \in \mathbb{I}_{N-1} \quad (1.5)$$

$$x(N) \in \mathcal{X}_f \quad (1.6)$$

where the current state of the system is x . Once the solution is obtained and following the receding horizon strategy, the control action $u(0)$ is applied to the system at instant k .

The set of states for which exists a sequence of N admissible control actions such the closed-loop system has an evolution inside the region \mathcal{X} and reach the terminal set \mathcal{X}_f , is the so called *domain of attraction* of the predictive controller and it is denoted as \mathcal{X}_N . The domain of attraction is enlarged by increasing the prediction horizon or by taking a larger terminal region.

1.2.2 Stability and recursive feasibility of nominal MPC

The receding horizon strategy introduces feedback and provides a certain degree of robustness. However nominal MPC formulations with finite horizons in general don't guarantee convergence to the origin even stability. This issue focused the attention of the research community on studying the closed-loop properties of this class of controllers, producing a set of formulations that guarantee the stability based on Lyapunov theory, in particular, proving that under certain assumptions the optimal cost of the open-loop optimization problem is a Lyapunov function of the closed-loop system. Several of these formulations

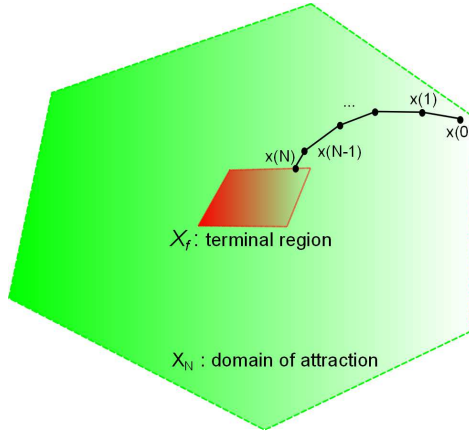


Figure 1.1 Characteristic regions on model predictive control.

can be found in Chisci et al. (1994); Mayne and Michalska (1990). In Mayne et al. (2000) is established that predictive control needs two basic ingredients to stabilize asymptotically a constrained nonlinear system, a terminal constraint and a terminal cost..

For a stage cost $\ell(x,u) \geq \alpha(|x|)$ in which α is a K_∞ function, recursive feasibility and asymptotic stability on \mathcal{X}_N are easily established if the *terminal cost* $V_f(\cdot)$ and *terminal region* \mathcal{X}_f satisfy the following two conditions

$$\forall x \in \mathcal{X}_f \subset \mathcal{X}, \exists u \in \mathcal{U} | V_f(f(x,u)) \leq V_f(x) - \ell(x,u), f(x,u) \in \mathcal{X}_f$$

These conditions can be summarized as follows:

- The *terminal region* \mathcal{X}_f is an admissible positive invariant set of the system, that is, there exists a control law which stabilizes the system in this terminal set guaranteeing that the system evolution and control actions in this set are admissible.
- The *terminal cost* $V_f(\cdot)$ is a control Lyapunov function related to the system controlled by the local controller corresponding to the terminal region such as its increment at one step is equal or lower than minus the stage cost for all state inside of the terminal set. Thus this local control law stabilizes asymptotically the system.

Then $\forall N \in \mathbb{I}_\infty$ and $\forall x \in \mathcal{X}_f$ it holds that

$$V_N^\circ(f(x, \kappa_N(x))) \leq V_N^\circ(x) - \ell(x, \kappa_N(x)) \tag{1.7}$$

$$V_{N+1}^\circ(x) \leq V_N^\circ(x) \tag{1.8}$$

Thus under reasonable conditions it follows that

$$V_N^\circ(x) \in [\alpha_1(|x|), \alpha_2(|x|)], \quad \forall x \in \mathcal{X}_N \quad (1.9)$$

$$V_N^\circ(f(x, \kappa_N(x))) \leq V_N^\circ(x) - \alpha_1(|x|), \quad \forall x \in \mathcal{X}_N \quad (1.10)$$

where $\alpha_1(\cdot)$ and $\alpha_2(\cdot)$ are K_∞ functions. The lower bound in (1.9) is a consequence of (1.7) and a lower bound on $\ell(\cdot)$. The upper bound follows from an upper bound on $V_N(\cdot)$ and (1.8). The inequality in (1.10) follows from the properties of $V_f(\cdot)$ and \mathcal{X}_f . From (1.9) follows that the origin is an asymptotically or exponentially stable equilibrium state for the controlled system with a region of attraction \mathcal{X}_N .

However this ingredients only ensures the asymptotic stability on \mathcal{X}_N . In some cases, the control law κ_N might be discontinuous even if the functions of \mathbb{P}_N are continuous. Thus in order to ensure *KL* asymptotic stability on \mathcal{X}_N is necessary to satisfy the following conditions:

- The controlled system and its value function have to be strong uniformly bounded on \mathcal{X}_N .
- The lower bound of $V_f(\cdot)$ is a K_∞ function.
- \mathcal{X}_N is bounded.

A significant contribution in the last decades is the conditions that ensures recursive feasibility and stability of model predictive control without a terminal stability constraint. See for example Grüne (2012) where it is not necessary terminal cost and terminal region. However the stability conditions are very limited and the recursive feasibility is not guaranteed. Another relevant contribution is shown in Limon et al. (2006b) where stability and recursive feasibility are guaranteed for linear system being necessary the terminal cost at least.

1.3 Set-point tracking model predictive control

The objective of MPC for tracking is to ensure that the tracking error, which is the difference between a reference or desired output and the actual output, tends to zero. The optimization problem of this control problem is posed as follows

$$\begin{aligned} \min_{x, u} \quad & \sum_{j=0}^{N-1} \|y(j) - r(j)\|_S^2 + \|u(j) - u^r(j)\|_R^2 \\ \text{s.t.} \quad & x(j+1) = Ax(j) + Bu(j), \quad j \in \mathbb{I}_{N-1} \\ & y(j) = Cx(j) + Du(j), \quad j \in \mathbb{I}_{N-1} \\ & x(j) \in \mathcal{X} \\ & u(j) \in \mathcal{U} \\ & x(N) \in \mathcal{X}_f \end{aligned} \quad (1.11)$$

where $x(j) \in \mathbb{R}^n$, $u(j) \in \mathbb{R}^m$ and $y(j) \in \mathbb{R}^p$ are the state, control and output vector respectively. $u^r(j) \in \mathbb{R}^m$ is the desired control vector obtained from the reference vector

$r(j) \in \mathbb{R}^p$. Posing the optimization problem (1.11) in terms of the tracking error signals $e_y(i) = y(i) - r(i)$, the resulting optimization problem is a standard regulation problem (Rawlings and Mayne, 2009) with a time varying set of constraints and a terminal equality constraint $e_y(N) = 0$.

If the evolution of the reference is known a priori, the tracking error can be predicted and then MPC can be designed to achieve asymptotic stability. However tracking control is an inherently uncertain control problem because in general the reference may be changed without a predefined deterministic law or even randomly. Therefore the tracking problem is considerably more difficult since MPC is naturally suited to deterministic control problems. This may render the MPC problem infeasible for the current state and the current reference due to the set of constraints. Thus, the recursive feasibility and the stability of the predictive control scheme can not be guaranteed when the reference is varying.

A number of solutions have been proposed in the literature to deal with the uncertainty derived from a varying reference. In (Pannocchia, 2004; Pannocchia et al., 2005) the set-point change is considered equivalent to a disturbance to be rejected and asymptotic stability and offset-free control is ensured by integrating a disturbance model in the prediction model. A different approach was proposed in the context of reference governors (Bemporad et al., 1997; Gilbert et al., 1999) that guarantees robust tracking without considering the performance of the obtained controller nor the domain of attraction. More recently, in (Ferramosca et al., 2009; Limon et al., 2008), an MPC for tracking constant references was proposed that guarantees that under any change of the set point, the closed-loop system maintains the feasibility of the controller and guarantees convergence if admissible.

1.4 Economic MPC

The main goal of an advanced control system in the process industries is to ensure a safe operation of the plant while the economic profits are maximized, attending the policies of the operator of the plant. The economic problem in a plant is traditionally solved using a multi-layer hierarchical control structure (see Tatjewski (2008); Darby et al. (2011); Engell (2007)). The low level control layer deals with the regulation of the plant usually done by programmable logic controllers (Programmable Logic Controllers (PLC)). The common controllers used in these industrial devices are a proportional-integral-derivative controllers (PID controllers) which are a control loop feedback mechanism commonly used in industrial control systems. The upper layer control is usually a high level control composed by a multi-variable advanced controller which function is the calculation of the set points of the low level controls in order to move or keep the system at the desired operation point. This operation point is calculated by a real time optimizer (RTO) calculates the economically optimal equilibrium point according to data from the plant, forecast information obtained from past data and economic criteria. A scheme of this hierarchical structure is shown in figure 1.2.

When the economic criteria or the forecast data change, the real time optimizer provides a new operation point and the task of the high level controller is to move/keep the system to/at this new desired operation point. In order to manage significant changes of the operation point and reduce the feasibility problems related to the mismatches between the

integrated model used in the RTO and the dynamic model used in the high level control layer, typically an MPC, this high level control is usually designed as a two layer structure (see Becerra et al. (1998)). The objective of this layer is to calculate the suitable targets for the advanced controller. This upper layer is usually called steady state target optimizer (Steady State Target Optimizer (SSTO)). The lower layer is composed by the advanced controller whose objective is to regulate the system to the new operation point.

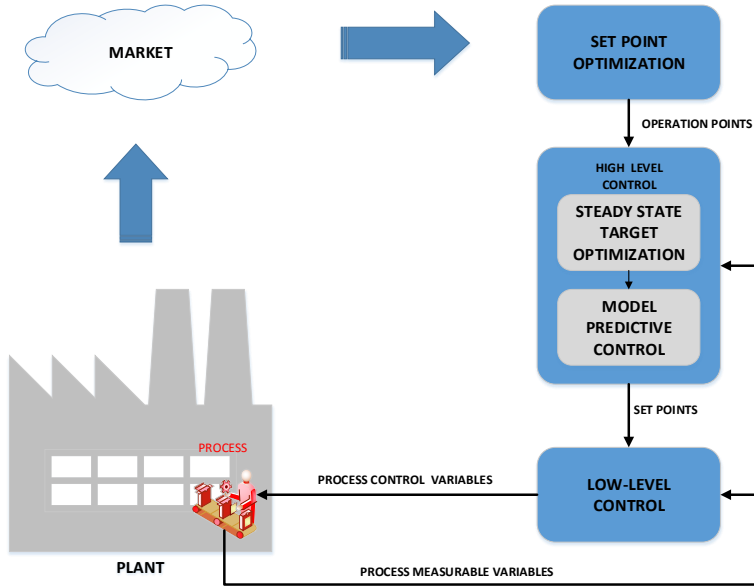


Figure 1.2 Hierarchical control structure.

The first disadvantage of this approach is that the most profitable operation of the plant may not happen at an equilibrium set-point and it may be a periodic cycle. The second one is that $\ell(\cdot)$ and $V_f(\cdot)$ are not chosen to reflect economic cost so the transient trajectory of the closed-loop system from the initial state to the target state may not be optimal from an economic point of view. Thirdly, the mismatches between the static model used in the RTO and the dynamic model used in the MPC may lead to unreachable targets or to a loss of feasibility of the predictive controller. In conclusion, this hierarchical structure under changes in the operational point provided by the real time optimizer doesn't guarantee important properties such as recursive feasibility and stability presenting a worse performance because every layer is designed independently.

In many control design procedures, the parameter of $\ell(\cdot)$, the stage cost, are regarded as being able to be adjusted in order to achieve traditional design objectives. However, in process industries profitability is often the main objective. In order to enhance the performance during the transient of the system, the so-called economic MPC was proposed

(Rawlings and Amrit (2009)). The main characteristic of this predictive controller is that its stage cost function is designed by using directly an economic criteria. This allows the controller to take into account the performance during the transient.

Economic MPC addresses this limitations by choosing $\ell(\cdot)$ to be the economic cost of operating the plant at (x,u) . The best operating point is then chosen to minimize this stage cost with respect to (x,u) . In contrast to standard MPC, the stage cost of the best operating point is not zero and standard results on MPC do not treat this case. Thus special techniques have to be employed. Considering a system subjected to state-control constraint, $(x,u) \in \mathcal{Z}$, this type of MPC should minimize the following average cost:

$$\lim_{N \rightarrow \infty} \frac{1}{N} \sum_{i=0}^{N-1} \ell(x(i), u(i))$$

In Heidarinejad et al. (2012, 2013a,b), Lyapunov based model predictive control designs, which are capable of optimizing closed-loop performance with respect to general economic considerations for a broad class of nonlinear process systems, including systems subject to asynchronous and delayed measurements and uncertain variables have been developed. The proposed techniques are based on two different modes of operation which guarantee that the closed-loop system is ultimately bounded in a small region containing the origin.

In Rawlings et al. (2012), recent results on the stabilizing design of economic MPC are summarized. In Grüne (2013) an stabilizing economic MPC without terminal constraint is presented. In Zanin et al. (2002) a single layer economic MPC has been proposed by integrating the RTO into the MPC as terminal cost function and the benefits of this controller has been practically validated.

1.5 Robust MPC

An important question about MPC design is whether the real plant controlled by an MPC designed for the nominal model of the plant is still stable when there exists mismatches between the prediction horizon and the real behavior of the plant. This can be analyzed using the notion of Input to State Stable (ISS) (input to state stable).

In Jiang and Wang (2001) has been establish that a system is ISS if and only if it admits an ISS-Lyapunov function. Examples of the use of ISS theory are included in Lazar et al. (2008); Limon et al. (2002); Limon et al. (2008); Limon (2002); Limon et al. (2009b).

This analysis is relevant because a system controlled with an MPC could be destabilized by an arbitrarily small disturbance, see Grimm et al. (2004). In Kellett and Teel (2004) is proved that the nominal system is inherently robustly stable if and only if it admits a continuous Lyapunov function. Usually in MPC, the value function $V_N^\circ(\cdot)$ of the optimal control problem solved online is employed as a control Lyapunov function (Control Lyapunov Function (CLF)) and continuity of the value function is established when state constraints are not present, the admissible set of control actions is compact and the model function, the stage cost function and the terminal cost function are continuous. This implies that we cannot expect nominal MPC to be robustly stable if a terminal constraint is employed. However, in Yu et al. (2014) is shown that nominal MPC without state constraints but

with a conventional terminal constraint and penalty is input to state stable (ISS). Hence, under the usual assumptions, the controlled system is ISS if the compact subset \mathcal{W} which contains the disturbances is sufficiently small. In order to deal with uncertainty, these issues should be taken into account in the design of the predictive controllers.

A classic approach is to minimize the cost function for the worst possible uncertainty realization, the so-called min-max approach first proposed in Witsenhausen (1968), but the resulting min-max optimization problems can be computationally very demanding, see Mayne and Langson (2001). In order to overcome this problem, several solutions have been proposed where a cost function that depends on nominal predictions is minimized while guaranteeing robust constraint satisfaction. In Chisci et al. (2001) is proposed a constraint tightening method which guarantees constraint satisfaction for a set of bounded uncertainties and a predictive controller based on nominal predictions is proposed. In Mayne et al. (2005) a robust MPC to control uncertain systems was proposed by the so called tubes where a tube centered in the nominal trajectory and with a section equal to the (preferably minimal) robust invariant set are used to contain the real trajectories of the uncertain system.

This class of formulations often needs computing a minimal robust invariant set (see Rakovic et al. (2005)), which can be difficult for large dimension systems. In Alvarado et al. (2010a), a formulation that under certain assumptions avoided the use of this set was proposed.

1.6 Model predictive controller for tracking periodic signals

In certain cases, the optimal operation of the plant from an economic point of view is not to remain at a given steady-state but to follow a non-steady trajectory, often periodical Lee et al. (2001). This is the case for instance when the system is subject to periodic disturbances (such as an exogenous periodic demand of a water distribution network or supply chains), fluctuating prices of the economic cost function (such as the electricity unitary cost), or time varying dynamics (such as batch nonlinear-process operation). In Huang et al. (2012) it is reported that processes such as simulated moving bed (SMB) and pressure swing adsorption (PSA) present a better economic performance if they are not operated at an equilibrium point, but at an periodic trajectory.

In order to obtain a good control strategy to solve problems which present a non-steady state periodic optimal control trajectory due to the nonlinearities of the dynamic systems or external pseudo-periodic disturbances such as demands or prices evolutions, it is gaining importance in the research community the development of predictive controllers for tracking periodic signals. These controllers are focused on improving the performance of the transient stage guaranteeing stability conditions.

Periodic references appears naturally in important control problems such as repetitive control (Lee et al., 2001), periodic systems (Kern et al., 2009; Gondhalekar et al., 2013) or economic operation of complex systems (Huang et al., 2012). In (Magni et al., 2001) a class of output feedback MPC for nonlinear discrete-time systems is proposed to solve the problem of tracking exogenous signals (and asymptotically rejecting disturbances) generated by systems with known dynamics. In (Mäder and Morari, 2010) a predictive

controller for the offset-free tracking of reference signals generated by arbitrary dynamics is proposed. This controller ensures that the tracking error tends to zero, but recursive feasibility and stability of the closed-loop system is not ensured in case of changing references.

The application of MPC to periodic systems was studied in Lee et al. (2001) where a model-based predictive control approach to repetitive control of continuous processes with periodic operations was proposed. This formulation was later extended to improve the performance with respect to period errors in Manish Gupta (2006) and nowadays different variations can be found in the literature. In addition to periodic systems and batch processes, economic operation of complex systems often leads to non-steady state operation, see for example Huang et al. (2012) or the water drinking network applications presented in Grosso et al. (2014a); Ocampo-Martínez et al. (2013).

To deal with non-steady operation of the plant, the predictive control structure must be modified. One solution proposed in the literature is to follow a two layer approach in which the optimal periodic trajectory is calculated by a dynamic real time optimizer (Dynamic Real Time Optimizer (DRTO)), which takes into account a dynamic model of the plant; and based on this optimal periodic trajectory, a MPC for tracking the optimal trajectory is applied, see for example Wurth et al. (2011). If the model predictive controller is designed appropriately Rawlings and Mayne (2009), asymptotic convergence of the closed-loop system to the optimal trajectory can be proved. In order to improve the economic performance during the transient, several authors propose to use economic MPC to track the optimal trajectory. In Angeli et al. (2012) an economic MPC that guarantees that the asymptotic average economic cost of the controlled system is no worse than the average economic cost of the optimal trajectory has been presented. Lyapunov stability of the controlled plant is derived if the initial state is in a neighborhood of the optimal trajectory. In Huang et al. (2012) stability and robustness of infinite horizon economic MPC is analyzed. In general, all the above mentioned control strategies require the calculation of the optimal periodic trajectory by the real time optimization layer for the given economic cost function. The economic cost function typically depends on exogenous parameters, such as unitary prices or expected demands, that may change throughout the operation of the plant. When these parameters are changed, then the optimal trajectory must be recalculated and the predictive controllers should be re-designed to this new scenario by adapting the constraints and/or the cost function appropriately. The subsequent variation of the constraints of the optimization problem could lead to feasibility loss Limon et al. (2012); Ferramosca et al. (2010).

1.7 Objectives of this thesis

The main objective of the thesis is to propose novel predictive controllers to stabilize the system in periodic trajectories. It is assumed that the provided periodic references to track may vary along the time and that there is model uncertainty and/or disturbances. The designed controllers must fulfill the following requirements:

- *Asymptotically convergence*: The closed-loop system has to converge asymptotically

to the optimal reachable trajectory, that is the optimal trajectory which the closed-loop system is able to reach taking into account all the constraints.

- *Constraint satisfaction*: The closed-loop system has to satisfy all the operational constraint related to the system such as limits on states, control inputs and outputs.
- *Recursive feasibility*: The closed-loop system can not lose feasibility at any time if the initial state of the system is feasible.
- *Feasibility under changing criteria* : The closed-loop system can not lose feasibility even when sudden changes in the optimization criteria take place.
- *Robustness under bounded additive uncertainties*: The closed-loop system must guarantee the satisfaction of the constraints, asymptotically convergence to the optimal robust reachable trajectory which minimizes a criteria and the maintenance of the feasibility and convergence properties in the presence of sudden changes in the criteria for all possible uncertainties.
- *Scalability*: The proposed controlled must be applicable to large scale systems satisfying the previous features.

In this thesis we will focus on periodic operation of linear systems. As mentioned in the previous section, periodic operation appears naturally in many relevant control applications. In addition, we will use the properties of periodic trajectories to design new predictive controllers that address all the relevant issues mentioned before.

1.8 Thesis outline

The outline of the thesis is the following:

- ✓ **Chapter 2. Model predictive controller for tracking periodic signals.** This chapter presents a new model predictive controller for tracking arbitrary periodic references. The proposed controller is based on a single layer that unites dynamic trajectory planning and control. A design procedure to guarantee that the closed-loop system converges asymptotically to the optimal admissible periodic trajectory while guaranteeing constraint satisfaction is provided. The proposed controller allows sudden changes in the reference without losing feasibility. The properties of the proposed controller are demonstrated with a simulation example of a ball and plate system.
- ✓ **Chapter 3. Economic periodic model predictive control.** Periodic optimal operation of constrained periodic linear systems is considered in this chapter in which it is proposed an economic model predictive controller based on a single layer that unites dynamic real time optimization and control. This new controller guarantees closed-loop convergence to the optimal periodic trajectory that minimizes the average operation cost for a given economic criterion. A-priori calculation of the optimal trajectory is not required and if the economic cost function is changed, recursive feasibility and convergence to the new periodic optimal trajectory is guaranteed. The results are demonstrated with two simulation examples, a four tank system, and a simplified model of a section of Barcelona's water distribution network.

- ✓ **Chapter 4. Periodic economic control of a non-isolated micro-grid.** This chapter presents the application of economic predictive control to minimize the cost of operating a non-isolated micro-grid connected to an electric utility subject to a periodic internal demand. The micro-grid considered is made of a set of photovoltaic panels, two storage systems and can buy and sell energy to a electric utility. The first storage system is made of a cluster of batteries of lead acid and the second storage system is based on hydrogen storage. A function that describes the economic cost of operating the plant taking into account aspects such as electric market costs, degradation of the micro-grid and amortization costs is proposed. Based on this cost and considering the periodic nature of the plant, the previous economic predictive controller capable of adapting to sudden changes on the cost function while guaranteeing stability and recursive feasibility has been successfully tested on a realistic nonlinear model of an experimental configurable test-bed located at the laboratories of the University of Seville.
- ✓ **Chapter 5. Robust model predictive controller for tracking periodic signals.** A novel robust model predictive control for tracking periodic signals formulation based on nominal predictions and constraint tightening is proposed in this chapter. In order to guarantee robust constraint satisfaction and convergence, a constraint tightening approach based on semi-feedback predictions is used. Two design procedures based on a robust positive invariant terminal region and on an equality terminal constraint which does not require the calculation of any invariant set are presented. The properties of the proposed controller are demonstrated with a simulation of a ball and plate system.
- ✓ **Chapter 6. Application to a large-scale drinking water network of robust MPC for tracking periodic references.** This chapter proposes to apply the previous robust predictive controller for tracking periodic references to an uncertain discrete time algebraic-differential linear model of a large scale drinking water network. The system considered has been obtained from the water balance equations of a section of Barcelona's drinking water network taking into account bounded additive perturbations. In this model, we assume that a prediction of the water demand is available and that the prediction error is bounded. To demonstrate the main properties of the controller and that it is possible to apply robust schemes with guaranteed closed-loop properties to large scale systems, three different simulation scenarios have been considered.
- ✓ **Chapter 7. Conclusions.** The thesis ends with an analysis of the most relevant contribution and points out future research lines in the field of predictive controllers.

1.9 List of publications

1.9.1 Journal papers

- Pereira,M.; Limon,D.; Muñoz de la Peña,D.; Valverde,L.; Alamo,T.; *Periodic economic control of a non-isolated micro-grid*, Transactions on Industrial Electronics,

United States, Institute Of Electrical And Electronics Engineers,2015.

- Limon,D.; Pereira,M.; Muñoz de la Peña,D.; Alamo,T.; Grosso,J.M.; *Single-layer economic model predictive control for periodic operation*, Journal of Process Control,2014.
- Limon,D.; Pereira,M.; Muñoz de la Peña,D.; Alamo,T.; Jones,C.N.; Zeilinger,M.N.; *MPC for Tracking periodic References*, IEEE Transactions on Automatic Control,2015.
- Pereira,M.; Muñoz de la Peña,D.; Limon,D.; Alvarado,I.; Alamo,T.; *Application to a large-scale drinking water network of robust MPC for tracking periodic references*, Control Engineering Practice (Submitted).
- Pereira,M.; Muñoz de la Peña,D.; Limon,D.; Alvarado,I.; Alamo,T.; *Robust model predictive controller for tracking periodic signals*, IEEE Transactions on Automatic Control, (submitted).

1.9.2 International conference papers

- Grosso,J.M.; Ocampo,C.; Puig,V. ; Limon,D.; Pereira,M.; *Economic MPC for the Management of Drinking Water Networks*; Ponencia en congreso, 2014 European Conference Control (ECC), Estrasburgo, Francia, 2014.
- Limon,D.; Alamo,T.; Pereira,M.; Ferramosca,A.; *Integrating the RTO in the MPC: an adaptive gradient-based approach*; Ponencia en congreso, 2013 European Control Conference (ECC), Zurich, Suiza,2013.
- Agüero,J.; Rodríguez, F.; Castilla,M.; Pereira,M.; *Productiveness and real time prices in Energy management for Hvac systems*, Comunicacion en Congreso, 39th Annual Conference of the IEEE Industrial Electronics Society, Viena, Austria, 2013.
- Limon,D.; Alamo,T.; Muñoz de la Peña,D.; Zeilinger,M.N.; Jones,C.N.; Pereira,M.; *MPC for tracking periodic reference signals*, Ponencia en Congreso, IFAC Nonlinear Model Predictive Control Conference International Federation of Automatic Control, Paises Bajos, 2012.
- Pereira, M.; Limon,D.; Alamo, T.; Valverde, L.; Bordons,C.; *Economic Model Predictive Control of a smartgrid with hidrogen storage and PEM fuel cell*, Ponencia en Congreso, IECON 2013 – 39th Annual conference of the IEEE Industrial Electronics Society, Viena, Austria, 2013.
- Pereira,M; Limon,D.; Alamo, T.; Valverde, L.; *Application of Periodic Economic MPC to a Grid-Connected Micro-grid*, Poster en Congreso, 5th IFAC Nonlinear Model Predictive Control Conference International Federation of Automatic control, Sevilla, España,2015.
- Pereira,M.; Muñoz de la Peña,D.; Limon,D.; Alvarado,I.; Alamo,T.; *Application to a large-scale drinking water network of robust MPC for tracking periodic references*, 2016 European Conference Control (ECC) (submitted).

- Pereira,M.; Muñoz de la Peña,D.; Limon,D.; Alvarado,I.; Alamo,T.; *Robust model predictive controller for tracking periodic signals*, 2016 European Conference Control (ECC), (submitted).

1.9.3 National conference papers

- Pereira,M.; Muñoz de la Peña,D.; Limon,D.; Alamo,T.; *MPC Implementation in a PLC base don Nesterov's fast gradient method*, Ponencia en congreso, 23rd Mediterranean Conference on Control and Automation (MED). Torremolinos, Malaga, 2015.

2 Model predictive controller for tracking periodic signals

Research is to see what everybody else has seen, and to think what nobody else has thought

ALBERT SZENT-GYORGYI

Traditionally, the most used strategy in industry to regulate a system to a given operation point is the hierarchical control structure composed by a real time optimization (RTO) layer to calculate the optimal operation point, taking into account economic and other considerations, and an advanced controller to regulate the system to this optimal operation point.

However, As it was shown in chapter 1, there exists many relevant application such that the economically optimal policy to be operated is tracking a time-varying, possibly periodic, trajectory. The standard hierarchical structure can be extended to deal with this case assuming that the optimal trajectory is calculated by a dynamic RTO, and that the advanced controller is designed to track a target periodic reference using state of the art formulations. The main disadvantages of this scheme are that the performance may be sub-optimal and that the system may lose feasibility because of the differences on the models of the system used by both layers. Moreover, the target reference may not even be feasible or reachable. In this case, the control objective is to follow the best possible trajectory that satisfies the constraints and the system dynamics. This trajectory is called the *optimal reachable trajectory* and it is calculated by solving an optimization problem where a given optimality criterion is minimized based on the dynamic control model and the constraints.

The control scheme presented in this chapter is based on a single layer, which unites the dynamic trajectory planning and a MPC stage which regulates the system to the provided trajectory by the upper stage. This single layer controller guarantees that the closed-loop system converges to the optimal trajectory. See figure 2.1.

The proposed scheme extends the method presented in (Ferramosca et al., 2009; Limon et al., 2008) for tracking constant set-points to periodic references and is based on augmenting the decision variables with a set of auxiliary variables that describe a future, periodic and admissible trajectory. The cost function penalizes both the tracking error of the predicted trajectory to the planned reachable one, and the deviation of the planned reachable trajectory to the target periodic reference.

A design procedure to guarantee that the closed loop system converges asymptotically to the optimal admissible periodic trajectory while guaranteeing constraint satisfaction and recursive feasibility is provided. Besides it is proved that these properties hold even in the case of sudden changes in the reference to be tracked. The properties of the proposed controller are demonstrated with a simulation example of a ball and plate system. The results of this chapter have been published in Limon et al. (2015).

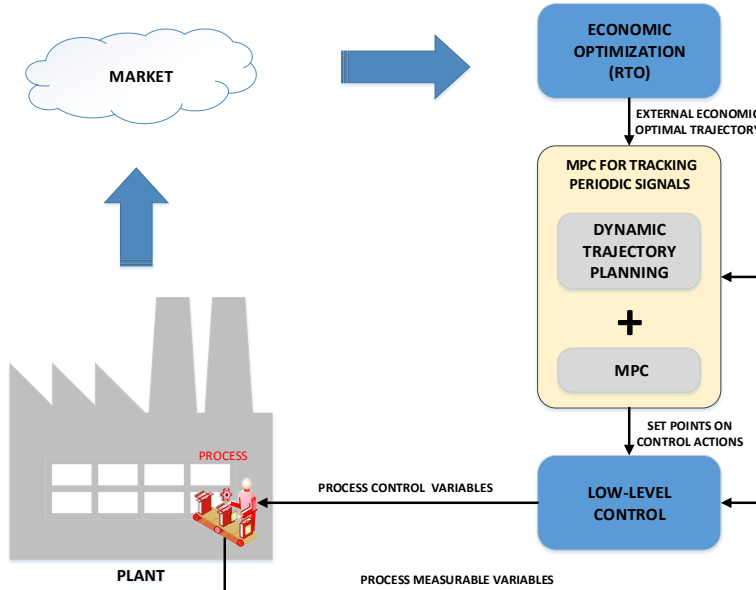


Figure 2.1 Hierarchical control structure of MPC for tracking periodic signals.

2.1 Problem formulation

Consider a discrete time linear system described by the following state-space model

$$\begin{aligned} x(k+1) &= Ax(k) + Bu(k) \\ y(k) &= Cx(k) + Du(k) \end{aligned} \quad (2.1)$$

where $x(k) \in \mathbb{R}^n$, $u(k) \in \mathbb{R}^m$ and $y(k) \in \mathbb{R}^p$ are the state, input and output of the system at time step k .

Assumption 2.1.1 *It is assumed that the pair (A,B) is controllable and (C,A) is observable.*

From this assumption it can be proved that there exists an integer $n_c \geq n$ such that the following matrices

$$\begin{aligned} &[A^{n_c-1}B, \dots, AB, B] \\ &[C^T, (CA)^T, \dots, (CA^{n_c-1})^T] \end{aligned}$$

are full row rank.

The controller must ensure that the closed-loop system satisfy the following state and input constraints

$$(x(k), u(k)) \in \mathcal{Z} \quad (2.2)$$

where set \mathcal{Z} is a convex and compact polyhedron that contains the origin.

The control objective is to steer the output $y(k)$ as close as possible to an exogenous periodic reference $r(k)$ with period T . Since no assumption is considered in the provided reference, there may not exist a control law capable of steering the system to this reference signal. This can be a consequence of the limits imposed by the constraints and/or by the dynamics. In this case the reference is said to be *unreachable*.

Next we define the notion of reachable periodic reference.

Definition 2.1.1 A periodic signal \mathbf{r} with period length T is said to be reachable if there exists state and input signals \mathbf{x} and \mathbf{u} such that

1. (\mathbf{x}, \mathbf{u}) are coherent with the system (2.1) and are periodic, i.e. for all $i \in \mathbb{I}_{[0, T-1]}$, $x(i+1) = Ax(i) + Bu(i)$ and $x(T) = x(0)$.
2. (\mathbf{x}, \mathbf{u}) are admissible, that is, for all $i \in \mathbb{I}_{[0, T-1]}$ $(x(i), u(i)) \in \mathcal{Z}^c$, where the set \mathcal{Z}^c is a closed polyhedron contained into the relative interior of \mathcal{Z} .
3. (\mathbf{x}, \mathbf{u}) maps the reference, that is, for all $i \in \mathbb{I}_{[0, T-1]}$, $r(i) = Cx(i) + Du(i)$.

The reason for considering a tighter constraint set \mathcal{Z}^c is to avoid the possible loss of controllability when the constraints are active Rao and Rawlings (1999). Notice that this is not limiting from a practical point of view since this set can be arbitrarily close to the set \mathcal{Z} .

If the reference is not reachable, then the controller cannot steer the output signal to the given reference. In this case the control goal is to steer the output to a reachable periodic trajectory that optimizes a certain criterion. This is referred to as the optimal reachable

trajectory which is defined by a periodic sequence of outputs and its corresponding state and inputs which are denoted $(\mathbf{y}^\circ, \mathbf{x}^\circ, \mathbf{u}^\circ)$ respectively.

In this formulation, the optimal reachable trajectory is chosen such that a cost function of the sum of the weighted squared error in a period T is minimized. This trajectory is calculated by following optimization problem that decides the initial state and the sequence of inputs that define the trajectory based on the target reference \mathbf{r} :

$$\begin{aligned} \min_{\mathbf{y}^r, \mathbf{x}^r, \mathbf{u}^r} \quad & V_p(\mathbf{r}; \mathbf{x}^r, \mathbf{u}^r) \\ \text{s.t.} \quad & \mathbf{x}^r(j+1) = A\mathbf{x}^r(j) + B\mathbf{u}^r(j) \\ & \mathbf{y}^r(j) = C\mathbf{x}^r(j) + D\mathbf{u}^r(j) \\ & (\mathbf{x}^r(j), \mathbf{u}^r(j)) \in \mathcal{X}^c \\ & \mathbf{x}^r(T) = \mathbf{x}^r(0) \end{aligned} \quad (2.3)$$

where

$$V_p(\mathbf{r}; \mathbf{x}^r, \mathbf{u}^r) = \sum_{j=0}^{T-1} \|\mathbf{y}^r(j) - \mathbf{r}(j)\|_S^2$$

The solution to this optimization problem is denoted $(\mathbf{y}^\circ, \mathbf{x}^\circ, \mathbf{u}^\circ)$.

If the reference \mathbf{r} is not reachable, there exists an error between the optimal reachable trajectory and the reference to be tracked. We denote this cumulative error as

$$V_p^\circ(\mathbf{r}) = V_p(\mathbf{r}; \mathbf{x}^\circ, \mathbf{u}^\circ) \quad (2.4)$$

Assumption 2.1.2 *The optimization problem (2.3) is strictly convex.*

Assumption 2.1.2 implies that the solution of the optimization problem is unique. Strict convexity can be checked easily since this is a quadratic programming problem. If the optimization problem would not be strictly convex, this can be regularized to be strictly convex by adding to the cost function a term, for instance $\|\mathbf{u}^r(j)\|_M^2$, with M positive definite.

Note that if the signal \mathbf{r} is known and periodic with period T , then the solution of the optimization problem (2.3) does not depend on the time instant in which the periodic reference is evaluated. The optimal reachable trajectory $(\mathbf{y}^\circ, \mathbf{x}^\circ, \mathbf{u}^\circ)$ is obtained from the periodic extension of the solution of (2.3).

The control objective is to design a state feedback tracking control law $u(k) = \kappa(\mathbf{x}(k), \mathbf{r}(k))$ such that given a periodic reference $r(k)$, the closed-loop system

$$\begin{aligned} \mathbf{x}(k+1) &= A\mathbf{x}(k) + B\kappa(\mathbf{x}(k), \mathbf{r}(k)) \\ \mathbf{y}(k) &= C\mathbf{x}(k) + D\kappa(\mathbf{x}(k), \mathbf{r}(k)) \end{aligned}$$

satisfies the constraints, is stable and converges to the optimal reachable trajectory. At each time step k , the periodic reference signal $\mathbf{r}(k)$ used to define the controller is different because the initial time of the sequence changes. With a slight abuse of notation, we define \mathbf{r} as the target periodic reference, and $\mathbf{r}(k)$ the reference fed to the controller which takes into account the time shift.

Notice that the sequence \mathbf{r} provided to the controller is the expected evolution of the periodic reference. As it will be demonstrated later on, the proposed control law will deal with the case that the periodic reference signal is suddenly changed and this may differ from expected. The only assumption is that the reference signal is periodic with period T .

Standard tracking schemes are usually based on a hierarchical architecture in which a trajectory planner computes the optimal reachable trajectory which is then used by a MPC as a target reference. This implies that the MPC controller depends on this optimal trajectory and that two different optimization problems have to be solved. In addition, standard MPC methods for tracking are generally based on optimization problems whose feasible region depends on the reference signal. This implies that feasibility can be lost if a sudden change in the reference takes place as mentioned before.

2.2 Proposed controller

In this section, a novel predictive tracking controller is proposed to solve the problem of tracking references that are asymptotically periodic. This controller ensures recursive feasibility and asymptotic stability of the closed loop system to the optimal reachable trajectory even in the case of sudden changes of the reference.

The proposed controller combines the trajectory planner and the MPC for tracking in a single optimization problem in which the decision variables are a planned reachable trajectory defined by its initial state x^r and the corresponding sequence of inputs \mathbf{u}^r as well as sequence of future control inputs \mathbf{u}_N . The optimization problem minimizes the cost function $V_N(x, \mathbf{r}; x^r, \mathbf{u}^r, \mathbf{u}_N)$, where the parameters (x, \mathbf{r}) stand for the current state and expected reference signal, and the decision variables $(x^r, \mathbf{u}^r, \mathbf{u}_N)$ stand for the initial state and sequence of future inputs of the planned reachable trajectory and the sequence of predicted control inputs respectively. The cost function is defined as follows:

$$V_N(x, \mathbf{r}; x^r, \mathbf{u}^r, \mathbf{u}_N) = V_t(x; x^r, \mathbf{u}^r, \mathbf{u}_N) + V_p(\mathbf{r}; x^r, \mathbf{u}^r)$$

with $N \leq T$, where

$$V_t(x; x^r, \mathbf{u}^r, \mathbf{u}_N) = \sum_{i=0}^{N-1} \|x(i) - x^r(i)\|_Q^2 + \|u(i) - u^r(i)\|_R^2 \quad (2.5)$$

$$V_p(\mathbf{r}; x^r, \mathbf{u}^r) = \sum_{i=0}^{T-1} \|y^r(i) - r(i)\|_S^2 \quad (2.6)$$

The term $V_t(x; x^r, \mathbf{u}^r, \mathbf{u}_N)$ penalizes the tracking error of the open-loop predicted trajectories with respect to the planned reachable reference along the prediction horizon N . The term $V_p(\mathbf{r}; x^r, \mathbf{u}^r)$ penalizes the error between the planned reachable trajectory and the reference to be tracked predicted for one period T .

In order to evaluate the MPC for tracking periodic references, the following optimization problem $P_N(x, \mathbf{r})$ is solved at each sampling time:

$$(x^{r*}, \mathbf{u}^{r*}, \mathbf{u}_N^*) = \underset{x^r, \mathbf{u}^r, \mathbf{u}_N}{\operatorname{argmin}} V_N(x, \mathbf{r}; x^r, \mathbf{u}^r, \mathbf{u}_N) \quad (2.7a)$$

$$s.t. \quad x(0) = x \quad (2.7b)$$

$$x(i+1) = Ax(i) + Bu(i) \quad i \in \mathbb{I}_{N-1} \quad (2.7c)$$

$$y(i) = Cx(i) + Du(i) \quad i \in \mathbb{I}_{N-1} \quad (2.7d)$$

$$(x(i), u(i)) \in \mathcal{Z} \quad i \in \mathbb{I}_{N-1} \quad (2.7e)$$

$$x^r(0) = x^r \quad (2.7f)$$

$$x^r(i+1) = Ax^r(i) + Bu^r(i) \quad i \in \mathbb{I}_{T-1} \quad (2.7g)$$

$$y^r(i) = Cx^r(i) + Du^r(i) \quad i \in \mathbb{I}_{T-1} \quad (2.7h)$$

$$(x^r(i), u^r(i)) \in \mathcal{Z}^c \quad i \in \mathbb{I}_{T-1} \quad (2.7i)$$

$$x^r(0) = Ax^r(T-1) + Bu^r(T-1) \quad (2.7j)$$

$$x(N) = x^r(N) \quad (2.7k)$$

The optimal solution of this optimization problem will be denoted by the superscript $*$. Thus, $\mathbf{x}_N^*(x, \mathbf{r}), \mathbf{y}_N^*(x, \mathbf{r})$ denotes the optimal predicted trajectories of the states and outputs of the system respectively. Analogously $\mathbf{x}^{r*}(x, \mathbf{r}), \mathbf{y}^{r*}(x, \mathbf{r})$ denotes the optimal planned reachable trajectories of the states and outputs of the system.

Constraints (2.7b-2.7d) define the predicted trajectories of the system starting from the current state. Constraints (2.7f-2.7h) define the planned reachable reference starting from the free initial state x^r . Constraints (2.7e) and (2.7i) include the state and input constraints for both the predicted states and the planned reachable reference. In addition, two terminal constraints are included to guarantee closed-loop convergence to the optimal reachable trajectory. Constraint (2.7j) is added to enforce that the reachable trajectory is periodic, while constraint (2.7k) guarantees that the terminal state of the predicted trajectory of the plant reaches the planned reachable trajectory at the end of the prediction horizon.

It is important to point out that the set of constraints of this optimization problem does not depend on the reference signal \mathbf{r} if and only if a set of states $\mathcal{X}_N \subseteq \mathbb{R}^n$ such that the optimization is feasible if $x \in \mathcal{X}_N$ for any reference signal. The domain of attraction \mathcal{X}_N is defined as the set of states that can admissibly reach any reachable periodic trajectory in N steps, and in general is large if compared with the set of states that can admissibly reach a particular reachable periodic trajectory.

The control law is given by

$$u(k) = \kappa_N(x(k), \mathbf{r}(k)) = u_N^*(0; k)$$

2.3 Stability analysis

In this section we study the closed-loop properties of the proposed control law. In particular we prove that the output converges asymptotically to the optimal reachable trajectory and that the controller maintains feasibility even in the presence of sudden changes in the target reference. To this end, we make use of the following slightly modified Lyapunov theorem, see Keerthi and Gilbert (1988):

Theorem 2.3.1 *Consider an autonomous system $z(k+1) = f(z(k))$ where $z(k) \in \mathbb{R}^n$. Let Γ be a positive invariant set and $\Omega \subseteq \Gamma$ be a compact set, both including the origin as an interior point. If there exists a function $W : \mathbb{R}^n \rightarrow \mathbb{R}^+$ and suitable K_∞ -class functions $\alpha_1, \alpha_2, \alpha_3$ such that*

$$(i) \quad W(z(k)) \geq \alpha_1(\|z(k)\|), \quad \forall z(k) \in \Gamma \quad (2.8a)$$

$$(ii) \quad W(z(k)) \leq \alpha_2(\|z(k)\|), \quad \forall z(k) \in \Omega \quad (2.8b)$$

$$(iii) \quad W(z(k+1)) - W(z(k)) \leq -\alpha_3(\|z(k)\|), \quad \forall z(k) \in \Gamma \quad (2.8c)$$

then $W(\cdot)$ is called a Lyapunov function in Γ and the origin is asymptotically stable for all initial states in Γ .

In the following theorem, we will use this result to prove the existence of a Lyapunov function and then derive the asymptotic stability of the optimal trajectory.

Theorem 2.3.2 *Assume that system (2.1) satisfies Assumptions 2.1.1 and 2.1.2, the weighting matrix Q is positive definite and the prediction horizon is such that $N \geq n_c$. Then system (2.1) controlled by the proposed control law is recursively feasible and the optimal reachable trajectory \mathbf{x}° given by $(x^\circ, \mathbf{u}^\circ)$ is asymptotically stable with region of attraction \mathcal{X}_N , i.e. the closed loop system is stable and $x(k)$ converges asymptotically to $\mathbf{x}^\circ(k)$ for all $x(0) \in \mathcal{X}_N$.*

Proof. Asymptotic stability will be proved by demonstrating that for the system that models the error between the state of the reachable optimal trajectory and the closed loop trajectory of the system, that is¹

$$z(k) = x(k) - x^\circ(k)$$

the function

$$W(z(k)) = W(x(k) - x^\circ(k)) = V_N^*(x(k), \mathbf{r}(k)) - V_p^\circ(\mathbf{r}) \quad (2.9)$$

satisfies the conditions of Theorem 2.3.1 in the region \mathcal{X}_N and provides a Lyapunov function. This function is defined as the difference between the optimal cost of the MPC problem at time k , $V_N^*(x(k), \mathbf{r}(k))$, and the cost value of the optimal reachable trajectory defined in (??). To simplify the notation, we have dropped the dependence of function

¹ The value of the state of the optimal reachable trajectory is obtained from the solution of problem (2.3) taking into account the periodic nature of the trajectory for values of k greater than the period.

$W(\cdot)$ on the target reference \mathbf{r} . In addition, we will not use the error $z(k)$ in the following derivations, but its definition, $x(k) - x^\circ(k)$.

In what follows, $y(i;k), x(i;k)$ are the output and state predicted at time i applying $\mathbf{u}(k)$ from the initial state $x(k)$; $y^r(i;k), x^r(i;k)$ are the output and state of the planned reachable reference at time i applying $\mathbf{u}^r(k)$ from the initial state $x^r(k)$; $y^\circ(i;k), x^\circ(i;k)$ are the output and state of the optimal reachable reference i applying $\mathbf{u}^\circ(k)$ from the initial state $x^\circ(k)$.

First, we will prove that the region \mathcal{X}_N is a positive invariant set for the system in closed-loop with the proposed controller, and hence, also for $x(k) - x^\circ(k)$. Consider the shifted sequences

$$\mathbf{u}_N^s(k) = \{u_N^*(1;k-1), \dots, u_N^*(N-1;k-1), u_N^{r*}(N;k-1)\} \quad (2.10a)$$

$$x^{rs}(k) = x^{r*}(1;k-1) \quad (2.10b)$$

$$\mathbf{u}^{rs}(k) = \{u^{r*}(1;k-1), \dots, u^{r*}(T-1;k-1), u^{r*}(0;k-1)\} \quad (2.10c)$$

Taking into account that the optimal solution at time $k-1$ is feasible by definition, it is easy to prove that the shifted sequences are also feasible at time k . Note that the constraints of problem 2.7 do not depend on the reference, so this is true even in the presence of arbitrary changes of \mathbf{r} . Therefore, if $x(k-1)$ is feasible, i.e. $x(k-1) \in \mathcal{X}_N$, then $x(k)$ will also be feasible, that is, $x(k) \in \mathcal{X}_N$, and hence \mathcal{X}_N is a positive invariant set.

Next, we will prove that the proposed Lyapunov function satisfies the conditions of theorem 2.3.1.

Condition (i): From the definition of $W(\cdot)$ we have that

$$\begin{aligned} W(x(k) - x^\circ(k)) &= \sum_{i=0}^{N-1} \|(x^*(i;k) - x^{r*}(i;k))\|_Q^2 + \|(u^*(i;k) - u^{r*}(i;k))\|_R^2 \\ &+ V_p(\mathbf{r}(k), x^{r*}(k), \mathbf{u}^{r*}(k)) - V_p^\circ(\mathbf{r}) \\ &\geq \|x(k) - x^{r*}(k)\|_Q^2 + V_p(\mathbf{r}(k), x^{r*}(k), \mathbf{u}^{r*}(k)) - V_p^\circ(\mathbf{r}) \end{aligned}$$

From the strictly convexity of optimization problem (2.3), there exists a $\pi_1 > 0$ such that

$$V_p(\mathbf{r}(k), x^{r*}(k), \mathbf{u}^{r*}(k)) - V_p^\circ(\mathbf{r}) \geq \pi_1 \|(x^{r*}(k) - x^\circ(k))\|^2$$

and therefore, since Q is positive definite,

$$\begin{aligned} W(x(k) - x^\circ(k)) &\geq \lambda_{\min}(Q) \|x(k) - x^{r*}(k)\|^2 + \pi_1 \|(x^{r*}(k) - x^\circ(k))\|^2 \\ &\geq \alpha_1 (\|x(k) - x^{r*}(k)\|^2 + \|(x^{r*}(k) - x^\circ(k))\|^2) \\ &\geq \frac{\alpha_1}{2} \|x(k) - x^\circ(k)\|^2 \end{aligned}$$

with $\alpha_1 = \min\{\lambda_{\min}(Q), \pi_1\} > 0$.

Condition (ii): Since the optimal reachable trajectory is contained in the relative interior of the set of constraints \mathcal{Z} , there exists a sufficiently small neighborhood Υ such that for

all $(x(k) - x^\circ(k)) \in \Upsilon$, the dead-beat control law (such that $x(k+N) = x^\circ(k+N)$)

$$u(k) = K_{db}(x(k) - x^\circ(k)) + u^\circ(k)$$

provides a feasible solution for $(x^r(k), \mathbf{u}^r(k)) = (x^\circ(k), \mathbf{u}^\circ(k))$, resulting in an admissible predicted trajectory. Notice that the dead-beat control law can be used since $N \geq n_c$ and the system is controllable as stated in Assumption 2.1.1.

Therefore, taking into account the optimality of the solution, for all $x(k)$ such that $(x(k) - x^\circ(k)) \in \Upsilon$, there exist a constant $c_w > 0$ such that

$$\begin{aligned} W(x(k) - x^\circ(k)) &\leq \sum_{i=0}^{N-1} \|x(i;k) - x^\circ(i;k)\|_Q^2 + \|u(i;k) - u^\circ(i;k)\|_R^2 \\ &\leq \sum_{i=0}^{N-1} c_w \|x(i;k) - x^\circ(i;k), u(i;k) - u^\circ(i;k)\|^2 \end{aligned}$$

Then taking into account the linearity of the system controlled with the dead-beat control law, there exists a constant $w_c > 0$ such that

$$\sum_{i=0}^{N-1} \|x(i;k) - x^\circ(i;k), u(i;k) - u^\circ(i;k)\|^2 \leq w_c \|x(k) - x^\circ(k)\|^2$$

Then we have that

$$W(x(k) - x^\circ(k)) \leq c_w w_c \|x(k) - x^\circ(k)\|^2$$

for all $(x(k) - x^\circ(k)) \in \Upsilon$.

Condition (iii): From standard arguments Rawlings and Mayne (2009) and periodicity of $\mathbf{r}, \mathbf{y}^{r*}(k), \mathbf{u}^{r*}(k)$, the following inequalities follow:

$$\begin{aligned} \Upsilon &= V_N^*(x(k), \mathbf{r}(k)) - V_N^*(x(k-1), \mathbf{r}(k-1)) \\ &\leq V_N(x(k), \mathbf{r}(k); x^{rs}(k), \mathbf{u}^{rs}(k), \mathbf{u}_N^s(k)) - V_N^*(x(k-1), \mathbf{r}(k-1)) \\ &\leq -\|x^*(0;k-1) - x^{r*}(k-1)\|_Q^2 - \|u_N^*(0;k-1) - u^{r*}(0;k-1)\|_R^2 \\ &\quad + V_p(\mathbf{r}(k); x^{rs}(k), \mathbf{u}^{rs}(k)) - V_p(\mathbf{r}(k-1); x^{r*}(k-1), \mathbf{u}^{r*}(k-1)) \\ &\leq -\|x^*(0;k-1) - x^{r*}(k-1)\|_Q^2 - \|u_N^*(0;k-1) - u^{r*}(0;k-1)\|_R^2 \end{aligned}$$

From lemma 2.3.1 we have that there exist $x^r(k), \mathbf{u}^r(k), \mathbf{u}_N(k)$ such that

$$V_N(x(k), \mathbf{r}(k); x^r(k), \mathbf{u}^r(k), \mathbf{u}_N(k)) - V_N^*(x(k-1), \mathbf{r}(k-1)) \leq -\gamma \|x(k-1) - x^\circ(k-1)\|^2$$

for all $x(k-1) \in \mathcal{X}_N$ and some $\gamma > 0$. ■

We have proved that $W(x(k) - x^\circ(k))$ is a Lyapunov function for the closed-loop system in \mathcal{X}_N , and then, the optimal reachable trajectory \mathbf{x}° given by $(x^\circ, \mathbf{u}^\circ)$ is asymptotically stable with region of attraction \mathcal{X}_N .

2.3.1 Technical Lemmata

In this section we present two technical lemmas used to prove condition (iii). Lemma 2.3.1 is itself condition (iii), while Lemma 2.3.2 is used to prove Lemma 2.3.1.

Lemma 2.3.1 *If Problem $P_N(x(k-1); \mathbf{r}(k-1))$ is feasible, then there exists a positive constant $\gamma > 0$ such that*

$$V_N^*(x(k), \mathbf{r}(k)) - V_N^*(x(k-1); \mathbf{r}(k-1)) \leq -\gamma \|x(k-1) - \mathbf{x}^\circ(k-1)\|^2$$

for all $x(k-1) \in \mathcal{X}_N$.

Proof. In this proof, the signals defined in the proof of Theorem 2.3.2 will be used.

Consider that for $x(k)$ and the shifted reference $(x^{rs}(k), \mathbf{u}^{rs}(k))$ the sequences introduced in Lemma 2.3.2 are defined. By feasibility we have that

$$(x^{rs}(i; k), u^{rs}(i; k)) \in \mathcal{L}^c$$

and then there exists an $\varepsilon > 0$ such that if $\|x(k) - x^{rs}(k)\| \leq \varepsilon$ then $(\mathbf{u}_N^a(k), x^{rs}(k), \mathbf{u}^{rs}(k))$ is a feasible solution of $P_N(x(k), \mathbf{r}(k))$.

Take the constant

$$\Gamma_k = \|x^{r*}(k-1) - x^\circ(k-1)\|^2$$

and let $\beta_k \in (0, 1)$ be a positive constant satisfying the conditions in Lemma 2.3.2. Take a $\beta \in (\beta_k, 1)$ such that

$$(1 - \beta) \|x^{rs}(k) - x^\circ(k)\| \leq \varepsilon$$

and define

$$\xi_k = (1 - \beta) \|x^{rs}(k) - x^\circ(k)\|$$

Then the following two cases are studied:

Case 1: $\|x(k) - x^{rs}(k)\| \geq \xi_k$

By the definition of $x(k)$ and since $x^{rs}(k) = x^{r*}(1; k-1)$ we obtain

$$\begin{aligned} \xi_k &\leq \|x(k) - x^{r*}(1; k-1)\| \\ &= \|A(x(k-1) - x^{r*}(k-1)) + B(u^*(0; k-1) - u^{r*}(0; k-1))\| \\ &\leq \rho \|x(k-1) - x^{r*}(k-1)\| + \rho \|u^*(0; k-1) - u^{r*}(0; k-1)\| \end{aligned}$$

where $\rho = \max\{\|A\|, \|B\|, 1\}$.

Consider the case that

$$\|u^*(0; k-1) - u^{r*}(0; k-1)\| \leq \frac{\xi}{2\rho}$$

then from the last inequality we have that

$$\|x(k-1) - x^{r*}(k-1)\| \geq \frac{\xi}{2\rho}$$

and then

$$\begin{aligned} & \| (x(k-1) - x^{r^*}(k-1)) \|_Q^2 + \| (u^*(0; k-1) - u^{r^*}(0; k-1)) \|_R^2 \\ \geq & \lambda_{\min}(Q) \| x(k-1) - x^{r^*}(k-1) \|^2 \geq \frac{\lambda_{\min}(Q) \xi^2}{4\rho^2}. \end{aligned}$$

On the other hand, if we consider the case that

$$\| (u^*(0; k-1) - u^{r^*}(0; k-1)) \| \geq \frac{\xi}{2\rho}$$

then

$$\begin{aligned} & \| (x(k-1) - x^{r^*}(k-1)) \|_Q^2 + \| (u^*(0; k-1) - u^{r^*}(0; k-1)) \|_R^2 \\ \geq & \| (u^*(0; k-1) - u^{r^*}(0; k-1)) \|_R^2 \\ \geq & \lambda_{\min}(R) \| (u^*(0; k-1) - u^{r^*}(0; k-1)) \|^2 \geq \frac{\lambda_{\min}(R) \xi^2}{4\rho^2} \end{aligned}$$

Let

$$\bar{\xi} := \max \left\{ \frac{\lambda_{\min}(Q) \xi^2}{4\rho^2}, \frac{\lambda_{\min}(R) \xi^2}{4\rho^2} \right\}$$

and choose

$$\gamma = \frac{\bar{\xi}}{\max \{ \|x - x^\circ\|^2, x \in \mathcal{X}_N, (x^\circ, u) \in \mathcal{L}^c \}}$$

Notice that constant γ is positive and bounded since set \mathcal{L} is assumed to be compact. Then,

$$\begin{aligned} & \| (x(k-1) - x^{r^*}(k-1)) \|_Q^2 + \| (u^*(0; k-1) - u^{r^*}(0; k-1)) \|_R^2 \\ \geq & \bar{\xi} = \gamma \max \{ \|x - x^\circ\|^2, x \in \mathcal{X}_N, (x^\circ, u) \in \mathcal{L}^c \} \\ \geq & \gamma \| (x(k-1) - x^\circ(k-1)) \|^2. \end{aligned}$$

Case 2: $\|x(k) - x^{rs}(k)\| \leq \xi_k$

Consider the sequences defined in lemma 2.3.2 at $x(k)$, for the feasible shifted reference trajectory $(x^{rs}(k), \mathbf{u}^{rs}(k))$ and taking the optimal unconstrained dead-beat control law gain as the stabilizing control law gain K .

Since $\|x(k) - x^{rs}(k)\| \leq \xi_k \leq \varepsilon$ and since the solution $(\mathbf{u}_N^a(k), x^{rs}, \mathbf{u}^{rs}(k))$ is a feasible solutions of $P_N(x(k), \mathbf{r}(k))$, the solution $(\hat{\mathbf{u}}_N^a(k), \hat{x}^r, \hat{\mathbf{u}}^r(k))$ is also feasible by convexity.

For the given Γ_k and β , since

$$\|x(k) - x^{rs}(k)\| \leq \xi_k = (1 - \beta) \|x^{rs}(k) - x^\circ(k)\|$$

we derive from lemma 2.3.2 that

$$\hat{V}_N(x(k), \mathbf{r}(k)) \leq V_N(x(k), \mathbf{r}(k)) - (1 - \beta)^2 \|x^{r^*}(k-1) - x^\circ(k-1)\|^2 \quad (2.11)$$

Since K is the optimal unconstrained control law, we have that

$$V_N(x(k), \mathbf{r}(k)) \leq V_N(x(k), \mathbf{r}(k); x^{rs}(k), \mathbf{u}^{rs}(k), \mathbf{u}_N^s(k))$$

and then we have that

$$\begin{aligned} \Delta^* &= \hat{V}_N(x(k), \mathbf{r}(k)) - V_N^*(x(k-1), \mathbf{r}(k-1)) \\ &\leq V_N(x(k), \mathbf{r}(k)) - (1-\beta)^2 \|x^{r*}(k-1) - x^\circ(k-1)\|^2 - V_N^*(x(k-1), \mathbf{r}(k-1)) \\ &\leq V_N(x(k), \mathbf{r}(k); x^{rs}(k), \mathbf{u}^{rs}(k), \mathbf{u}_N^s(k)) - V_N^*(x(k-1), \mathbf{r}(k-1)) \\ &\quad - (1-\beta)^2 \|x^{r*}(k-1) - x^\circ(k-1)\|^2 \\ &\leq -(\|x(k-1) - x^{r*}(k-1)\|_Q^2 + \|u^*(0; k-1) - u^{r*}(0; k-1)\|_R^2) \\ &\quad - (1-\beta)^2 \|x^{r*}(k-1) - x^\circ(k-1)\|^2 \\ &\leq -\lambda_{\min}(Q) \|x(k-1) - x^{r*}(k-1)\|^2 - (1-\beta)^2 \|x^{r*}(k-1) - x^\circ(k-1)\|^2 \\ &\leq -\gamma \|x(k-1) - x^\circ(k-1)\|^2 \end{aligned}$$

with $\gamma = \frac{1}{2} \min\{\lambda_{\min}(Q), (1-\beta)^2\}$. ■

Lemma 2.3.2 *Let $x(k)$ be a given state and let $(x^r(k), \mathbf{u}^r(k))$ be such that the associated trajectory is admissible. Let $(\mathbf{x}_N^a(k), \mathbf{u}_N^a(k))$ be a sequence of states and control inputs derived from the control law $\kappa^a(x(i), x^r(k), \mathbf{u}^r(k)) = K(x(i) - x^r(i; k)) + \mathbf{u}^r(i; k)$ such that $x^a(N; k) = x^r(N; k)$. Let $V_N(x(k), \mathbf{r}(k))$ be the cost associated to this solution, that is*

$$V_N(x(k), \mathbf{r}(k)) = V_N(x(k), \mathbf{r}(k); \mathbf{u}_N^a(k), x^r(k), \mathbf{u}^r(k))$$

Let $(\hat{x}^r(k), \hat{\mathbf{u}}^r(k))$ be defined as

$$(\hat{x}^r(k), \hat{\mathbf{u}}^r(k)) = \beta(x^r(k), \mathbf{u}^r(k)) + (1-\beta)(x^\circ(k), \mathbf{u}^\circ(k)) \quad (2.12)$$

for $\beta \in (0, 1)$, and let $\hat{\mathbf{u}}_N^a(k)$ be a sequence of control inputs derived from the dead-beat control law $\kappa^a(x(i), \hat{x}^r(k), \hat{\mathbf{u}}^r(k)) = K(x(i) - \hat{x}^r(i; k)) + \hat{\mathbf{u}}^r(i; k)$. Let $\hat{V}_N(x(k), \mathbf{r}(k))$ be the cost associated to this solution, that is

$$\hat{V}_N(x(k), \mathbf{r}(k)) = V_N(x(k), \mathbf{r}(k); \hat{\mathbf{u}}_N^a(k), \hat{x}^r(k), \hat{\mathbf{u}}^r(k))$$

Then, for any positive constant $\Gamma > 0$, there exists a constant $\beta \in (0, 1)$ such that

$$\|x(k) - x^r(k)\| \leq (1-\beta) \|x^r(k) - x^\circ(k)\| \quad (2.13)$$

implies that

$$\hat{V}_N(x(k), \mathbf{r}(k)) - V_N(x(k), \mathbf{r}(k)) \leq -(1-\beta)^2 \Gamma$$

Proof. We denote $A_{cl} = A + BK$. From the definition of the dead-beat control law we obtain

$$u^a(i; k) = KA_{cl}^i(x(k) - x^r(k)) + \mathbf{u}^r(i; k) \quad (2.14a)$$

$$x^a(i; k) = A_{cl}^i(x(k) - x^r(k)) + x^r(i; k) \quad (2.14b)$$

and similarly for $\hat{\mathbf{u}}_N^a(k)$ $\hat{\mathbf{x}}_N^a(k)$. Taking into account (2.14), we can show that

$$\begin{aligned} \Phi &= \sum_{i=0}^{N-1} \left(\|\hat{x}^a(i; k) - \hat{x}^r(i; k)\|_Q^2 + \|\hat{u}^a(i; k) - \hat{u}^r(i; k)\|_R^2 \right) \\ \Psi &= \sum_{i=0}^{N-1} \left(\|x^a(i; k) - x^r(i; k)\|_Q^2 - \|u^a(i; k) - u^r(i; k)\|_R^2 \right) \\ \Phi - \Psi &= \|x(k) - \hat{x}^r(k)\|_H^2 - \|x(k) - x^r(k)\|_H^2 \\ &= \|x(k) - x^r(k) + (1 - \beta)(x^r(k) - x^\circ(k))\|_H^2 - \|x(k) - x^r(k)\|_H^2 \\ &= (1 - \beta)^2 \|x^r(k) - x^\circ(k)\|_H^2 + 2(1 - \beta)(x(k) - x^r(k))^T H(x^r(k) - x^\circ(k)) \\ &\leq (1 - \beta)^2 \|x^r(k) - x^\circ(k)\|_H^2 + 2(1 - \beta) \|H\| \|x(k) - x^r(k)\| \|x^r(k) - x^\circ(k)\| \\ &\leq (1 - \beta)^2 \lambda_H \|x^r(k) - x^\circ(k)\|^2 + 2(1 - \beta) \lambda_H \|x(k) - x^r(k)\| \|x^r(k) - x^\circ(k)\| \\ &\leq (1 - \beta)^2 \lambda_H \|x^r(k) - x^\circ(k)\|^2 + 2(1 - \beta)^2 \lambda_H \|x^r(k) - x^\circ(k)\|^2 \\ &= 3(1 - \beta)^2 \lambda_H \|x^r(k) - x^\circ(k)\|^2 \end{aligned}$$

where H is defined as

$$H = \sum_{i=0}^{N-1} A_{cl}^{iT} (Q + K^T R K) A_{cl}^i$$

which is positive definite. The constant $\lambda_H = \lambda_{\max}(\|H\|)$. Convexity of $V_p(\cdot)$ provides that

$$V_p(\mathbf{r}(k), \hat{x}^r(k), \hat{\mathbf{u}}^r(k)) \leq \beta V_p(\mathbf{r}(k), x^r(k), \mathbf{u}^r(k)) + (1 - \beta) V_p^\circ \quad (2.15)$$

Using these results, it can then be seen that for any $\Gamma > 0$

$$\begin{aligned} \Xi &= \hat{V}_N(x(k), \mathbf{r}(k)) - V_N(x(k), \mathbf{r}(k)) + (1 - \beta)^2 \Gamma \\ &\leq (1 - \beta)^2 \Gamma + 3(1 - \beta)^2 \lambda_H \|x^r(k) - x^\circ(k)\|^2 \\ &\quad - (1 - \beta)(V_p(\mathbf{r}(k), x^r(k), \mathbf{u}^r(k)) - V_p^\circ) \end{aligned}$$

Since $V_p(\mathbf{r}(k); x^r(k), \mathbf{u}^r(k)) > V_p^\circ$ by optimality of the optimal reachable reference, for any $\Gamma > 0$ there exists a $\beta \in (0, 1)$, such that

$$\hat{V}_N(x(k), \mathbf{r}(k)) - V_N(x(k), \mathbf{r}(k)) + (1 - \beta)^2 \Gamma \leq 0$$

■

2.4 Some properties of the proposed controller

The proposed controller has a number of interesting properties that we present in the following list:

1. The proposed optimization problem is a standard multi-parametric quadratic program in $(x, \mathbf{r}(k))$ that can be solved for a given $(x(k), \mathbf{r}(k))$ using specialized algorithms (Boyd and Vandenberghe, 2004). Furthermore, taking into account (Bemporad et al., 2002), it is proved that the resulting control law is a piecewise affine function of $(x(k), \mathbf{r}(k))$.
2. As it was illustrated in (Limon et al., 2008), the inclusion of the reachable reference in the MPC formulation leads to an enlargement of the domain of attraction of the predictive controller. This property is improved by the proposed controller, the domain of attraction is the set of states that can be reached in N steps any periodic reachable signal of the system. Since a constant reference is a possible periodic reachable signal, the domain of attraction of the proposed controller is larger than the one presented in (Limon et al., 2008), but at expense of a larger number of decision variables.
3. One of the main properties of this controller is that recursive feasibility is guaranteed for any reference signal $\mathbf{r}(k)$, even in the case that it is non-periodic. Besides, the controller steers the system to the closest possible periodic reachable signal (taking $V_p(\cdot)$ as measure). Furthermore the calculation of the optimal trajectory is not required to derive the control law.

At a certain sampling time, k , the control action is calculated for a provided expected reference signal $\mathbf{r}(k)$ used in the predictions. If at the next sampling time $k + 1$, the provided reference $\mathbf{r}(k + 1)$ is suddenly changed and hence it is not consistent with $\mathbf{r}(k)$, i.e. $r(j; k + 1) \neq r(j + 1; k)$, then the optimization problem remains feasible and the control law will be also well defined. Therefore, the control law will steer the system to the new optimal trajectory as long as the provided expected reference is consistent.

Moreover, if the reference signal is not periodic but converges to a periodic reference signal, then the control law steers the system to the optimal periodic trajectory of the limit periodic reference. This is a consequence of the continuity of the control law $\kappa(x, \mathbf{r})$ with respect to the predicted reference \mathbf{r} .

4. As \mathcal{Z} is compact, then the control law $\kappa_N(x(k), \mathbf{r}(k))$ is also Lipschitz continuous with respect the state $x(k)$. As the model is continuous, then the closed loop system is input-to-state stable (ISS) with respect to additive disturbances (Limon et al., 2009b) in a robust positively invariant set.

2.5 Example

In this section we apply the proposed controller to a linear approximation of a ball and plate system. The system consists of a plate pivoted at its center such that the slope of the plate can be manipulated in two perpendicular directions. A servo system consisting of motors is used for tilting the plate and control the two angles of rotation θ_1, θ_2 . An appropriate sensor for measurement of the ball position z_1, z_2 is assumed to be available, for example an intelligent vision system. The basic control task is to control the position of a ball freely rolling on a plate. This system is a dynamic system with two inputs and two outputs. Figure 2.2 shows a schematic of the system.

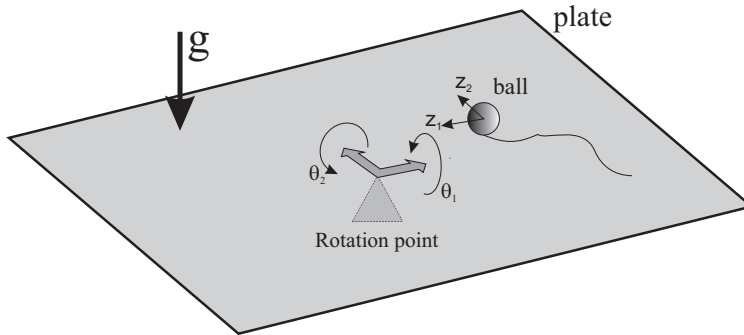


Figure 2.2 Ball and plate system.

To carry out the simulations a nonlinear continuous time model is obtained from the rigid body dynamics of the ball on the plate. In particular, applying the Lagrange-Euler formulation to each coordinate $(z_1, z_2, \theta_1, \theta_2)$ and assuming that the ball holds always contact with the plate and does not slip when moving, the following model is obtained:

$$\begin{aligned}\ddot{z}_1 &= \frac{5}{7}(z_1 \dot{\theta}_1^2 + \dot{\theta}_1 z_2 \dot{\theta}_2 + g \sin \theta_1) \\ \ddot{z}_2 &= \frac{5}{7}(z_2 \dot{\theta}_2^2 + z_1 \dot{\theta}_1 \dot{\theta}_2 + g \sin \theta_2)\end{aligned}$$

The inputs of the ball and plate system are the accelerations applied in each rotation axis and they are denoted as $\mathcal{U} = [u_1, u_2]^t = [\ddot{\theta}_1, \ddot{\theta}_2]^t$. The state $x \in \mathbb{R}^8$ is defined as follows

$$x^T = [z_1, \dot{z}_1, \theta_1, \dot{\theta}_1, z_2, \dot{z}_2, \theta_2, \dot{\theta}_2]^T$$

We consider the following constraints on the position, angles and inputs:

$$\begin{aligned}|z_i| &\leq 6 \text{ cm}, i = 1, 2 \\ |\theta_i| &\leq \frac{\pi}{2} \text{ rad}, i = 1, 2 \\ |u_i| &\leq 110 \text{ rad/s}^2, i = 1, 2\end{aligned}$$

To apply the proposed MPC control scheme, a discrete time linear system is obtained taking as equilibrium point the origin for all the states and inputs and a sampling time $T_m = 0.05$ seconds (see details in (Moreno-Armendáriz et al., 2010),(Wang et al., 2014)). The matrices that define system (2.1) are the following

$$A = \begin{pmatrix} 1 & 0.05 & 0.0088 & 0.0001 & 0 & 0 & 0 & 0 \\ 0 & 1 & 0.35 & 0.0088 & 0 & 0 & 0 & 0 \\ 0 & 0 & 1 & 0.05 & 0 & 0 & 0 & 0 \\ 0 & 0 & 0 & 1 & 0 & 0 & 0 & 0 \\ 0 & 0 & 0 & 0 & 1 & 0.05 & 0.0088 & 0.0001 \\ 0 & 0 & 0 & 0 & 0 & 1 & 0.35 & 0.0088 \\ 0 & 0 & 0 & 0 & 0 & 0 & 1 & 0.05 \\ 0 & 0 & 0 & 0 & 0 & 0 & 0 & 1 \end{pmatrix}$$

$$B = \begin{pmatrix} 0 & 0 \\ 0.0001 & 0 \\ 0.0013 & 0 \\ 0.05 & 0 \\ 0 & 0 \\ 0 & 0.0001 \\ 0 & 0.0013 \\ 0 & 0.05 \end{pmatrix}; C = \begin{pmatrix} 1 & 0 & 0 & 0 & 0 & 0 & 0 & 0 \\ 0 & 0 & 0 & 0 & 1 & 0 & 0 & 0 \end{pmatrix}$$

This system satisfies Assumption (2.1.1). It is important to remark that the dynamics of variables z_1 and z_2 are decoupled, however we will take into account coupled constraints in the controller definition. This model is used both to design the controller and to carry out the simulations.

To demonstrate the main properties of the proposed controller we consider two different scenarios. In both scenarios, the weighting matrices of the controller are $R = 10 \cdot I^2$, $Q = 100 \cdot I^8$, $S = 7000 \cdot I^2$ where I is the identity matrix of appropriate dimension. The simulations were done in Matlab 2013a using the solver quadprog.

In the first scenario, the ball must follow a pentagram of radius $8cm$ centered in the origin of the plate with a speed of $8.4 \frac{cm}{s}$. The period of the reference, that is, the time that the ball takes to follow the geometric figure is 4.5 seconds. Hence the period is 90 samples. In this scenario we consider a long prediction horizon equal to the period, that is, the horizon of the MPC control problem is $N = 90$. The number of decision variables of the problem is $n_u \cdot (N + T) + n_x = 368$. The initial state of this scenario is the ball in equilibrium at $(z_1, z_2) = (0, -5)cm$. In order to demonstrate the approach for coupled states, in this scenario the following state constraint is included:

$$\begin{aligned} |z_1 + z_2| &\leq 6 \text{ cm} \\ |-z_1 + z_2| &\leq 6 \text{ cm} \end{aligned}$$

The first scenario shows how the closed-loop system converges asymptotically to the

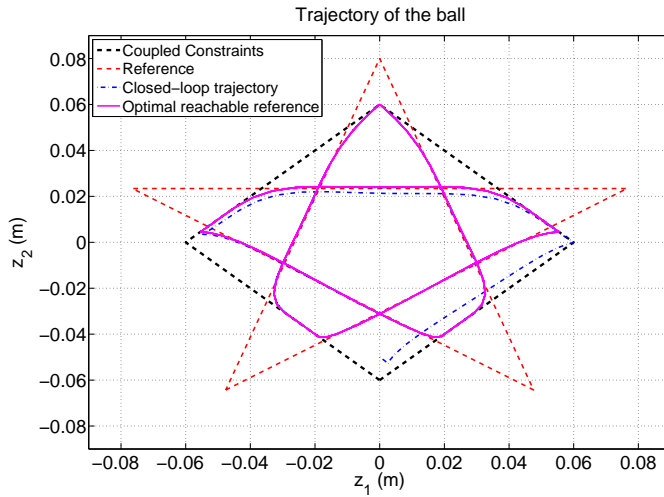


Figure 2.3 Trajectories of z_1, z_2 for the closed loop system (dash-dot blue), the trajectory planner (continuous magenta) and the target reference (discontinuous red). The artificial coupled constraints are shown (yellow) (scenario 1).

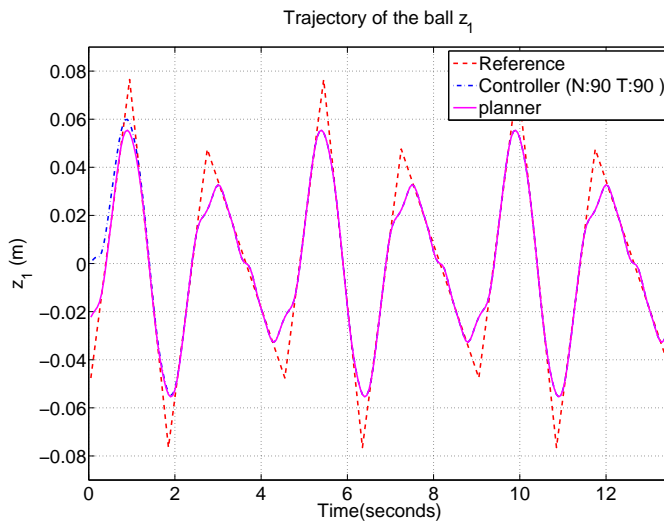


Figure 2.4 Trajectories of z_1 for the closed loop system (dash-dot blue), the trajectory planner (continuous magenta) and the target reference (discontinuous red) (scenario 1).

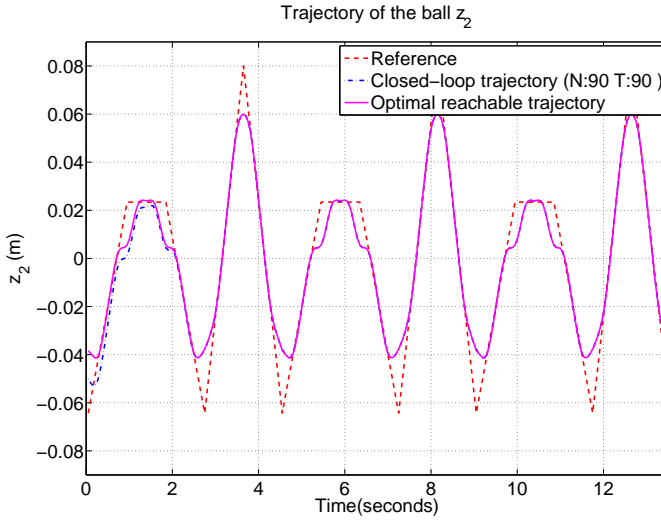


Figure 2.5 Trajectories of z_2 for the closed loop system (dash-dot blue), the trajectory planner (continuous magenta) and the target reference (discontinuous red) (scenario 1).

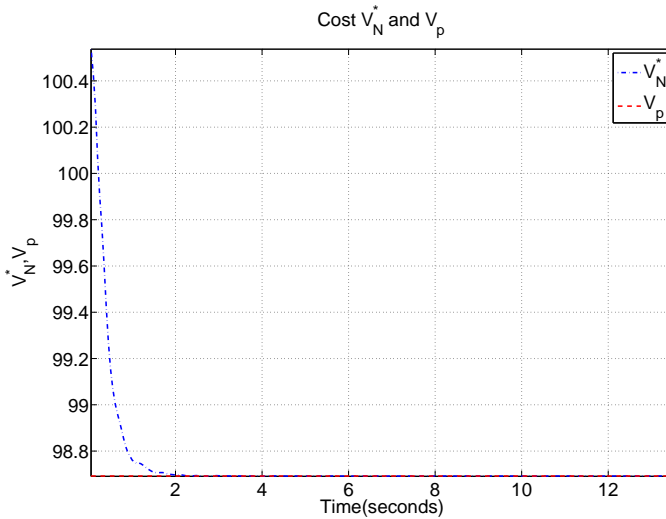


Figure 2.6 Trajectories of the optimal cost V_N^* (discontinuous blue) and trajectory planner cost V_p^o (discontinuous red) (scenario 1).

optimal reachable trajectory satisfying the coupled constraints. Figure 2.3 shows the trajectories of z_1, z_2 for the closed loop system (dash-dot blue), the trajectory planner or optimal reachable reference (continuous magenta) and the target reference (discontinuous red) in the z_1, z_2 plane. Figures 2.4, 2.5 show the trajectory of the ball on each axis. In these figures, it can be seen that the trajectory of the closed-loop system converges to the trajectory of the trajectory planner with zero error. This trajectory is the best trajectory that the ball can follow without violating the constraints. It can be seen that there exists a deviation between the trajectory of the planner and the target reference. For this reason the optimal cost of the optimization problem (2.3) is non zero. Figure 2.6 shows that the cost of the proposed controller converges to the cost of the trajectory planner in a non-increasing manner, demonstrating that the difference between both values is a Lyapunov function for the error between the state of the system and the trajectory planner state, as proved in Theorem 2.3.2.

In the second scenario, a short prediction horizon is chosen to demonstrate that the proposed controller has a large domain of attraction that has a low dependence on the prediction horizon N . In particular, for this scenario the prediction horizon is $N = 5$. The number of decision variables is $n_u \cdot (N + T) + n_x = 74$. In addition, in order to prove that recursive feasibility is not lost even in the presence of a sudden change in the target reference, in this scenario the reference switches between two geometric figures. First the ball must draw a rectangle of size $6 \times 4 \text{ cm}$ and is centered in $(4, 5) \text{ cm}$ with a speed of $11.43 \frac{\text{cm}}{\text{s}}$. At time 2.8 seconds the reference changes in order to draw a circumference with center on $(-4, -4) \text{ cm}$ and a radius of 1 cm . The target speed of the second trajectory is $2.3 \frac{\text{cm}}{\text{s}}$. The period length of both references is the same, that is $T = 28$. The initial state of this scenario is the ball in equilibrium at $(z_1, z_2) = (-5, 5) \text{ cm}$.

This scenario shows that when the reference changes suddenly, the trajectory of the ball converges to the new trajectory of the planner satisfying the constraints and without losing feasibility even when the prediction horizon is much lower than the period length. Figure 2.7 shows the trajectories of z_1, z_2 for the closed loop system (dash-dot blue), the trajectory planner (continuous magenta) and the target reference (discontinuous red) in the z_1, z_2 plane. Figures 2.10, 2.11 show the trajectory of the ball on each axis. Figures 2.8, 2.9 show the temporal evolution of the accelerations and that the constraints on the input were satisfied at all times. In these figures, it can be seen that the trajectory of the closed-loop system converges to the optimal reachable reference trajectories with zero error, first to the trajectory planner of the rectangle, and then to the trajectory planner of the circle. All these figures show a sudden change in when the reference switches from the rectangle to the circle. It can be seen that there exists a deviation between the trajectory of the planner and the target reference for the rectangle, but that the error is zero for the circle reference, which is reachable. For this reason the optimal cost of the optimization problem 2.3 is non zero for the rectangle and zero for the circle. Figure 2.6 shows that the cost of the proposed controller converges to the cost of the trajectory planners in a non-increasing manner, demonstrating that the difference between both values increases suddenly when the reference changes, but that then it converges again to the new optimal trajectory planner cost. It is important to remark, that when the target reference changes, all the state variables are far away from the optimal reachable reference, and that they take more than 5 time steps to reach it, however, the MPC maintains feasibility as proved in

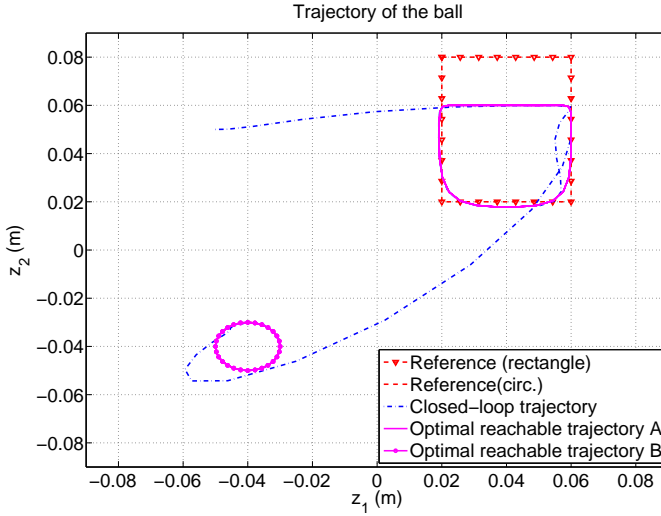


Figure 2.7 Trajectories of z_1, z_2 for the closed loop system (dash-dot blue), the trajectory planner (continuous magenta) and the target reference (discontinuous red) (scenario 2).

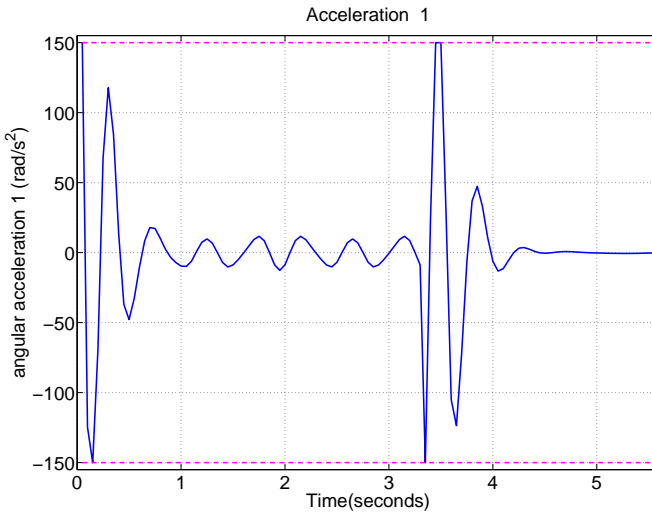


Figure 2.8 Trajectories of $\ddot{\theta}_1$ for the closed loop system (blue). The constraints are shown in red (scenario 2).

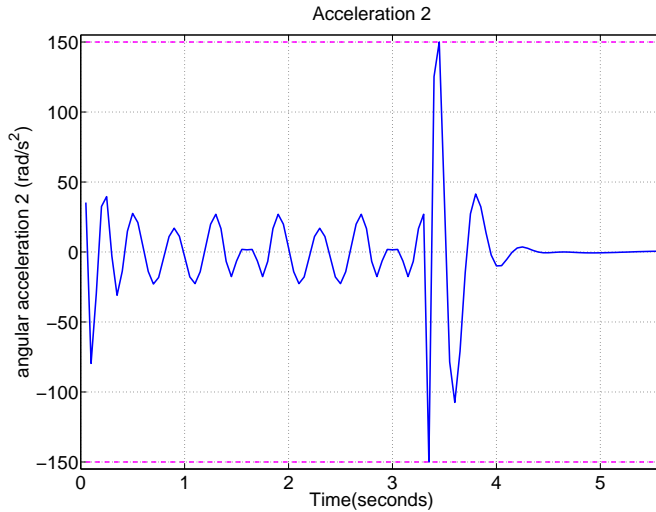


Figure 2.9 Trajectories of $\ddot{\theta}_2$ for the closed loop system (blue). The constraints are shown in red (scenario 2).

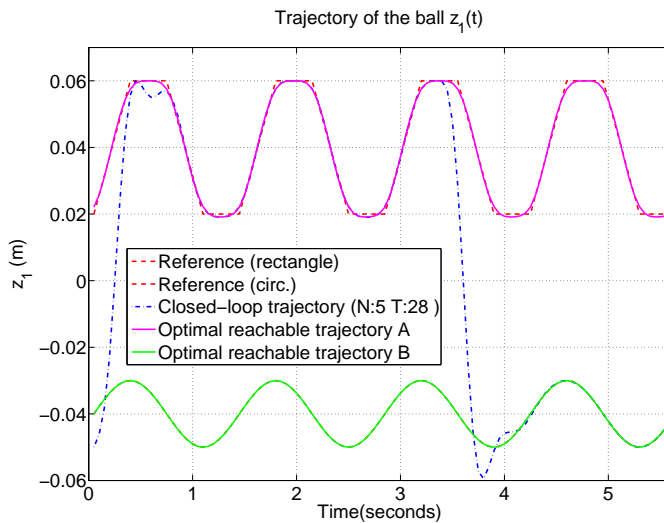


Figure 2.10 Trajectories of z_1 for the closed loop system (dash-dot blue), the trajectory planner (continuous magenta) and the target reference (discontinuous red) (scenario 2).

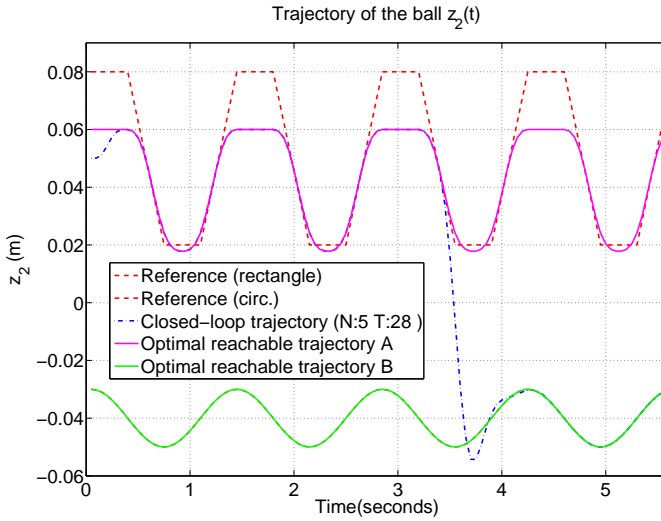


Figure 2.11 Trajectories of z_2 for the closed loop system (dash-dot blue), the trajectory planner (continuous magenta) and the target reference (discontinuous red) (scenario 2).

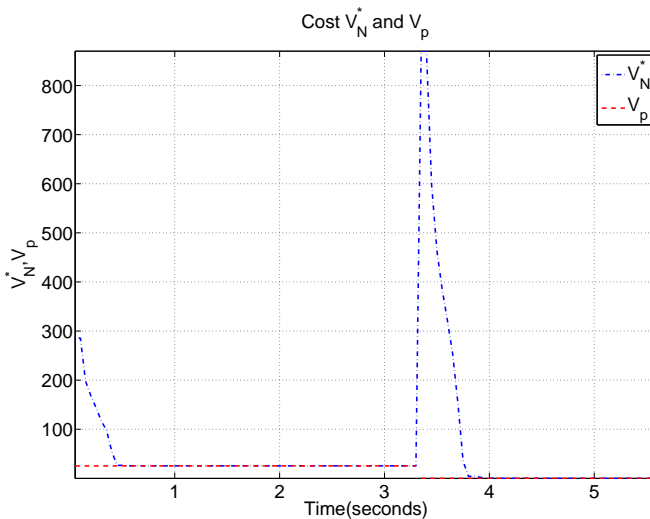


Figure 2.12 Trajectories of the optimal cost V_N^* (discontinuous blue) and trajectory planner cost V_p^o (discontinuous red) (scenario 1).

Theorem 2.3.2.

3 Economic MPC for changing periodic operation

If we knew what it was we were doing, it would not be called research, would it?

ALBERT EINSTEIN

As it was shown in chapter 2, the economic operation of a plant is typically based on a two-layer control structure, where the economically optimal trajectory of the plant is calculated and provided as the target to the predictive controller. The economic cost function typically depends on exogenous parameters, such as unitary prices or expected demands, that may be changed throughout the operation of the plant. When these parameters are changed, then the optimal trajectory must be recalculated and submitted to the MPC for tracking periodic references.

In particular, in this chapter is considered the economic periodic operation of constrained linear systems. Thus we propose an economic model predictive controller based on a single layer that unites dynamic real time optimization and control following the idea of Zanin et al. (2002). Then the two layer approach may lead to a loose of optimality. The proposed control scheme is shown in figure 3.1 where it can be seen that the inputs are the external economic parameters of which depend the economic cost function, and not a target trajectory as in figure 2.1.

The proposed controller guarantees closed-loop convergence to the *optimal periodic reachable trajectory* that minimizes average operation cost for a given economic criterion. In addition of guaranteeing stability, convergence to the optimal periodic reachable trajectory, recursive feasibility and constraint satisfaction, if the economic cost function is changed, recursive feasibility and convergence to the new optimal periodic reachable trajectory continue been guaranteed. The results are demonstrated with two simulation examples, a four tank system, and a simplified model of a section of Barcelona's water distribution network (see Ocampo-Martinez et al. (2013)).

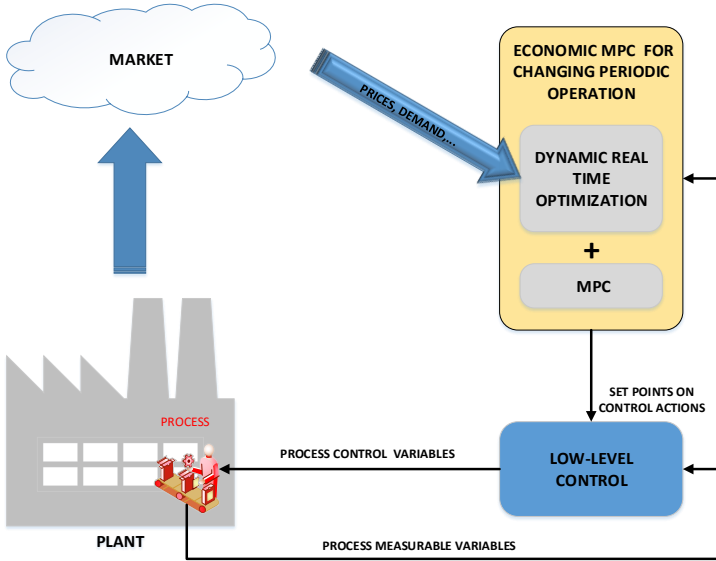


Figure 3.1 Hierarchical control structure of the economic periodic model predictive control.

The results of this chapter have been published in Limon et al. (2014).

3.1 Problem formulation

In this work we focus of the following class of time-varying linear systems

$$x(k+1) = A(k)x(k) + B(k)u(k) + w(k) \tag{3.1}$$

where $x(k) \in \mathbb{R}^n$, $u(k) \in \mathbb{R}^m$ and $w(k) \in \mathbb{R}^n$ are the state, input and disturbance vectors of the system at time step k respectively. The evolution of the matrices $A(k)$ and $B(k)$ as well as the disturbance signal $w(k)$ are known.

The dynamic model can be considered as a time varying affine system denoted as

$$x(k+1) = f(k,x(k),u(k)) \tag{3.2}$$

with $f(k,x,u) = A(k)x + B(k)u + w(k)$.

The state and input must satisfy the following constraints

$$(x(k),u(k)) \in \mathcal{Z}(k) \subseteq \mathbb{R}^{n+m} \tag{3.3}$$

where $\mathcal{Z}(k)$ is a closed convex polyhedron that may vary in time. It is assumed that $\mathcal{Z}(k)$ is known and contains the origin in its interior.

The performance of the evolution of the plant is measured by an economic stage cost function $\ell(k,x,u,p)$ that depends on the current state and input of the plant, on the time and on a set of exogenous parameters p . The value of exogenous parameter p may be changed during the operation of the plant and this variation is not known a priori. This function is assumed to be positive $\ell(k,x,u,p) \geq 0$ for all (k,x,u,p) and convex in (x,u) for all k and p .

We focus on the periodic operation of a closed-loop system with a fixed period T . The periodic behaviour may be a consequence of the time-varying system dynamics, the exogenous disturbances, the constraints and/or the time varying economic stage cost function. Thus, these functions are considered to be periodic, as it is stated in the following assumption.

Assumption 3.1.1 *The system is periodic and its period is T . That is, for all k , the following equations hold for all $(x,u) \in \mathcal{Z}(k)$ and p*

$$\begin{aligned} A(k) &= A(k+T) \\ B(k) &= B(k+T) \\ w(k) &= w(k+T) \\ \mathcal{Z}(k) &= \mathcal{Z}(k+T) \\ \ell(k,x,u,p) &= \ell(k+T,x,u,p) \end{aligned}$$

3.1.1 Economically optimal periodic operation

The main objective of the control system is to operate the plant to achieve an optimal economic performance. This performance cost function is typically posed the average of the economic cost function of the closed-loop system trajectories, that is

$$L_\infty(0,x(0),\mathbf{u}_\infty(0),p) = \lim_{M \rightarrow \infty} \frac{1}{M} \sum_{j=0}^{M-1} \ell(j,x(j),u(j),p)$$

where $x(0)$ is the initial state and $\mathbf{u}_\infty(0)$ is corresponding closed-loop input trajectories.

The optimal trajectory in which the system could be operated $(\mathbf{x}_\infty^*, \mathbf{u}_\infty^*)$ is derived from the solution of the following optimization problem in which the initial state is a free variable

$$\min_{x(0), \mathbf{u}_\infty} L_\infty(0,x(0),\mathbf{u}_\infty,p) \quad (3.4a)$$

$$s.t. \quad x(j+1) = f(j,x(j),u(j)), \quad (3.4b)$$

$$(x(j),u(j)) \in \mathcal{Z}_r(j), \quad \forall j \geq 0, \quad (3.4c)$$

where the set $\mathcal{L}_r(j)$ is a closed polyhedron contained into the relative interior of $\mathcal{L}(j)$ in order to ensure that the constraint $\mathcal{L}(j)$ is not active in the optimal trajectory¹.

The optimal state and input trajectories are \mathbf{x}_∞^* and \mathbf{u}_∞^* respectively. It is assumed that the solution of the optimization problem (3.4), and therefore the optimal trajectory, is unique for a given p . The optimal economic cost function is denoted as $L_\infty^*(p)$. Notice that this optimal trajectories depend on the value of the exogenous parameter p . This dependence will be emphasized by denoting the optimal trajectories as $\mathbf{x}_\infty^*(p)$ and $\mathbf{u}_\infty^*(p)$.

In general, problem (3.4) has an infinite number of decision variables, however given the periodic nature of the dynamics, the constraints, the cost function, and the assumption of uniqueness of the solution, the optimal trajectories can be obtained solving a finite horizon open-loop problem that optimizes the average cost of a period Angeli et al. (2012). In particular, the optimal solution can be obtained from the solution of the following optimization problem at any given time instant k , which we denote as $P_{DRTO}(k,p)$:

$$\mathcal{L}_T^o(k,p) = \min_{x(0), \mathbf{u}_T} \sum_{j=0}^{T-1} \ell(k+j, x(j), u(j), p) \quad (3.5a)$$

$$s.t. \quad x(j+1) = f(k+j, x(j), u(j)) \quad (3.5b)$$

$$(x(j), u(j)) \in \mathcal{L}(k+j), \quad j \in \mathbb{I}_{[0, T-1]} \quad (3.5c)$$

$$x(0) = x(T) \quad (3.5d)$$

This is the so-called dynamic real-time optimization problem and it is used in practice to adapt the optimal trajectories to possible variations on exogenous signals such as p .

Theorem 3.1.1 *The optimal solution $P_{DRTO}(k,p)$ satisfies the following equations*

$$x^o(j;k) = x^*(k+j)$$

$$u^o(j;k) = u^*(k+j)$$

$$\mathcal{L}_T^o(k,p) = \mathcal{L}_T^o(0,p) = TL_\infty^*(p)$$

Proof. Let us assume that $k \in \mathbb{I}_{[0, T-1]}$, then the solution $x(0;k) = x^o(1; k-1)$ and $u(j;k) = u^o(j+1; k-1)$ for $j \in \mathbb{I}_{[0, T-2]}$ and $u(T-1;k) = u^o(0; k-1)$ is a feasible solution of $P_{DRTO}(k,p)$. The cost function of this feasible solution is equal to the optimal cost function of $P_{DRTO}(k-1,p)$, $\mathcal{L}_T^o(k-1,p)$, and then, from optimality we have that $\mathcal{L}_T^o(k,p) \leq \mathcal{L}_T^o(k-1,p)$. Then it holds that

$$\mathcal{L}_T^o(T,p) \leq \mathcal{L}_T^o(k,p) \leq \mathcal{L}_T^o(k-1,p) \leq \mathcal{L}_T^o(0,p)$$

Since the system is periodic, $\mathcal{L}_T^o(0,p) = \mathcal{L}_T^o(T,p)$ and $\mathcal{L}_T^o(k,p) = \mathcal{L}_T^o(0,p)$ for all k . ■

The infinite horizon optimal trajectory $(\mathbf{x}_\infty^*, \mathbf{u}_\infty^*)$ is obtained extending the obtained solution periodically. In general, the initial state of the system will be different to the

¹ This tighter set of constraints is added to avoid the possible loss of controllability due to the existence of active constraints. This is not a limitation from a practical point of view since this set can be chosen arbitrarily close to the real constraint set.

corresponding state of the optimal trajectory. The control objective is to derive a control law $u(k) = \kappa(k, x(k), p)$ such that the evolution of the closed-loop system

$$x(k+1) = f(k, x(k), \kappa(k, x(k), p))$$

fulfils the constraints (3.3) and the average economic performance is asymptotically minimized, that is, $(x(k), u(k))$ converges to $(x^*(k; p), u^*(k; p))$.

3.2 Economic MPC for changing periodic operation

The proposed predictive controller combines the dynamic real time optimization and the control decision in a single optimization problem. To this aim an artificial periodic trajectory is added as a new decision variable. The cost function is then a sum of two terms: (i) a tracking term that penalizes the deviation between the predicted trajectory and the artificial periodic trajectory and (ii) an economic term that measures the economic cost function of the artificial periodic trajectory. The cost function of the controller optimization problem is defined as follows:

$$\begin{aligned} V_N(k, x, p, \bar{\mathbf{u}}_N, x^a(0), \mathbf{u}_T^a) &= \sum_{i=0}^{N-1} \|\bar{x}(i) - x^a(i)\|_Q^2 + \|\bar{u}(i) - u^a(i)\|_R^2 \\ &+ \sum_{j=0}^{T-1} \ell(k+j, x^a(j), u^a(j), p) \end{aligned}$$

where N is the prediction horizon and T is the period of the system. It is assumed that $N \leq T$.

The control law is derived from the solution of following optimization problem $P_N(k, x, p)$:

$$\min_{\bar{\mathbf{u}}_N, x^a(0), \mathbf{u}_T^a} V_N(k, x, p, \bar{\mathbf{u}}_N, x^a(0), \mathbf{u}_T^a) \quad (3.6a)$$

$$s.t. \quad \bar{x}(0) = x \quad (3.6b)$$

$$\bar{x}(i+1) = f(k+i, \bar{x}(i), \bar{u}(i)) \quad (3.6c)$$

$$(\bar{x}(i), \bar{u}(i)) \in \mathcal{Z}(k+i), \quad i \in \mathbb{I}_{[0, N-1]} \quad (3.6d)$$

$$x^a(j+1) = f(k+j, x^a(j), u^a(j)) \quad (3.6e)$$

$$(x^a(j), u^a(j)) \in \mathcal{Z}^r(k+j), \quad j \in \mathbb{I}_{[0, T-1]} \quad (3.6f)$$

$$x^a(0) = x^a(T) \quad (3.6g)$$

$$\bar{x}(N) = x^a(N) \quad (3.6h)$$

where $\bar{\mathbf{u}}_N$ is the predicted input trajectory and (x_0^a, \mathbf{u}_T^a) are the artificial initial state and input trajectories respectively.

Constraints (3.6b)-(3.6d) guarantee that the predicted trajectory of the system is admissible. The set of constraints on the artificial periodic trajectory (3.6e)-(3.6g) are identical to the constraints of the DRTO optimization problem (3.5), and guarantee that this trajectory is admissible and periodic. The terminal constraint (3.6h) forces the predicted trajectory to reach the artificial trajectory in N steps.

$P_N(k,x,p)$ is a convex optimization problem in which the cost function is convex and the constraints are linear. This problem can be efficiently solved using specialized algorithms such as interior point methods Boyd and Vandenberghe (2004). The optimal solution is denoted $(\bar{\mathbf{u}}_N^o, x^{ao}(0), \mathbf{u}_T^{ao})$ and it is assumed to be unique for a given p . The proposed control law is derived from the receding horizon policy

$$u(k) = \bar{u}^o(0) = \kappa(k,x,p)$$

Notice that the set of constraints (3.6b)-(3.6h) does not depend on the exogenous parameter p . This implies that a change of the value of p cannot cause a loss of feasibility of the optimization problem. Indeed, a change on the economic stage cost function affects only the cost function of the optimization problem. The set of states where the optimization problem $P_N(k,x,p)$ is feasible is denoted as $X_N(k)$. The set of feasible initial states $X_N(0)$ will be denoted as X_N .

We will prove next the following properties of the proposed controller: (i) if the initial state is such that $P_N(0,x(0),p(0))$ is feasible, then all the subsequent optimization problems $P_N(k,x(k),p(k))$ will be feasible even in the case that the parameter p is changed and (ii) the optimal trajectory is an asymptotically stable trajectory of the closed-loop system in the Lyapunov sense.

Before stating the main theorem of this chapter the notion of stability is introduced and a Lyapunov sufficient condition is shown.

3.2.1 Lyapunov asymptotic stability of a periodic trajectory

Consider a closed-loop system given by

$$x(k+1) = f(k,x(k),\kappa(k,x(k))) = f_\kappa(k,x(k)) \quad (3.7)$$

subject to the constraints $x(k) \in \mathcal{X}_\kappa(k) = \{x : (x,\kappa(x)) \in \mathcal{Z}\}$. Assume that the trajectory $x_t(k)$ is a trajectory of system (3.7) such that $x_t(k) \in X_{\kappa_r}(k)$, where $X_{\kappa_r}(k)$ is the relative interior of $X_\kappa(k)$.

A Lyapunov stability notion is adopted: the state $x(k)$ converges to the optimal trajectory $x_t(k)$ and, near the optimal trajectory, small changes in the initial state $x(0)$ cause small changes in the subsequent trajectory. Denoting the tracking error as follows

$$e(k) = x(k) - x_t(k)$$

the trajectory $x_t(k)$ is an asymptotic stable trajectory of the system if there exists a set of initial states Γ and a \mathcal{KL} function², $\beta(\cdot, \cdot)$, such that for all $x(0) \in \Gamma$, then

$$\|e(k)\| \leq \beta(\|e(0)\|, k)$$

and $x(k) \in X_{\kappa}(k)$ for all k .

Asymptotic stability can be proved by the conditions of the following theorem.

Theorem 3.2.1 *Let $\Omega(k)$ be a closed set that contains $x_t(k)$ in its interior, and is contained in $X_{\kappa}(k)$, such that for all $x(k) \in \Omega(k)$, then $x(k+1) \in \Omega(k+1)$. Assume that there exists a continuous function $W(k, x) : \mathbb{R} \times \mathbb{R}^n \rightarrow \mathbb{R}$ such that*

$$W(k, x(k)) \geq \alpha_1(\|e(k)\|), \quad \forall x(k) \in \Omega(k) \quad (3.8a)$$

$$W(k, x(k)) \leq \alpha_2(\|e(k)\|), \quad \forall e(k) \in B_r \quad (3.8b)$$

$$W(k+1, x(k+1)) - W(k, x(k)) \leq -\alpha_3(\|e(k)\|), \quad \forall x(k) \in \Omega(k) \quad (3.8c)$$

where $\alpha_i(\cdot)$ are \mathcal{K}_{∞} functions and B_r is a neighborhood of the origin $B_r = \{z : \|z\| \leq r\}$. Then $x_t(k)$ is an asymptotic stable trajectory of the system (3.7) for all $x(0) \in \Omega(0)$.

Proof. Since $W(k, x)$ is continuous and $x_t(k)$ is contained in the interior of $\Omega(k)$, by means of Proposition 2 of the postface to the book Rawlings and Mayne (2009), there exists a \mathcal{K}_{∞} function $\tilde{\alpha}_2(\cdot)$ such that

$$W(k, x(k)) \leq \tilde{\alpha}_2(\|e(k)\|), \quad \forall x(k) \in \Omega(k)$$

Notice that this implies that $\|e(k)\| \geq \tilde{\alpha}_2^{-1}(W(k, x(k)))$ and then

$$\begin{aligned} W(k+1, x(k+1)) &\leq W(k, x(k)) - \alpha_3(\tilde{\alpha}_2^{-1}(W(k, x(k)))) \\ &\leq \phi(W(k, x(k))) \end{aligned}$$

where $\phi(\cdot)$ is a certain \mathcal{K}_{∞} function such that $\phi(s) < s$ for all $s > 0$ (see Jiang and Wang (2001)). From this inequality we have that

$$\alpha_1(\|e(k)\|) \leq W(k, x(k)) \leq \phi^k(W(0, x(0))) \leq \phi^k(\tilde{\alpha}_2(\|e(0)\|))$$

where $\phi^k(s)$ is the k -th composition of function $\phi(\cdot)$, that is, $\phi^k(s) = \phi^{k-1}(\phi(s))$ with $\phi^0(s) = s$.

Taking into account that $\beta(s, t) = \alpha_1^{-1}(\phi^t(\tilde{\alpha}_2(s)))$ is a \mathcal{KL} function (see Limon et al. (2006a)), then

$$\|e(k)\| \leq \beta(\|e(0)\|, k)$$

for all $x(0) \in \Omega(0)$. On the other hand, by definition $x(k) \in \Omega(k) \subseteq X_{\kappa}(k)$. ■

² A function $\beta(s, t)$ is a \mathcal{KL} function if $\beta(\cdot, t)$ is a \mathcal{K}_{∞} function for all $t \geq 0$ and if $\beta(s, \cdot)$ is strictly decreasing converging to zero for all $s > 0$.

Once the stability framework is defined, then the stability properties of the proposed controller are stated in the following section.

3.2.2 Stabilizing design of the proposed controller

Asymptotic stability of the optimal trajectory for system 3.1 controlled by the proposed controller will be proved defining a function based on the optimal cost function $V_N^o(k, x, p)$ of problem $P_N(k, x, p)$ that serves as Lyapunov function. To this aim, the following controllability condition on the system is assumed.

Assumption 3.2.1 For integers $0 \leq i \leq j \leq T$, let define

$$\Psi(j, i) = A(j) \cdot A(j-1) \cdots A(i+1)B(i).$$

Then it is assumed that there exists an integer n_c such that the matrix

$$[\Psi(n_c - 1, 0), \cdots, \Psi(n_c - 1, n_c - 2), B(n_c - 1)]$$

is full row rank.

Furthermore, it is necessary to remark that in virtue of theorem C.34 in Rawlings and Mayne (2009) the optimal cost function $V_N^o(k, x, p)$ is a continuous function in x .

We present next the main theorem of this chapter:

Theorem 3.2.2 Let $\mathbf{x}_\infty^*(p)$ and $\mathbf{u}_\infty^*(p)$ be the economically optimal trajectory of the system derived from (3.4), let the prediction horizon N be equal to or larger than the integer n_c defined in Assumption 3.2.1 and let Q be a positive definite function, then the system controlled by the proposed control law is recursively feasible and the optimal trajectory is asymptotic stable for all feasible initial state, i.e. $x(0) \in X_N$.

Proof. First it will be proved that the optimization problem is recursively feasible and then the convergence of the closed-loop system will be shown.

Feasibility will be proved by recursion. Consider that the optimization problem is feasible at time instant k , i.e. $x(k) \in X_N(k)$. Let $\bar{\mathbf{u}}_N^o(k)$, $x_0^{ao}(k)$ and $\mathbf{u}_T^{ao}(k)$ be the optimal solution at sample k and let define the following solutions for the next sampling time $k+1$,

$$\begin{aligned} \bar{\mathbf{u}}_N(k+1) &= (u^o(1; k), \cdots, u^o(N-1; k), u^{ao}(N; k)) \\ x^a(0; k+1) &= x^{ao}(1; k) \\ \mathbf{u}_T^a(k+1) &= (u^{ao}(1; k), \cdots, u^{ao}(T-1; k), u^{ao}(0; k)). \end{aligned}$$

Taking into account that $\bar{x}^o(N; k) = x^{ao}(N; k)$, that the artificial trajectory is periodic, i.e. $x^{ao}(0; k) = x^{ao}(T; k)$ and considering that $x(k+1) = \bar{x}^o(1; k)$, then the predicted trajectories are

$$\begin{aligned} \bar{\mathbf{x}}_{N+1}(k+1) &= (\bar{x}^o(1; k), \cdots, \bar{x}^o(N-1; k), x^{ao}(N; k), x^{ao}(N+1; k)) \\ \mathbf{x}_{T+1}^a(k+1) &= (x^{ao}(1; k), \cdots, x^{ao}(T-1; k), x^{ao}(0; k), x^{ao}(1; k)) \end{aligned}$$

From the definition of the optimization problem constraints and taking into account that the optimal solution at time k is feasible, it can be proved that the aforementioned defined trajectory is feasible for time step $k + 1$, and hence that $x(k + 1) \in X_N(k + 1)$.

Taking into account that $x(0) \in X_N$, this implies that $x(k) \in X_N(k)$ for all k . Asymptotic stability will be proved demonstrating that the function

$$W(k, x) = V_N^o(k, x, p) - TL_\infty^*(p)$$

is a Lyapunov function for the optimal trajectory $\mathbf{x}_\infty^*(p)$ and satisfies the assumptions of Theorem 3.2.1. Let denote the error signal

$$e(k) = x(k) - x^*(k; p)$$

Next the following statements are proved:

- (1) $W(k, x(k)) \geq \alpha_1(\|e(k)\|)$ for all $x(k) \in X_N(k)$

From the definition of the Lyapunov function we have that

$$W(k, x(k)) \geq \|x(k) - x^{ao}(0; k)\|_Q^2 + TL_T(k, x^{ao}(0; k), \mathbf{u}_T^{ao}(k), p) - TL_\infty(p)$$

From the convexity and uniqueness of $P_{DRT0}(k, p)$ we have have that there exists a \mathcal{H}_∞ function $\pi_1(\cdot)$ such that

$$L_T(k, x^{ao}(0; k), \mathbf{u}_T^{ao}(k), p) \geq L_\infty(p) + \pi_1(\|x^{ao}(0; k) - x^*(k; p)\|)$$

and then in virtue of the properties of the \mathcal{H} functions we have that

$$\begin{aligned} W(k, x(k)) &\geq \|x(k) - x^{ao}(0; k)\|_Q^2 + T\pi_1(\|x^{ao}(0; k) - x^*(k; p)\|) \\ &\geq \alpha_1(\|x(k) - x^{ao}(0; k)\| + \|x^{ao}(0; k) - x^*(k; p)\|) \\ &\geq \alpha_1(\|x(k) - x^*(k; p)\|) \end{aligned}$$

for a some \mathcal{H}_∞ function $\alpha_1(\cdot)$.

- (2) $W(k, x(k)) \leq \alpha_2(\|e(k)\|)$ for all $e(k) \in B_\varepsilon$:

From the lemma 3.2.3 we have that $W(k, x(k)) \leq \alpha_2(\|x(k) - x^*(k; p)\|)$ for all $\|x(k) - x^*(k; p)\| \leq \varepsilon$, for a certain $\varepsilon > 0$.

- (3) $W(k + 1, x(k + 1)) - W(k, x(k)) \leq -\alpha_3(\|e(k)\|)$ for all $x(k) \in X_N(k)$:

Denoting $J^o(k) = V_N^o(k, x(k), p)$ and

$$J(k + 1) = V_N(k + 1, x(k + 1), p, \bar{\mathbf{u}}_N(k + 1), x_0^a(k + 1), \mathbf{u}_T^a(k + 1))$$

and taking into account the definition of the proposed feasible solution at $k + 1$ we have that

$$\begin{aligned} J(k+1) - J^o(k) &= -\|x(k) - x^a(0)\|_Q^2 - \|u(k) - u^a(0)\|_R^2 \\ &+ \ell(k+T, x^{ao}(0;k), u^{ao}(0;k), p) \\ &- \ell(k, x^{ao}(0;k), u^{ao}(0;k), p) \end{aligned}$$

Since the economic cost function is periodic, and considering the optimality of the solution, we have that

$$J^o(k+1) - J^o(k) \leq -\|x(k) - x^{ao}(0;k)\|_Q^2 - \|u(k) - u^{ao}(0;k)\|_R^2$$

From the definition of the Lyapunov function, it can be deduced that

$$W(k+1, x(k+1)) - W(k, x(k)) \leq -\|x(k) - x^{ao}(0;k)\|_Q^2$$

This means that the increment of $W(k, x(k))$ is a function of the difference between the state and the artificial state. In virtue of lemma 3.2.2 we have that this difference is a measure of the tracking error $e(k)$. That is, there exists a \mathcal{K}_∞ function $\alpha_3(\cdot)$ such that

$$\|x(k) - x^{ao}(0;k)\|_Q^2 \geq \alpha_3(\|e(k)\|).$$

Then we have that

$$W(k+1, x(k+1)) - W(k, x(k)) \leq -\alpha_3(\|e(k)\|)$$

This proves that $W(k, x(k))$ is a Lyapunov function and in virtue of theorem 3.2.2 for $\Omega(k) = X_N(k)$ and implies that the optimal trajectory is asymptotic stable. \blacksquare

Technical lemmata

This proof is based in three technical lemmas. The first one is the most important and states that if the system reaches the optimal artificial trajectory, i.e. $x(k) = x^{ao}(0;k,p)$, then the artificial trajectory has also reached the optimal trajectory, that is $\mathbf{x}_T^{ao}(k,p) = \mathbf{x}_T^*(k)$.

Lemma 3.2.1 *Let $x(k)$ be such that the solution of the optimization problem $P_N(k, x(k), p)$ satisfies $x(k) = x^{ao}(0;k)$, then $\bar{\mathbf{x}}_T^o(k) = \mathbf{x}_T^{ao}(k,p) = \mathbf{x}_T^*(k)$ and $\bar{\mathbf{u}}_T^o(k) = \mathbf{u}_T^{ao}(k,p) = \mathbf{u}_T^*(k)$.*

Proof. The proof will be done by contradiction. Assume that $(\bar{\mathbf{x}}_T^o, \bar{\mathbf{u}}_T^o)$ is not the optimal trajectory $(\mathbf{x}_T^*(k), \mathbf{u}_T^*(k))$, then from the uniqueness of 3.4 we have that

$$\sum_{j=0}^{T-1} \ell(k+j, x^{ao}(j), u^{ao}(j), p) > TL_\infty(p)$$

Let denote the sequences

$$(\hat{\mathbf{x}}_T^a(k), \hat{\mathbf{u}}_T^a(k)) = \beta(\mathbf{x}_T^{ao}(k), \mathbf{u}_T^{ao}(k)) + (1-\beta)(\mathbf{x}_T^*(k), \mathbf{u}_T^*(k))$$

where $\beta \in (0, 1]$.

Since $(\mathbf{x}_T^{ao}(k), \mathbf{u}_T^{ao}(k))$ and $(\mathbf{x}_T^*(k), \mathbf{u}_T^*(k))$ satisfy constraints (3.6e)-(3.6g), by convexity $(\hat{\mathbf{x}}_T^a(k), \hat{\mathbf{u}}_T^a(k))$ also satisfy them.

The controllability assumption 3.2.1 ensures that there exists a sequence of control actions

$$\hat{\mathbf{u}}_N(k) = M(k)(x(k) - \hat{x}^a(k)) + \hat{\mathbf{u}}_N^a(k)$$

for a suitable matrix $M(k)$, such that reaches $\hat{x}^a(k+N)$ in N steps.

Because the optimal trajectory $\mathbf{x}_\infty^*(p)$ and $\mathbf{u}_\infty^*(p)$ is contained in the relative interior of the constraint set, a β arbitrarily close to 1 can be found such that the resulting trajectory satisfies constraints (3.6b)-(3.6d) and (3.6h). Therefore the triplet $(\hat{\mathbf{u}}_N(k), \hat{x}^a(0;k), \hat{\mathbf{u}}_T^a(k))$ is a feasible solution of $P_N(k, x(k), p)$. The cost associated to this feasible solution is denoted as $\hat{V}_N(k)$ and satisfies that

$$\hat{V}_N(k) = \|x(k) - x^*(k; p)\|_{H(k)}^2 + \sum_{j=0}^{T-1} \ell(k+j, \hat{x}^a(j;k), \hat{u}^a(j;k), p)$$

for a certain matrix $H(k)$. Taking a constant λ_H as the maximum eigenvalue of $H(j)$ for all $j \in \mathbb{I}_{[0, T-1]}$ and considering the optimality of the solution we have that

$$\hat{V}_N(k) \leq \lambda_H \|x(k) - \hat{x}^a(0;k)\|^2 + \sum_{j=0}^{T-1} \ell(k+j, \hat{x}^a(j;k), \hat{u}^a(j;k), p) \quad (3.9)$$

From the optimality of the solution this cost is such that $\hat{V}_N(k) \geq V_N^o(k; x(k), p)$. Since the optimal solution at $x(k) = x^{ao}(0;k)$ is $(\mathbf{u}_N^{ao}, x^{ao}(0;k), \mathbf{u}_N^{ao})$ we have that

$$V_N^o(k; x(k), p) = \sum_{j=0}^{T-1} \ell(k+j, x^{ao}(j;k), u^{ao}(j;k), p)$$

and then

$$\hat{V}_N(k) \geq \sum_{j=0}^{T-1} \ell(k+j, x^{ao}(j;k), u^{ao}(j;k), p) \quad (3.10)$$

On the other hand, from the definition of $(\hat{\mathbf{x}}_T^a(k), \hat{\mathbf{u}}_T^a(k))$ and taking into account that $x(k) = x^{ao}(0;k)$, we have that

$$x(k) - \hat{x}^a(0;k) = (1 - \beta)(x(k) - x^*(k))$$

Besides, from the convexity of $\ell(k, x, u, p)$ we have that $\sum_{j=0}^{T-1} \ell(k+j, \hat{x}^a(j;k), \hat{u}^a(j;k), p)$ is less than or equal to

$$\beta \sum_{j=0}^{T-1} \ell(k+j, x^{ao}(j;k), u^{ao}(j;k), p) + (1 - \beta)TL_\infty(p) \quad (3.11)$$

Using (3.9) and (3.11) the following inequality is obtained:

$$\begin{aligned}\hat{V}_N(k) &\leq (1-\beta)^2 \lambda_H \|x(k) - x^*(k)\|^2 \\ &\quad + \beta \sum_{j=0}^{T-1} \ell(k+j, x^{ao}(j;k), u^{ao}(j;k), p) \\ &\quad + (1-\beta) TL_\infty(p)\end{aligned}$$

The right hand side of this inequality will be denoted as $F(\beta)$. This function is such that

$$F(1) = \sum_{j=0}^{T-1} \ell(k+j, x^{ao}(j;k), u^{ao}(j;k), p)$$

and hence, from (3.10) we have that $F(\beta) \geq F(1)$. Taking the partial of $F(\cdot)$ with respect to β function we have that

$$\frac{\partial F}{\partial \beta} = -2(1-\beta) \lambda_H \|x(k) - x^*(k)\|^2 + \sum_{j=0}^{T-1} \ell(k+j, x^{ao}(j;k), u^{ao}(j;k), p) - TL_\infty(p)$$

Evaluating this derivative at $\beta = 1$

$$\left. \frac{\partial F}{\partial \beta} \right|_{\beta=1} = \sum_{j=0}^{T-1} \ell(k+j, x^{ao}(j;k), u^{ao}(j;k), p) - TL_\infty(p)$$

From the initial assumption we have that

$$\left. \frac{\partial F}{\partial \beta} \right|_{\beta=1} > 0$$

Then there exists a β arbitrarily close to one such that $F(\beta) < F(1)$. Summarizing we have proved that for a certain β ,

$$F(1) \leq F(\beta) < F(1)$$

which is a contradiction and hence, the lemma is proved. ■

The following two lemmas are necessary to derive the bounds of the Lyapunov function.

Lemma 3.2.2 *Consider that $x(0) \in X_N$, then the optimal solution at each sampling time is such that there exists a \mathcal{H}_∞ function θ such that*

$$\|x(k) - x^{ao}(0;k)\| \geq \theta(\|x(k) - x^*(k)\|)$$

Proof. First we will prove that

$$\|x(k) - x^{ao}(0;k)\| = 0$$

if and only if $\|x(k) - x^*(k)\| = 0$. If $\|x(k) - x^{ao}(0; k)\| = 0$, then thanks to the lemma 3.2.1, we infer that $\|x(k) - x^*(k)\|$ is zero.

On the other hand if $\|x(k) - x^*(k)\| = 0$, then the triplet $(\mathbf{u}_N^*(k), x^*(k), \mathbf{u}_T^*(k))$ is the optimal solution to the optimization problem and hence $\|x(k) - x^{ao}(0; k)\| = 0$.

As a consequence of this statement, it can be inferred that $\|x(k) - x^{ao}(0; k)\| > 0$ for all $\|x(k) - x^*(k)\| > 0$.

Finally the optimization problem $P_N(k, x, p)$ is a multi-parametric convex optimization problem and the optimizers are continuous functions of the state x defined in the compact set X_N Rockafellar (1970). Then $x^{ao}(0; k)$ is a continuous function of $x(k)$ and hence $x(k) - x^{ao}(0; k)$ is a continuous function of $x(k) - x^*(k)$.

From Vidyasagar (1993) we derive that there exists a \mathcal{K}_∞ function such that

$$\|x(k) - x^{ao}(0; k)\| \geq \theta(\|x(k) - x^*(k)\|) \quad \blacksquare$$

Lemma 3.2.3 *There exists a $\varepsilon > 0$ and a \mathcal{K}_∞ function $\alpha_2(\cdot)$ such that*

$$W(k, x(k)) \leq \alpha_2(\|x(k) - x^*(k)\|)$$

for all $\|x(k) - x^*(k)\| \leq \varepsilon$.

Proof. The controllability Assumption 3.2.1 ensures that there exists a sequence of control actions

$$\tilde{\mathbf{u}}_N(k) = M(k)(x(k) - x^*(k; p)) + \mathbf{u}_N^*(k; p)$$

for a suitable matrix $M(k)$, such that the resulting trajectory reaches $x^*(k + N; p)$ in N steps.

Furthermore, as the optimal trajectory $\mathbf{x}_\infty^*(p)$ and $\mathbf{u}_\infty^*(p)$ are contained in the relative interior of the constraint sets, then there exists a small enough positive number $\varepsilon > 0$ such that the resulting trajectory $\tilde{\mathbf{x}}_N(k)$ is admissible if $\|x(k) - x^*(k; p)\| \leq \varepsilon$.

Consequently the triplet $(\tilde{\mathbf{u}}_N(k), x^*(k), \mathbf{u}_T^*(k))$ is a feasible solution of $P_N(k, x(k), p)$ and the corresponding cost is

$$V_N(k, x(k), p, \tilde{\mathbf{u}}_N(k), x^*(k), \mathbf{u}_T^*(k)) = \|x(k) - x^*(k; p)\|_{H(k)}^2 + TL_\infty(k)$$

for a given matrix $H(k)$. Taking a constant λ_H as the maximum eigenvalue of $H(j)$ for all $j \in \mathbb{I}_{[0, T-1]}$ and considering the optimality of the solution we have that

$$V_N^o(k, x(k), p) \leq \lambda_H \|x(k) - x^*(k; p)\|^2 + TL_\infty(k)$$

and then

$$W(k, x(k)) \leq \lambda_H \|x(k) - x^*(k; p)\|^2$$

The lemma is proved taking $\alpha_2(s) = \lambda_H s^2$. \blacksquare

The proposed controller has a number of interesting properties:

1. The proposed controller guarantees convergence of the closed-loop system to the optimal trajectory $(\mathbf{x}_\infty^*(p), \mathbf{u}_\infty^*(p))$ and the calculation of this trajectory by a DRTO is not required.
2. The feasibility region of the optimization problem does not depend on the economic stage cost function. The proposed optimization problem is guaranteed to be recursively feasible even if the economic cost function changes (and hence, the corresponding optimal periodic trajectory). Besides, if the parameter p is varying and converges to a constant value p_∞ , the control law steers the system to the optimal trajectory $(\mathbf{x}_\infty^*(p_\infty), \mathbf{u}_\infty^*(p_\infty))$.
3. The proposed optimization problem is the minimization of a convex function subject to linear constraints that can be efficiently solved using specialized algorithms (Boyd and Vandenberghe, 2004). In fact, for some choices of economic cost functions, such as linear or quadratic functions, the optimization problem is a standard quadratic programming problem.
4. The domain of attraction of the proposed controller, X_N is in general very large and particularly, larger than the set of initial states that can reach a particular optimal trajectory $\mathbf{x}_\infty(p)$ in N steps.
5. The control law $\kappa_N(k, x(k), \mathbf{r}_k)$ is Lipschitz continuous with respect to the state $x(k)$. As the model is continuous, then the closed-loop system is input-to-state stable (ISS) with respect to additive disturbances (Limon et al., 2009b), whenever the evolution of the plant is admissible. This implies that the closed-loop system is robust to small variations of the disturbance signal $w(k)$ and/or the matrices $A(k)$, $B(k)$.
6. The proposed controller takes into account the economic cost of the transient, since the dynamic real time optimizer is integrated into the predictive controller. The artificial trajectory can be seen as a reachable periodic trajectory that minimizes the average cost function. This trajectory is updated at each sample time and converges to the optimal trajectory.

3.3 Application to a four tank plant

In this section we present the application of the proposed controller to the multivariable laboratory plant of four interconnected tanks with nonlinear dynamics and subject to operational state and input constraints presented in Alvarado (2007), see figure 3.2. The inputs are the water flows through the two pumps denoted q_a, q_b . The outputs are the water levels in the lower two tanks (h_1 and h_2) and the states of the model are the water levels of the four tanks (h_1, h_2, h_3 and h_4).

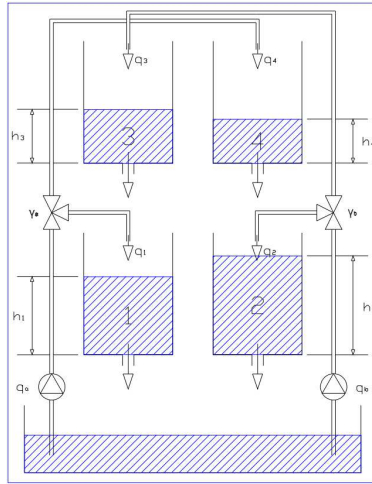


Figure 3.2 Four tank scheme.

The four tank plant can be approximated by the following nonlinear model (see Johansson (2000)):

$$\dot{h}_1 = -\frac{a_1}{A}\sqrt{2gh_1} + \frac{a_3}{A}\sqrt{2gh_3} + \frac{\gamma_1}{3600 \cdot A}q_a \quad (3.12a)$$

$$\dot{h}_2 = -\frac{a_2}{A}\sqrt{2gh_2} + \frac{a_4}{A}\sqrt{2gh_4} + \frac{\gamma_2}{3600 \cdot A}q_b \quad (3.12b)$$

$$\dot{h}_3 = -\frac{a_3}{A}\sqrt{2gh_3} + \frac{1-\gamma_2}{3600 \cdot A}q_a \quad (3.12c)$$

$$\dot{h}_4 = -\frac{a_4}{A}\sqrt{2gh_4} + \frac{1-\gamma_1}{3600 \cdot A}q_b \quad (3.12d)$$

subject to the following state and input constraints

$$\begin{aligned} Q_j^{\min} &\leq q_j \leq Q_j^{\max} & j = a, b \\ H_i^{\min} &\leq h_i \leq H_i^{\max} & i = 1, 2, 3, 4 \end{aligned}$$

where the values of the parameters of the system can be found in table 3.1. The nonlinear model will be used to carry out all the simulations of this section.

To apply the proposed controller, we will use a discrete time linear model obtained by linearizing the nonlinear model around the equilibrium point defined by h_i^o, q_j^o with $i = 1, 2, 3, 4$ and $j = a, b$, (see table 3.1). To reduce the steady linearization errors, the state of the linear model is defined as $x_i = \sqrt{h_i} - \sqrt{h_i^o}$ and inputs are defined as $u_j = q_j - q_j^o$ where $j = a, b$ and $i = 1, 2, 3, 4$. The linearized model has been discretized using the Tusting method with a sampling time of five seconds. The resulting matrices for the linear model

are the following:

$$A = \begin{pmatrix} 0.9419 & 0 & 0.0401 & 0 \\ 0 & 0.9334 & 0 & 0.0380 \\ 0 & 0 & 0.9587 & 0 \\ 0 & 0 & 0 & 0.9607 \end{pmatrix}; \quad B = \begin{pmatrix} 0.0083 & 0.0003 \\ 0.0004 & 0.0111 \\ 0 & 0.0168 \\ 0.0196 & 0 \end{pmatrix}$$

Note that in this application, the model is time invariant and disturbances are not taken into account.

Table 3.1 Parameters of the four tank plant.

	Value	Unit	Description
H_1^{max}	1.20	m	Maximum level of the tank 1
H_2^{max}	1.20	m	Maximum level of the tank 2
H_3^{max}	1.20	m	Maximum level of the tank 3
H_4^{max}	1.20	m	Maximum level of the tank 4
H_i^{min}	0.2	m	Minimum level of the tanks
Q_a^{max}	2.50	m^3/h	Maximal flow
Q_b^{max}	2.50	m^3/h	Maximal flow
Q_i^{min}	0	m^3/h	Minimal flow
a_1	$1.341e^{-4}$	m^2	Discharge constant of the tank 1
a_2	$1.533e^{-4}$	m^2	Discharge constant of the tank 2
a_3	$9.322e^{-5}$	m^2	Discharge constant of the tank 3
a_4	$9.061e^{-5}$	m^2	Discharge constant of the tank 4
A	0.03	m^2	Cross-section of all tanks
γ_a	0.3	n.u.	Parameter of the 3-ways valve
γ_b	0.4	n.u.	Parameter of the 3-ways valve
h_1^o	0.627	m	Equilibrium level tank 1
h_2^o	0.636	m	Equilibrium level tank 2
h_3^o	0.652	m	Equilibrium level tank 3
h_4^o	0.633	m	Equilibrium level tank 4
Q_a^o	1.6429	m^3/h	Equilibrium flow a
Q_b^o	2.0000	m^3/h	Equilibrium flow b

The economic cost function $\ell(k,x,u,p)$ is made of two terms. The first term penalizes the water flow through the pumps, while the second term is inversely proportional to the water stored in the lower tanks.

$$\ell(k,x,u,p) = (q_a(u)^2 + c(k)q_b(u)^2) + p \frac{V_{min}}{A(h_1(x) + h_2(x))}$$

where V_{min} is the minimum volume of water that can be stored in the lower two tanks, that is

$$V_{min} = A \cdot (H_1^{min} + H_2^{min})$$

The parameter $c(k)$ is the unitary cost of the cost of the flow q_b . This is time varying and its evolution is defined by the following periodic function with period 150 seconds:

$$c(k) = 0.15 \sin\left(\frac{2 \cdot \pi \cdot t}{30}\right) + 1 \quad t = 0, \dots, N_r - 1$$

The parameter p can change abruptly during operation, modeling a different economic criterion. In this case study, we consider two scenarios: In the first scenario, p is constant and equal to 15 and then there is an abrupt change at time step $t = 300s$ in which p changes from 15 to 25 leading to a second scenario.

The cost matrices Q, R of the proposed control scheme for both scenarios are the following

$$Q = \mathbb{I}^4, \quad R = \mathbb{I}^2 \tag{3.13}$$

The resulting optimization problem has been solved using the *fmincon* function of *Matlab 2013a*. The number of decision variables of the problem is 120.

The model used to carry out the simulations is the nonlinear model 3.12a-3.12d. The initial state of all the simulations is

$$\begin{pmatrix} h_1(0) \\ h_2(0) \\ h_3(0) \\ h_4(0) \end{pmatrix} = \begin{pmatrix} 0.4594 \\ 0.9534 \\ 0.4587 \\ 0.9521 \end{pmatrix}$$

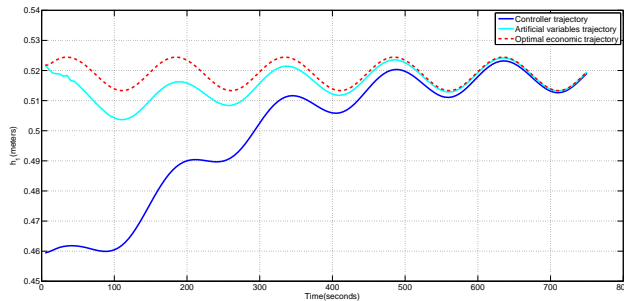


Figure 3.3 Closed-loop (blue), artificial (cyan) and optimal economic (red) trajectories of the level of tank 1 for scenario 1.

Figures 3.3-3.6 show the closed-loop (blue), artificial (cyan) and optimal economic (red) trajectories of the level of the four tanks for scenario 1. The artificial trajectory level is

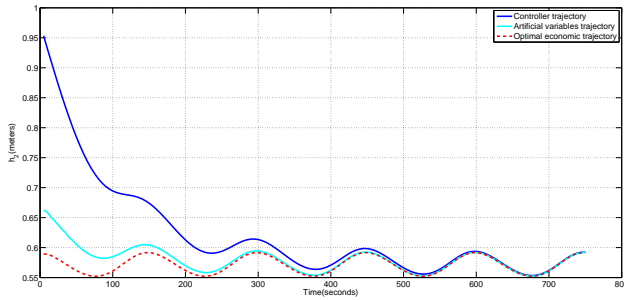


Figure 3.4 Closed-loop (blue), artificial (cyan) and optimal economic (red) trajectories of the level of tank 2 for scenario 1.

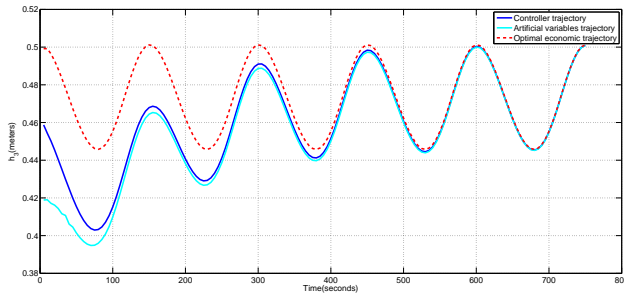


Figure 3.5 Closed-loop (blue), artificial (cyan) and optimal economic (red) trajectories of the level of tank 3 for scenario 1.

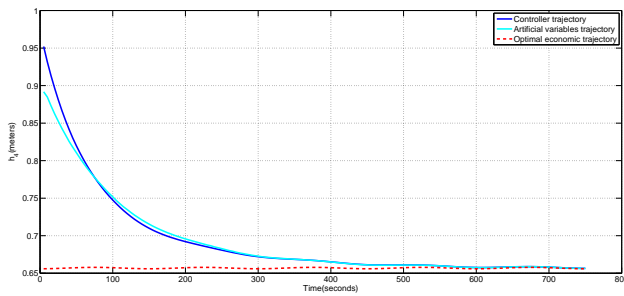


Figure 3.6 Closed-loop (blue), artificial (cyan) and optimal economic (red) trajectories of the level of tank 4 for scenario 1.

obtained at each sampling time from the corresponding optimal initial state of the artificial trajectory.

Figures 3.7-3.8 show the closed-loop (blue), artificial (cyan) and optimal economic

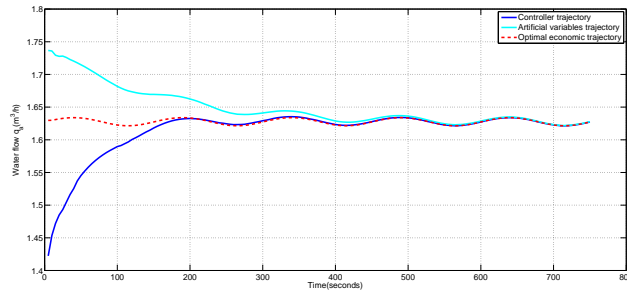


Figure 3.7 Closed-loop (blue), artificial (cyan) and optimal economic (red) trajectories of the water flow a for scenario 1.

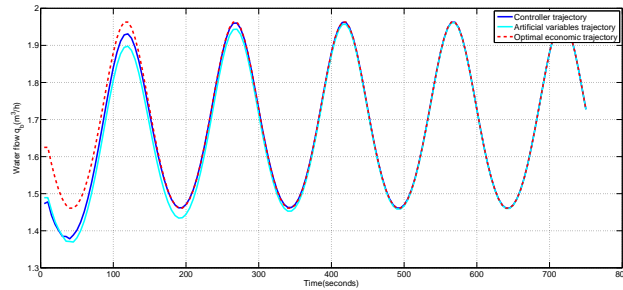


Figure 3.8 Closed-loop (blue), artificial (cyan) and optimal economic (red) trajectories of the water flow b for scenario 1.

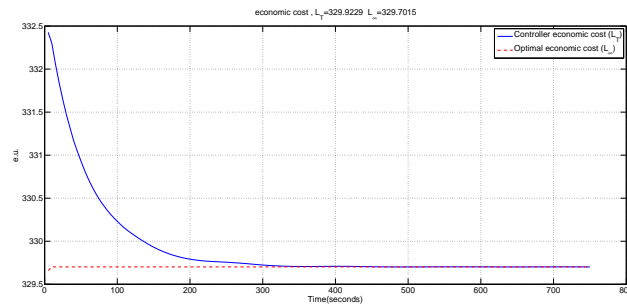


Figure 3.9 Evolution $\frac{1}{T} \mathcal{L}_T(k, \mathbf{x}, \mathbf{u}, \mathbf{p})$.

(red) trajectories of the water flows of pumps a and b . The artificial trajectory water flow is obtained at each sampling time from the corresponding optimal initial input of the artificial trajectory.

The simulation starts in an initial state far away from the optimal trajectory, but the

system is driven to an appropriate optimal periodic trajectory that minimizes the economic periodic function, i.e., the optimal trajectory. In figure 3.9 the convergence of $\frac{1}{T} \mathcal{L}_T(k, \mathbf{x}, \mathbf{u}, \mathbf{p})$ to $L_\infty(k, \mathbf{x}, \mathbf{u}, \mathbf{p})$ is shown.

This implies that the average economic cost in a period of the obtained trajectory converges to cost corresponding to the optimal trajectory.

In the second scenario, the robustness of the proposed controller with respect to abrupt changes in the economic stage cost is shown. In this case, the parameter p changes at $t = 300s$ from 15 to 25.

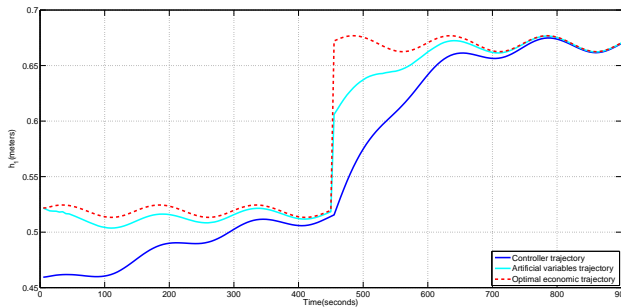


Figure 3.10 Closed-loop (blue), artificial (cyan) and optimal economic (red) trajectories of the level of tank 1 for scenario 2.

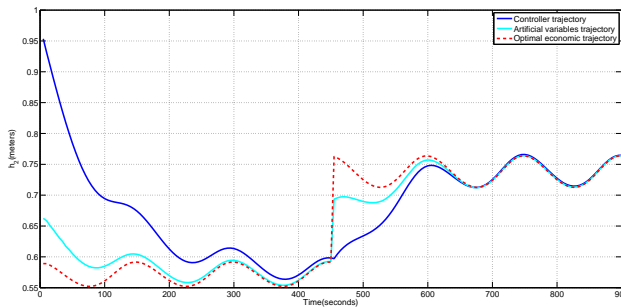


Figure 3.11 Closed-loop (blue), artificial (cyan) and optimal economic (red) trajectories of the level of tank 2 for scenario 2.

Figures 3.10-3.15 show the level and water flow trajectories for scenario 2. The simulation shows an abrupt change in all the trajectories at the sampling time in which the economic stage cost is changed. It is important to remark that the corresponding optimal periodic trajectories are very different between the two cost functions considered, which in general implies that the target trajectories for the controller are very different, however, the controller remains feasible because the optimization problem constraints do not depend on the optimal trajectory.

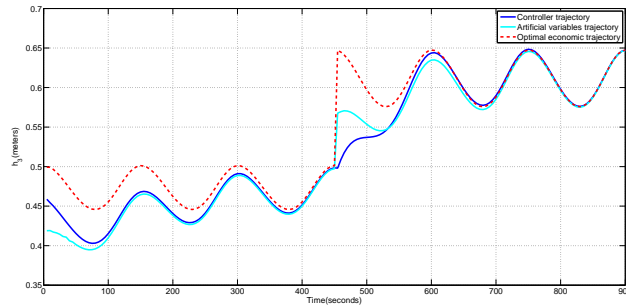


Figure 3.12 Closed-loop (blue), artificial (cyan) and optimal economic (red) trajectories of the level of tank 3 for scenario 2.

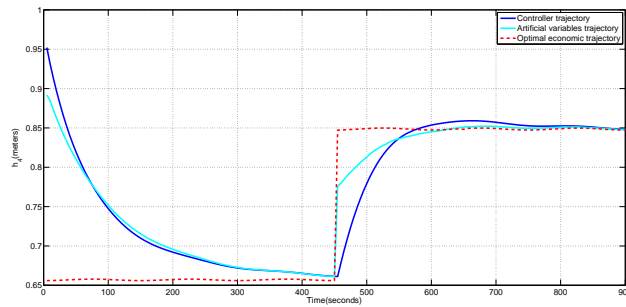


Figure 3.13 Closed-loop (blue), artificial (cyan) and optimal economic (red) trajectories of the level of tank 4 for scenario 2.

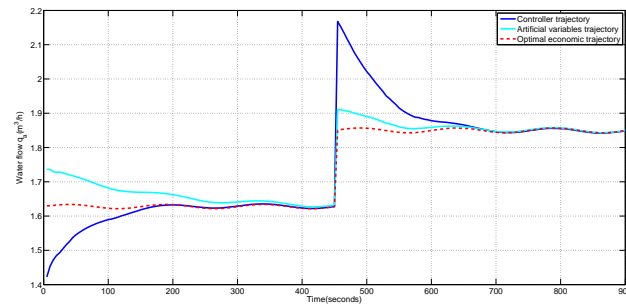


Figure 3.14 Closed-loop (blue), artificial (cyan) and optimal economic (red) trajectories of the water flow a for scenario 1.

Figure 3.16 shows the strong change in the optimal average economic cost when the variable p changes its value.

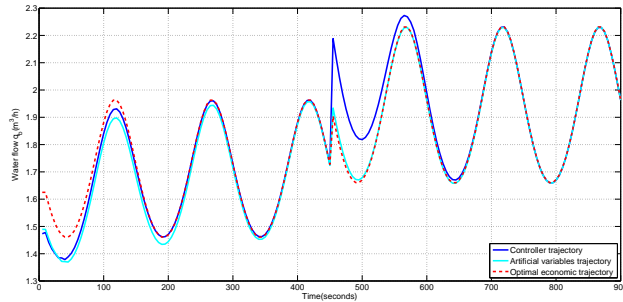


Figure 3.15 Closed-loop (blue), artificial (cyan) and optimal economic (red) trajectories of the water flow b for scenario 2.

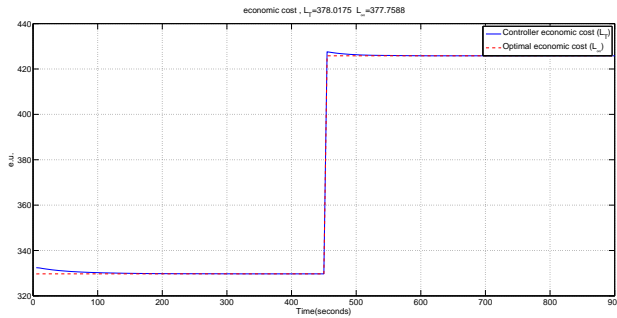


Figure 3.16 Evolution of $\frac{1}{T} \mathcal{L}_T(\mathbf{k}, \mathbf{x}, \mathbf{u}, \mathbf{p})$.

3.4 Application to a drinking water network

In this example we consider a simplified model of a section of Barcelona's drinking water network (Drinking Water Network (DWN)) presented in Ocampo-Martinez et al. (2013). Figure 3.17 and table 3.2 show a scheme of this network which consists on three water tanks, three valves and three water pumps. The network is connected to four demand points from which water is consumed (drinking water demand), and two water supply points from which the water is obtained.

The results of this section are obtained of applying the economic controller described in the previous sections. The proposed system is modelled as discrete time invariant model with a sampling time of one hour.

$$x(k+1) = A \cdot x(k) + B \cdot u(k) + B_d \cdot d(k) \quad (3.14a)$$

$$0 = E \cdot u(k) + E_d \cdot d(k) \quad (3.14b)$$

where $x(k) \in \mathbb{R}^3$ denotes de vector of volume in storage tanks (in m^3) and $u(k) \in \mathbb{R}^6$ denotes de vector of water flows through the six actuators given in $\frac{m^3}{s}$. Vector $d(k) \in \mathbb{R}^4$

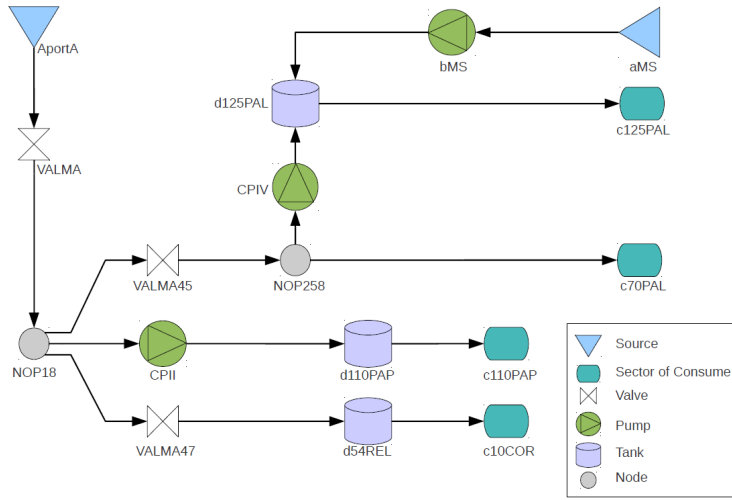


Figure 3.17 Topology of the three-tanks DWN example.

Table 3.2 Glossary of the topology of the DWN example.

Variable	Designed by	Description
u_1	VALMA	Valve
u_2	VALMA45	Valve
u_3	VALMA47	Valve
u_4	bMS	Pump
u_5	CPIV	Pump
u_6	CPII	Pump
x_1	d125PAL	Tank 1
x_2	d110PAP	Tank 2
x_3	d54REL	Tank 3
d_1	c125PAL	Demand point 1
d_2	c70PAL	Demand point 2
d_3	c101PAP	Demand point 3
d_4	c10COR	Demand point 4
a_1	AportA	Water supply A
a_2	aMS	Water supply B

denotes the network demands and it is also given in m^3 . The relationship between these variables and the variables of the real model can be found in table 3.2. Constraint 3.14b models that the DWN must satisfy the water demand defined by $d(k)$ at nodes $NOP18$ and $NOP25B$ as shown in figure 3.17. The equations that must be fulfilled on the nodes

$NOP18$ and $NOP25B$ are the following:

$$\begin{aligned}u_1(k) &= u_2(k) + u_3(k) + u_6(k) \\u_2(k) &= u_5(k) + d_2(k)\end{aligned}$$

The matrices A, B and B_d that define the model are the following

$$\begin{aligned}A &= \begin{pmatrix} 1 & 0 & 0 \\ 0 & 1 & 0 \\ 0 & 0 & 1 \end{pmatrix} & B &= \begin{pmatrix} 0 & 0 & 0 & 3600 & 3600 & 0 \\ 0 & 0 & 0 & 0 & 0 & 3600 \\ 0 & 0 & 3600 & 0 & 0 & 0 \end{pmatrix} \\ B_d &= \begin{pmatrix} -3600 & 0 & 0 & 0 \\ 0 & 0 & -3600 & 0 \\ 0 & 0 & 0 & -3600 \end{pmatrix}\end{aligned}$$

The matrices E, E_d are the following

$$\begin{aligned}E &= \begin{pmatrix} 1 & -1 & -1 & 0 & 0 & -1 \\ 0 & 1 & 0 & 0 & -1 & 0 \end{pmatrix} \\ E_d &= \begin{pmatrix} 0 & 0 & 0 & 0 \\ 0 & -1 & 0 & 0 \end{pmatrix}\end{aligned}$$

System ?? is subject to the following constraints on inputs and state

$$\begin{aligned}U_{min} &\leq u(k) \leq U_{max} \\ X_{min} &\leq x(k) \leq X_{max}\end{aligned}$$

where

$$\begin{aligned}U_{min} &= (0 \ 0 \ 0 \ 0 \ 0 \ 0)^T \\ U_{max} &= (1.2970 \ 0.0500 \ 0.1200 \ 0.0150 \ 0.0317 \ 0.0220)^T \\ X_{min} &= (0 \ 0 \ 0)^T \\ X_{max} &= (470 \ 960 \ 3100)^T\end{aligned}$$

The economic goal of the management of the DWN is to minimize the cost of water production and water transport supplying a periodic demand, typically of 24h. There are two operational goals that are included in the economic cost function. The operational goals are to guarantee the availability of water in every tank in order to satisfy the stochastic changes on the periodic demands and operate the network under smooth control actions.

The first operational criteria is taken into account including a penalty equal to the square of the deviation of the volume in each tank below the minimum values estimated for robust

operation:

$$J_S(k) = \sum_{i=1}^3 \|\delta_i(k)\|^2$$

where $\delta_i(k)$ denotes the deviation of the stored volume in tank i below the desired minimum volume $x_i^{sf}(k)$.

$$\delta_i(k) \triangleq \begin{cases} 0 & x_i(k) > x_i^{sf}(k) \\ x_i^{sf}(k) - x_i(k) & x_i(k) < x_i^{sf}(k) \end{cases} \quad i = 1,2,3$$

The second operational criteria is taken into account including a penalty on the square of the variations of the water flows in the pump and valves,

$$J_{\Delta u}(k) \triangleq \|\Delta u(k)\|^2$$

where $\Delta u(k) = u(k) - u(k-1)$.

Finally the economic cost of the water is included. This cost takes into account both the cost from the supply points and the transportation cost of operating the valves and pumps of the network.

$$J_E(k,p) \triangleq (\alpha_1 + p \cdot \alpha_2(k))^T \cdot u(k)$$

The cost is made up of a fixed water production cost denoted as $\alpha_1 \in \mathbb{R}^6$ and a time-varying (periodic) water cost denoted as $\alpha_2(k) \in \mathbb{R}^6$. Table 3.3 shows the value of the cost parameters α_1 and $\alpha_2(k)$ for each water flow. The parameter p is used to express an incremental change in electric prices at certain instant.

Table 3.3 Cost selection.

α	u_1	u_2	u_3	u_4	u_5	u_6	Time zone
α_1	2	0	0	2	0	0	0 - 24 hours
$\alpha_2(k)$	0	0	0	0.5	0.1	1	0 - 9 hours
$\alpha_2(k)$	0	0	0	3	4	3	9 - 20 hours
$\alpha_2(k)$	0	0	0	0.1	0.5	0.5	20 - 24 hours

Summing up, the economic stage cost function is the following

$$\ell(k,x,u,p) \triangleq \lambda_1 \cdot J_E(k,p) + \lambda_2 \cdot J_S(k) + \lambda_3 \cdot J_{\Delta u}(k)$$

where $\lambda_1, \lambda_2, \lambda_3$ are tuning parameters that set the influence of each objective on the overall economic cost function. The value of the parameters in this example are $\lambda_1 = 100$, $\lambda_2 = 10$, $\lambda_3 = 0.005$.

For tracking terms, the weighting matrices $Q = 0.01 * \mathbb{I}^3$ and $R = 10 * \mathbb{I}^6$. The prediction horizon and the periodic horizon are 24 hours and the sampling time is one hour. The initial state of the network is $x(0) = (160.44, 646.23, 633.89)$ given in m^3 and $u(0) = u(-1) = (0,0,0,0,0,0)$ given in m^3/h . The demands on points *c125PAL*, *c70PAL*, *c110PAP* and *c10COR* are periodic signals with a period of 24 hours, see figure 3.18.

In this example, the simulation horizon is six days. We consider a scenario in which the cost changes abruptly after $72h$ of operation. During the first $72h$, the parameter p is equal to zero and then the parameter takes the value of $p = 1$. This is equivalent to increase the unitary cost of pumping according to a given pricing policy.

For the simulation test, the optimization problem has been implemented using an epigraph formulation Ocampo-Martinez et al. (2013) and this has been carried out using *qpOASES* toolbox on Matlab 2013a and an Intel Core *i7* – 4700 with 16 GB of RAM.

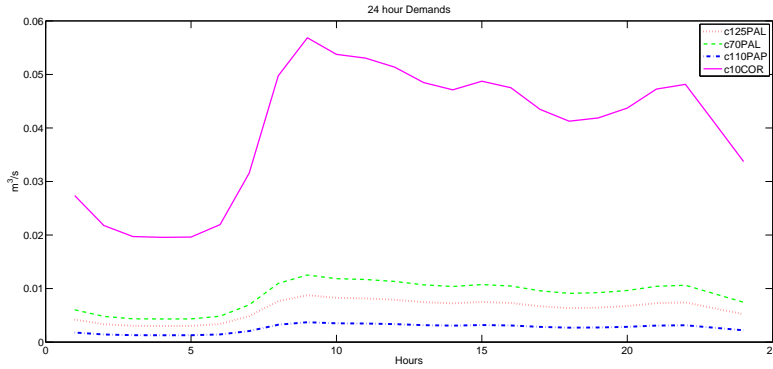


Figure 3.18 24h demand on points $c125PAL, c70PAL, c110PAP$ and $c10COR$.

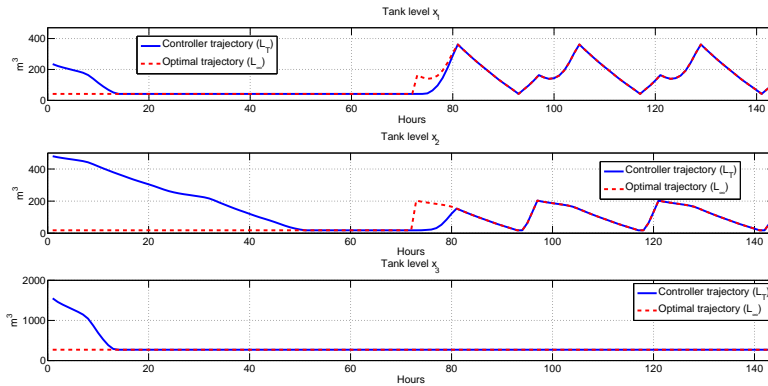


Figure 3.19 Stored volume in the Tank [m^3].

Figure 3.19 shows the evolution of the three tanks along 144 hours. It can be seen that during the first 72 hours, the optimal volumes of the three tanks is equal to the minimum levels because the costs of the water and transport are constant along the 24 hour period, so the optimal policy is to satisfy the demand and have the minimum amount of water in the tanks. When the cost of the water is modified and becomes time varying, then it is more

profitable to accumulate water when the cost is lower, to provide this water to the demand during the high cost time periods. In addition, it can be seen, that the supply points are also used at different time periods, depending on the value of their corresponding $\alpha_2(k)$.

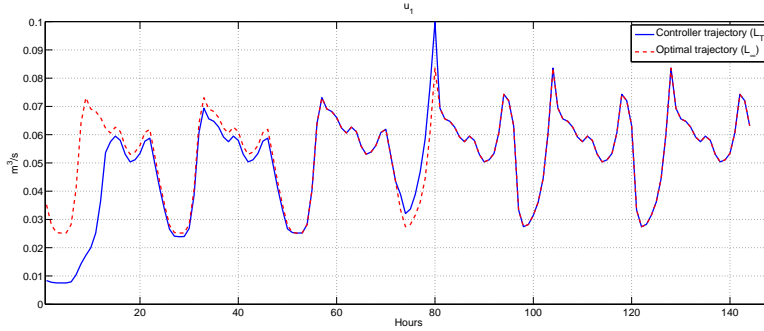


Figure 3.20 Optimal periodic (red) and closed-loop (blue) trajectories of valve *VALMA*.

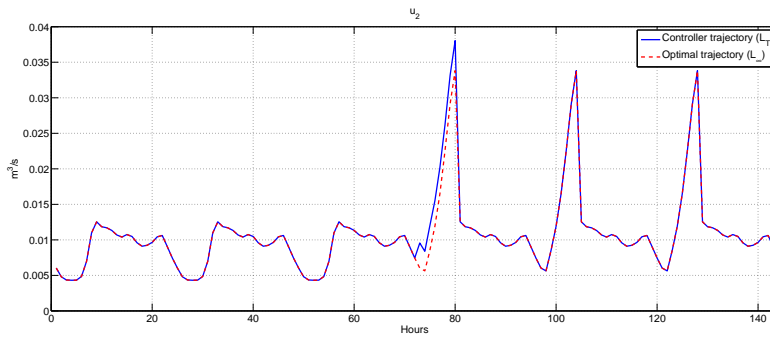


Figure 3.21 Optimal periodic (red) and closed-loop (blue) trajectories of valve *VALMA45*.

Figures 3.20-3.25 show the corresponding trajectories of optimal periodic control inputs (red) $u^*(k)$ and closed-loop (blue) inputs $u(k)$. Notice that during the first 72 hours, no water is accumulated, and in fact, the initial stored volume of water is used to satisfy the demand. After parameter p is changed, the new pricing policy produces a significant change in the optimal operation of the plant. This can be seen in figures 3.25-3.25 where the flows of the pumps change from a smooth periodic operation to a fast transition between its limits. This is also illustrated in figure 3.19, where the evolution of the volume of water in the tanks 1 and 2 changes from a steady evolution to a periodic evolution, storing water whenever the pumping price is lower.

Figure 3.26 shows the average economic cost of the optimal trajectory during a period (red) and optimal cost of the controller optimization problem (blue) trajectories. It can be seen that the optimal cost of the controller converges to the optimal cost as stated in the main theorem. The feasibility and robustness properties of this controller can be

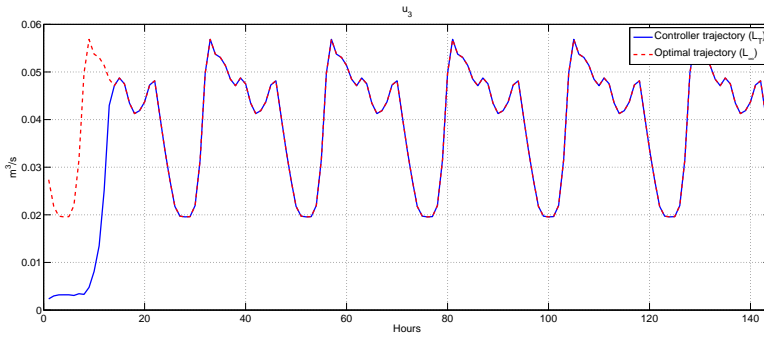


Figure 3.22 Optimal periodic (red) and closed-loop (blue) trajectories of valve *VALMA47*.

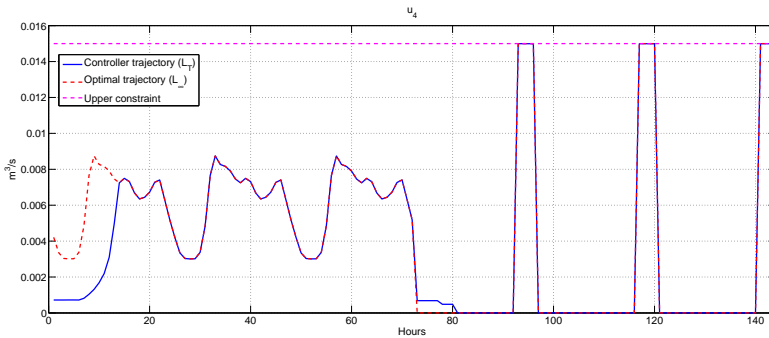


Figure 3.23 Optimal periodic (red) and closed-loop (blue) trajectories of pump *bms*.

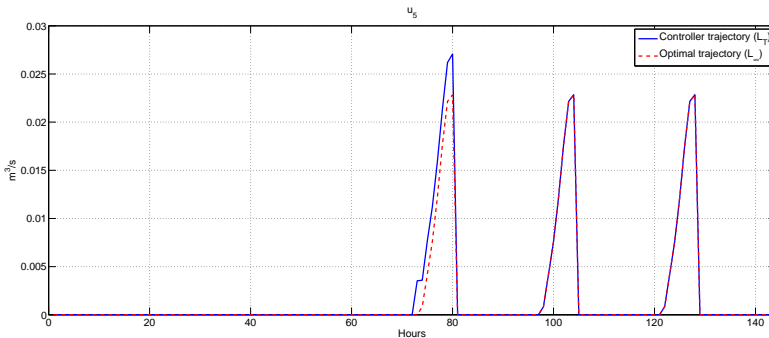


Figure 3.24 Optimal periodic (red) and closed-loop (blue) trajectories of pump *CPIV*.

observed when the cost changes after 72h. There is a sudden change in the optimal periodic trajectory when the parameter p changes. Note that the controller continues without loss of feasibility and that the closed-loop trajectories converge to the new optimal ones.

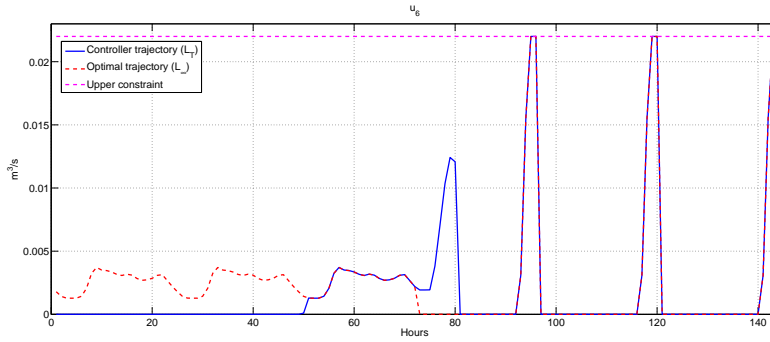


Figure 3.25 Optimal periodic (red) and closed-loop (blue) trajectories of pump *CPII*.

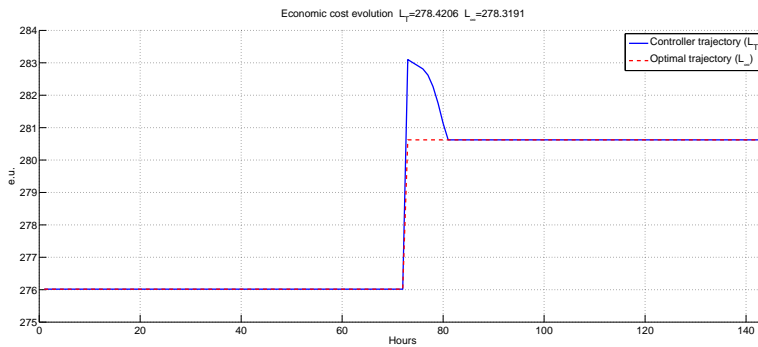


Figure 3.26 Average economic cost of the optimal trajectory during a period (red) and optimal cost of the controller optimization problem (blue) trajectories.

4 Periodic economic control of a non-isolated micro-Grid

A microgrid is a group of interconnected loads and distributed energy resources within clearly defined electrical boundaries that acts as a single controllable entity with respect to the grid. A microgrid can connect and disconnect from the grid to enable it to operate in both grid-connected or island-mode.

U.S. DEPART. OF ENERGY MICROGRID E. G.

Modern countries must face the energy problem caused by an increasing demand with limited fossil fuel sources and environmental restrictions. Among the actions that have been taken to deal with this problem are the support to the use of renewable energy sources and the improvement of the efficiency of the equipments and energy systems. These actions have led to a change in the energy management policies allowing for more flexible scenarios that take into account the uncertain nature of the renewable energy sources and the consumers demand. In these scenarios, microgrids; that is, a group of interconnected loads and distributed energy resources with clearly defined electrical boundaries that acts as a single controllable entity with respect to the grid, have a relevant role. These systems can operate in both grid connected or island mode and in general try to satisfy their internal demand and if possible sell the excess of produced energy to the grid. To this end, microgrids rely on energy storage systems such as batteries or hydrogen based storage systems.

The control of micro-grids has received a lot of attention over the last years and nowadays there exist several commercial solutions, however there are still open issues for research, see (Arefifar et al., 2015; Wang et al., 2015). In (Miland and Ulleberg, 2012) an experimental small-scaled stand-alone power system based on hydrogen is presented. Model predictive control (MPC) has also been applied to this class of systems, see for example (Choi and Lee, 2015; Parisio et al., 2014b,a; Valverde et al., 2012). In (Qi et al., 2012, 2011a,b) nonlinear

MPC techniques were applied to supervise a microgrid with wind-solar energy generation systems and water system based load. In (Heidarinejad et al., 2012) a Lyapunov-based economic controller for nonlinear systems was proposed and applied to a microgrid with renewable generation. In (Garcia and Bordons, 2013b; Salazar et al., 2013; Garcia and Bordons, 2013a) MPC techniques were applied to supervise a hybrid model of a microgrid with hydrogen storage system. In (Touretzky and Baldea, 2014) a strategy for the optimal economic control of building heating, ventilation and air conditioning systems with chilled water thermal energy storage was proposed.

One issue that micro-grid control systems must take into account is the time varying operation conditions that result from the varying power generation of renewable energy systems, the periodic character of distributed loads and the fluctuations of the prices of the electric market. In this case, the optimal operation of a microgrid from an economic point of view is not to remain at a certain steady state but to follow a non-steady trajectory, often periodic Lee et al. (2001); Huang et al. (2012). Several model predictive control schemes that deal with this problem have been recently proposed, see for example (Gondhalekar et al., 2013; Pinheiro et al., 2011)

In addition, efficient operation of microgrids can be enhanced if economic costs are taken into account in the control system design. For example, changing weather conditions and passing cloud cover produce a varying power generation from solar systems such as photovoltaic. This may cause large, rapid power fluctuations. The exposition of the fuel cell and electrolyzer to such short term and highly variable power conditions may lead to degradation of performance and life time of these hydrogen based power systems. In order to make these systems economically competitive, the cost associated with performance and life time degradation should be reduced. Using better power management strategies to operate these storage systems under the most favorable operating regimes has great potential to improve its life time.

Taking into account the results of the economic periodic predictive controller presented in chapter 3, we consider that it is very interesting the application of this controller to manage this class of systems which are gaining a lot of importance and attention by the research community. The strong periodic feature which presents some renewable energy sources and demands make this controller ideal. This chapter is focused on the application of this economic periodic predictive controller to minimize the cost of operating a non-isolated microgrid connected to an electric utility (Electric Utility (EU)) and subject to a periodic internal demand, see figure 4.1. The results of this chapter have been published in Pereira et al. (2015a).

4.1 Control of a non-isolated microgrid

The micro-grid considered is made of a set of photovoltaic panels, two storage systems and can buy and sell energy to an EU. The first storage system is made of a cluster of batteries of lead acid and the second storage system is based on hydrogen storage. We consider an scenario in which the microgrid has signed a contract with the electric utility in which it has to provide a predefined amount of energy in a given period of time each day. Out of this interval of time the energy the energy cannot be sold and is wasted,

although the microgrid can still purchase energy. To this end, we propose a cost function that takes into account the economic profit of the operation of the microgrid in the energy market as well as the economic cost of the operation of the plant in a realistic setting, in particular the proposed cost function takes into account the benefit of selling energy from the microgrid, a non-linear penalty for deviating from an energy bid and the degradation of the batteries and the hydrogen storage systems. Assuming that precise predictions on the photovoltaic generation, internal demands and energy bid contract are available, the efficient management of the facility is posed as an economic control problem of a periodic system.

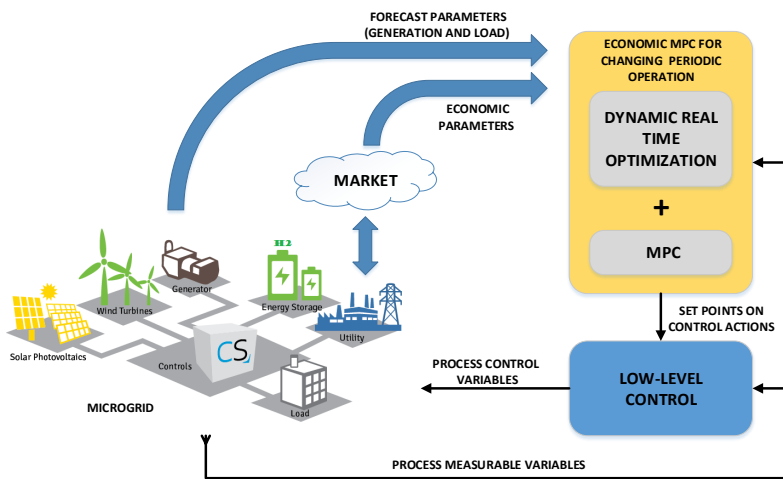


Figure 4.1 Hierarchical control structure of the application of the previous economic controller to a non-isolated microgrid.

The results presented in this chapter have been obtained on a nonlinear realistic model of a real micro-grid (Valverde et al., 2013b), (Valverde et al., 2013a) located in the University of Seville. This test-bed is operative since 2011 and was designed to implement and study different modes of operation and control strategies to optimize hydrogen smart-grids operation.

This micro-grid is made of a photovoltaic (PV) energy source, an energy consumer, a cluster of batteries, an energy storage system based on hydrogen and a connection to an electric utility (EU) to which the micro-grid can buy/sell energy from/to. The microgrid must try to sell an agreed power to the EU only during an certain interval of time. This power and interval of time are agreed with the EU.

The microgrid has two storage systems: a batteries cluster and a hydrogen based storage system. The hydrogen storage system is composed by a proton exchange membrane fuel cell that provides energy consuming hydrogen, and a polymer electrolyte membrane electrolyzer that produces hydrogen consuming energy. The hydrogen is stored in a metal hydride deposit. The batteries cluster included is used to support the short transitory power peaks due to its fast dynamic and the hydrogen storage system was installed in order to support the long power peaks due to its high investment cost.

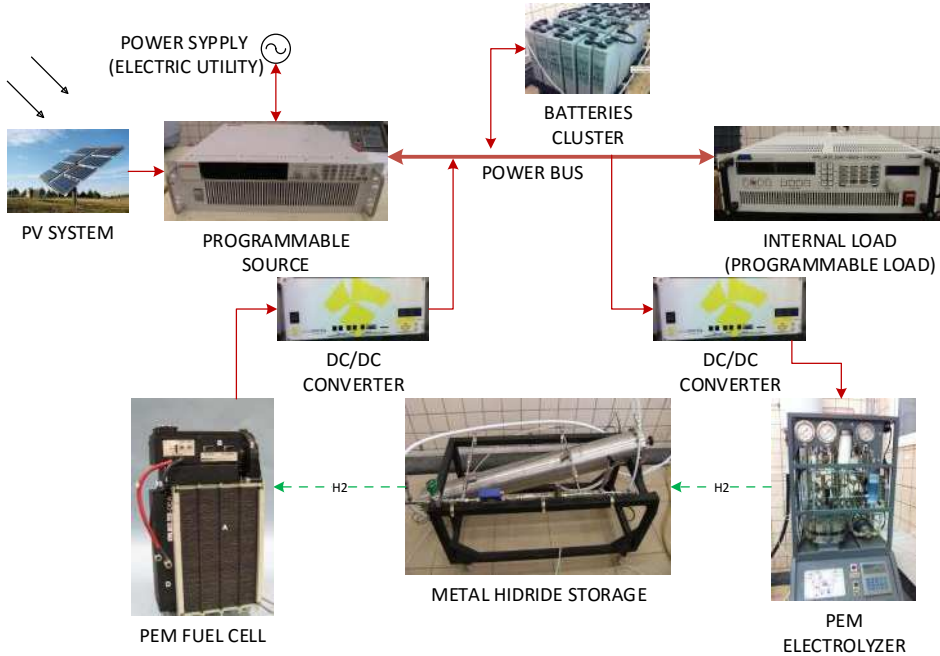


Figure 4.2 Micro-grid scheme simulated in the test-bed located in the University of Seville..

The manipulable inputs are the power reference of electrolyzer and fuel cell (P_{H_2}) and the power associated to the buying and selling of electric energy (P_{grid}) which is positive when it is selling energy. The power generation of the PhotoVoltaic panels (PV) system (P_{PV}) and the internal demand of the micro-grid (P_{load}) are considered as known disturbances. The outputs of the plant are the stored energy rate in both storage systems: the stage of charge of the batteries (Stage Of Charge of the batteries (SOC)) and the level of stored hydrogen in the metal hydride deposit (Metal Hydride Level (MHL)). The dynamics of the batteries are assumed to be very fast so the power of the battery (P_{bat}) is obtained from the power balance in the power bus which can be expressed as:

$$P_{bat} + P_{H_2} + P_{PV} = P_{load} + P_{grid}$$

We consider the difference between the power produced by the PV system and the power consumed by the inner load as an exogenous disturbance of the system and is defined as

$$P_{net} = P_{PV} - P_{load}$$

The objective of this kind of microgrid is not only to satisfy the internal demand and the energy contract with the EU, which we assume to be periodic, while maintaining the operational limits of the plant, but also to keep the equipment at their maximum efficiency points while minimizing the economic cost taking into account the electricity market costs. The main control objectives can be described as follows:

- (i) Maximize the profit of the energy exchange between the microgrid and the EU taking into account the prices of the intraday electricity market and the contract constraints.
- (ii) Fulfill a known periodic internal demand.
- (iii) Try to extend the life time of the equipments of the microgrid.
- (iv) Fulfill the operational constraint in order to prevent damage the equipments.

The proposed controller is based on the assumption that the internal demand is known which implies the use of a forecasting tool. The profile of large scale distribution grids presents periodicity and some predictability, however unpredictability is much more intense in small scale microgrids with few loads. Nevertheless, we consider that the use of a prediction of the demand is one of the main advantages of using a model based approach, and can improve the overall performance even in the presence of deviations from the nominal predictions thanks to the receding horizon scheme and the possibility of adapting to possible changes in these predictions.

4.1.1 Simulation model

In this approach we use the non-linear high order model of non-isolated microgrid presented in our previous work (Valverde et al., 2013b) to carry out the simulations. In this work, a model based on first principles was developed and validated on the experimental configurable test-bed located at the laboratories of the University of Seville. This test-bed is operative since 2011 and was designed to implement and study different modes of operation and control strategies to optimize hydrogen smart-grids operation. The test-bed has the following equipment: a 6 kW programmable electronic source to emulate the renewable energy sources, a 1 kW PEM electrolyzer for the production of hydrogen, a 7 Nm³ hydrogen storage tank based on metal hydride alloy, a 367 Ah lead-acid battery bank, a 1.5 kW PEM fuel cell and finally a 2.5 kW programmable electronic load to emulate different demand profiles. The programmable electronic source was programmed to emulate the behavior of a photovoltaic generation system as shown in figure 4.2. The test-bed has a programmable control system that allows implementing advanced control strategies based on the Matlab-Simulink environment which communicates using OLE for Process Control foundation specifications (OPC) with a PLC that controls the low level inputs.

In (Valverde et al., 2013b), the nonlinear and complex nature of the dynamics of the plant are described by a set of nonlinear algebraic and differential equations. The reader can refer

to this work for a detailed description of the model. These equations were implemented in a Simulink and a set of suitable parameters were identified and validated on the test-bed. The equations of the simulation model and its validation can be found in (Valverde et al., 2013b),(Valverde et al., 2013a). The main parameters of the models that compose the storage systems are shown in tables 4.1,4.2,4.3,4.4.

Table 4.1 PEM electrolyzer model parameters.

PEM electrolyzer model parameters		
Comments	Values	Units
Stack area	212.5	cm^2
H_2 Partial pressure	6.9	bar
O_2 Partial pressure	1.3	bar
Anode current density	1.0631^{-6}	A/cm^2
Cathode current density	1^{-3}	A/cm^2
Membrane thickness	178	μm
Membrane conductivity	0.14	S/cm
Membrane water content	21	$molH_2/molSO_3$
Thermal capacity	402400	J/K

Table 4.2 PEM fuel cell model parameters.

PEM fuel cell model parameters		
Comments	Values	Units
Fuel cell stack mass	5	kg
Fuel cell heat capacity	1100	$Jkg^{-1}K^{-1}$
Fuel cell emissivity	0.9	–
Radiation ex. area	0.1410	m^2
Fuel cell natural ex. area	0.0720	m^2
Fuel cell forced ex. area	1.2696	m^2
Natural heat transfer coef.	14	$WK^{-1}m^{-2}$
Forced heat transfer coef.	19.65	$WK^{-1}m^{-2}$

There are technological constraints on the hydrogen systems (production, storage and consumption) that limit the values of power for this manipulated input in order to avoid possible damages of the equipments. Power P_{grid} is limited between -2.5 kW and 2 kW. Power P_{H_2} is limited between -0.9 kW and 0.9 kW. In addition, the batteries need to maintain a certain level in the SOC in order to maintain the voltage at appropriate values in the power bus of micro-grid and in the hydrogen storage system is necessary to maintain the hydrogen levels between a minimum and maximum to avoid damage to the equipment. To this end the proposed controller will be designed to maintain the SOC and MHL between 40% and 90% when possible, including these constraints as soft constraints in the MPC optimization problem.

Table 4.3 Metal hydride model parameters.

Metal hydride tank model parameters		
Comments	Values	Units
MH powder porosity	0.55	–
MH density	3240	kg/m^3
Max. abs./desor. H_2 w. frac.	1.2174	$%w/w$
MH spec. heat const. vol.	419	$J/(molK)$
Heat transfer area	1.1453	m^2
MH volume ratio	1	–
Absorbed radiation	21.18	KJ/nik
Activation energy	59.187	$1/s$
Desor. heat trans. coef.	966.1980	$W/(m^2K)$
Absor. heat trans. coef.	833.144	$W/(m^2K)$

Table 4.4 Battery model parameters.

Battery model parameters		
Comments	Values	Units
Max. battery capacity	367	Ah
Battery voltage	48	V
Charge/disch. polariz. const.	0.006215	V
Exp. zone amplitude	11.053	V
Exp. zone inv. time const.	2.452	Ah^{-1}

4.1.2 Controller design model

In order to implement the control law proposed in (Limon et al., 2014) a discrete time linear model is needed. After analyzing the response of the system, the microgrid was modeled as two integrators with weighted inputs. A series of simulations were carried out using the nonlinear model to identify the slope of the step response to each input. For each input, over 300 simulations of 30 minutes with different initial states and step amplitudes were done. The parameters of the system were obtained as the mean value of these slopes. The resulting continuous time linear model was the following:

$$\dot{x} = \begin{bmatrix} 0.2712 & 0.1986 \\ -0.5096 & 0 \end{bmatrix} u(t) + \begin{bmatrix} 0.1986 \\ 0 \end{bmatrix} w(t)$$

with $x = [SOC \ MHL]^T$, $u = [P_{H_2} \ P_{grid}]^T$ and $w = P_{net}$. The following discrete time linear model used to design the controller was obtained using a Tustin method and a sampling

time of 1800 second (30 minutes):

$$x(k+1) = x(k) + \begin{bmatrix} 8.1360 & 5.9568 \\ -15.2886 & 0 \end{bmatrix} u(k) + \begin{bmatrix} 5.9568 \\ 0 \end{bmatrix} w(k)$$

The sampling time chosen is satisfactory for a long-term analysis assuming smooth irradiation profiles. The structure of the microgrid considered includes a set of batteries to compensate the effects of intermittence by PVs. At any given time, the batteries provide the power needed to balance the energy in the microgrid. This implies that short intermittence by PVs may affect the level of the batteries between sampling times, but in general the batteries have enough energy needed to provide the energy that the PV did not generate. In the next sampling time, the controller takes into account this disturbance in the SOC.

4.2 Economic cost function

We present next an economic cost function that takes into account the calculation of the power exchanged in the electricity market as well as technological issues and equipment operational costs. The cost of the battery bank, hydrogen storage, fuel cell and electrolyzer have been defined to reduce the intensive use these equipments might be subject to during normal operation.

The economic cost function h_{eco} is evaluated for a trajectory of the plant outputs and inputs along an operation period T , that is,

$$\begin{aligned} \mathbf{y} &= (y(0), y(1), \dots, y(T-1)) \\ \mathbf{u} &= (u(0), u(1), \dots, u(T-1)) \end{aligned}$$

The economic function depends on a set of time varying parameters, such as the price of power in the electricity hourly spot market C_{poolh} measured on *e.u./KWh*, the price of buying power to the EU C_{buy} and the power agreed with the EU P_{of} . The predictions of these parameters are included in a vector denoted as $\mathbf{c} = [C_{poolh} \ C_{buy} \ P_{of}]^T$. These parameters may change along the operation of the plant and they are assumed to be periodic. The trajectory of these parameters along an operation period is denoted as

$$\mathbf{c} = (c(0), c(1), \dots, c(T-1))$$

and it is such that C_{poolh} and C_{buy} remain constant along the period while P_{of} may vary.

The economic cost function is denoted by $h_{eco}(\mathbf{c}; \mathbf{y}, \mathbf{u})$. This function is defined as the sum of a number of costs that measures different economic aspects of the plant:

$$\begin{aligned} h_{eco}(\mathbf{c}; \mathbf{y}, \mathbf{u}) &= \beta_1 (h_{mg}(\mathbf{c}; \mathbf{y}, \mathbf{u}) + h_{sp}(\mathbf{c}; \mathbf{y}, \mathbf{u})) \\ &+ \beta_2 (h_b(\mathbf{y}, \mathbf{u}) + h_{fc}(\mathbf{y}, \mathbf{u}) + h_{ez}(\mathbf{y}, \mathbf{u}) + h_{mh}(\mathbf{y}, \mathbf{u}) + h_{op}(\mathbf{y}, \mathbf{u})) \end{aligned} \quad (4.1)$$

where h_{mg} is the economic cost of the power exchanged with the EU and includes the benefits of electricity sold and the penalty for possible deviations from the agreed energy bid, h_{sp} includes the cost to purchase energy from the EU, h_b, h_{fc}, h_{ez} and h_{mh} are costs

related with the degradation of the microgrid equipment, and h_{op} is a cost related with operational constraints of the microgrid. All these costs are described in detail in the following sections. The parameters β_1 and β_2 are fixed by the designer to weight the term of the economic profit versus the term of the operation cost.

The economic costs considered in this work have terms that depend on the sign of a given value. The sign function is a non-differentiable function. In order to use gradient base techniques to solve the optimization problems that define the model predictive controller, the following functions will be used instead of the sign function:

$$\begin{aligned}\delta_1(x) &= (0.5 + (0.5/\pi) \cdot \arctan(a \cdot x)) \\ \delta_2(x) &= (0.5 - (0.5/\pi) \cdot \arctan(a \cdot x))\end{aligned}$$

Function $\delta_1(x)$ is 0 when $x < f(a)$, is 1 when $x > f(a)$ and $f(a) \rightarrow 0$ when $a \rightarrow \infty$. Function $\delta_2(x)$ is 1 when $x < f(a)$, is 0 when $x > f(a)$ and $f(a) \rightarrow 0$ when $a \rightarrow \infty$. Figure 4.3 shows $\delta_1(x)$ for $a = 10$.

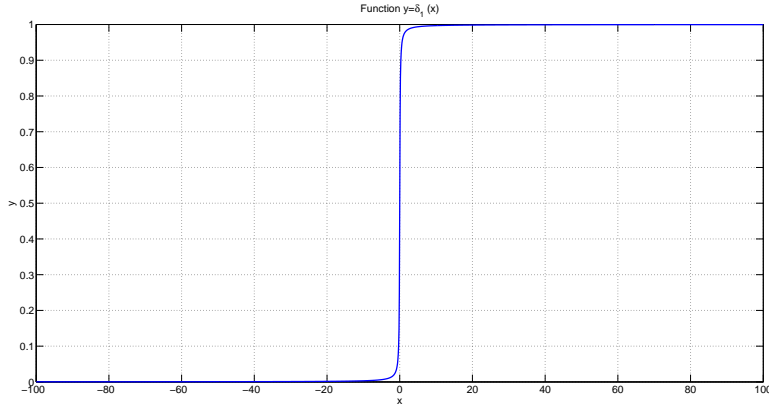


Figure 4.3 Function $\delta_1(x)$, $x = [100, -100]$ and $a=10$.

If mixed-integer linear inequalities are used to model the sign cost function, the resulting optimization problem would be nonlinear mixed integer, for which general purpose solvers are not available, making the implementation a much harder issue. We propose to use a nonlinear smooth approximation to simplify the implementation and inherit the closed-loop properties of the Economic MPC scheme applied. In the simulations done, the resulting controller is not sensible to this approximation, however, the resulting optimization problem can be badly conditioned if this parameter is not chosen appropriately.

4.2.1 Sold energy cost h_{mg}

The term h_{mg} models the average benefit of selling energy to the PV and the penalty of a deviation between the energy bought or sold the the PV and the agreed value of the

contract, often call the energy bid.

$$h_{mg}(\mathbf{c}; \mathbf{y}, \mathbf{u}) = \frac{1}{T} \sum_{j=0}^{T-1} f_{mg}(j)$$

where $f_{mg}(j) = f_{mg}(c(j), y(j), u(j))$ is the economic stage cost of the energy sold at sampling time j .

The term f_{mg} models the benefit of selling energy to the PV and the penalty of the energy bid, that is, the deviation between the energy bought or sold to the PV, P_{grid} , and the agreed value of the contract, P_{of} . The penalty for not fulfilling the contract is in general a complex function that depends on the deviation. In this work we consider two different linear costs depending on whether the deviation is negative (energy deficit) or positive (surplus of energy). $P_{enalc}^{up}(\%)$ is the penalization percentage due to a positive deviation and $P_{enalc}^{lw}(\%)$ is the penalization percentage due to a negative deviation. Using δ_1 and δ_2 in order to approximate these costs we obtain the following expression:

$$f_{mg}(j) = f_{mg}^{up}(j) + f_{mg}^{lw}(j) - C_{poolh} \cdot P_{grid}(j)$$

where

$$\begin{aligned} f_{mg}^{up}(j) &= -\delta_1((P_{of}(j) - P_{grid}(j))) \cdot P_{enalc}^{up}(\%) \cdot C_{poolh} \cdot (P_{of}(j) - P_{grid}(j)) \\ f_{mg}^{lw}(j) &= -\delta_2((P_{of}(j) - P_{grid}(j))) \cdot P_{enalc}^{lw}(\%) \cdot C_{poolh} \cdot (P_{of}(j) - P_{grid}(j)) \end{aligned}$$

4.2.2 Purchased or wasted energy h_{sp}

The term h_{sp} models the average cost of energy supplied by the EU as follows

$$h_{sp}(\mathbf{c}; \mathbf{y}, \mathbf{u}) = \frac{1}{T} \sum_{j=0}^{T-1} f_{sp}(j)$$

where $f_{sp}(j) = f_{sp}(c(j), y(j), u(j))$ is the economic stage cost of the energy sold at sampling time j .

The energy provided by the EU is purchased in order to provide a power supply when the cost of use the stored energy are high. Positive values of P_{grid} imply returning or selling energy and negative values imply purchasing energy. The cost that represent the waste of energy (when $P_{of} = 0$, i.e. there are not power agreed with the EU) is a quadratic term and the purchase of energy ($P_{of} > 0$) is a linear term. This cost is expressed as follows

$$f_{sp}(j) = \delta_2(P_{grid}) \cdot C_{buy} \cdot \|P_{grid}(j)\| + (1 - \delta_1(P_{of})) \cdot \delta_1(P_{grid}) \cdot 10 \cdot \|P_{grid}(j)\|^2$$

where the weight of the quadratic term is a technological-economic weight chosen to avoid that the microgrid throws away energy instead of storing it.

4.2.3 Degradation cost of equipments

Battery cost h_b

The degradation cost of the lead acid batteries can be posed as follows

$$h_b(\mathbf{y}, \mathbf{u}) = \frac{C_{ibat} \cdot \frac{1}{3600}}{CN \cdot V_{dc} \cdot N_{cycles} \cdot \eta_{bat}} \cdot \frac{1}{T} \sum_{j=0}^{T-1} \|P_{bat}(j)\|$$

where C_{ibat} is the investment cost of the batteries and it has a value of 2548 e.u., CN is the nominal capacity of the batteries and has a value of 333 Ah. V_{dc} is the voltage of the batteries and has a value of 48 V, N_{cycles} is the numbers of equivalent cycles and it has a value of 96. Finally η_{bat} models the performances of the batteries and has a value of 0.8.

Hydrogen cost h_{fc}, h_{ez}, h_{mh}

Each charging and discharging cycle of the metal hydride tank has a cost because of the limited number of cycles that the alloy can stand and the gradual loss of capacity. The cost of the electrolyzer and the fuel cell it is composed by two terms: a cost associated to the time that both systems stay on in a period T and a cost associated to the number of ignitions of any of these systems in a period T .

$$\begin{aligned} h_{fc}(\mathbf{y}, \mathbf{u}) &= J_{TON}^{fc} + J_{NON}^{fc} \\ h_{ez}(\mathbf{y}, \mathbf{u}) &= J_{TON}^{ez} + J_{NON}^{ez} \end{aligned}$$

where J_{TON} penalizes the time that the equipment (the fuel cell or the electrolyzer) is switched on and J_{NON} penalizes the number of times that the equipment is switched on. These are described as follows:

$$\begin{aligned} J_{TON}^{fc} &= \frac{C_{ifc}}{N_{TH}^{fc}} \cdot Tm \cdot \frac{1}{T} \sum_{j=0}^{T-1} \delta_1(P_{H2}(j)) \\ J_{NON}^{fc} &= \frac{C_{ifc}}{N_{TH}^{fc}} \cdot \frac{1}{T} \sum_{j=1}^{T-1} \left(\delta_1(P_{H2}(j)) - \delta_1(P_{H2}(j-1)) \right) \\ J_{TON}^{ez} &= N_{TH}^{ez} \cdot Tm \cdot \frac{1}{T} \sum_{j=0}^{T-1} \left(\delta_2(P_{H2}(j)) \cdot (5 \cdot \|P_{H2}(j)\| + 1.5) \right) \\ J_{NON}^{ez} &= \frac{C_{ieez}}{N_{TH}^{ez}} \cdot \frac{1}{T} \sum_{j=1}^{T-1} \left(\delta_2(P_{H2}(j)) - \delta_2(P_{H2}(j-1)) \right) \end{aligned}$$

where C_{ifc} is the investment cost of the fuel cell (7000e.u./Kw), N_{TH}^{fc} is the total number of the life time hours of the fuel cell (30000hours), N_{TH}^{ez} is the total number of the life time hours of the electrolyzer (55000hours) and C_{ieez} is the investment cost of the electrolyzer (7000e.u./Kw).

Metal hydride tank h_{mh} :

This cost penalizes the usage of the hydrogen based storage system. If this term is penalized then the batteries are prioritized as storage system. This cost is calculated as the average cost of the deviation of the metal hydride level from its initial value. This cost can be expressed as follows

$$h_{mh}(\mathbf{y}, \mathbf{u}) = \frac{V_{H_2}}{100 \cdot N_{TC}} \cdot \frac{1}{T} \sum_{j=0}^{T-1} \|MHL(j) - MHL(0)\|$$

where V_{H_2} is the total volume of the deposit, N_{TC} is the total number of estimated cycles of life time of the metal hydride deposit (30600 *cycles*), and $MHL(k)$ is the level of stored hydrogen of the metal hydride deposit at time k .

4.2.4 Operation costs f_{op}

This cost takes into account three different aspects of the operation of the plant: the cost J_{SM} penalizes sequence of control actions that are aggressive and it is formulated as follows:

$$J_{SM} = \frac{1}{T} \sum_{j=0}^{T-1} \|\Delta u(j)\|$$

The cost J_{DZ} penalizes values of P_{H_2} in the zone of $(-0.1, 0.1)$ as it is recommended by the vendor. This is given by:

$$J_{DZ} = \frac{1}{T} \sum_{j=0}^{T-1} \delta_1(\|P_{H_2}(j) - 0.1\|) \cdot \|P_{H_2}(j)\|^2$$

The cost J_{RB} penalizes those trajectories of SOC and MHL that are close to their operation limits, acting as a soft constraint on the limits on the outputs.

$$\begin{aligned} J_{RB} = \frac{1}{T} \sum_{j=0}^{T-1} & \left(\delta_1(\|SOC(j) - 48\|) \cdot \|SOC(j) - 48\|^4 \cdot k_1 \right. \\ & + \delta_2(\|SOC(j) - 75\|) \cdot \|SOC(j) - 75\|^4 \cdot k_2 \\ & + \delta_1(\|MHL(j) - 48\|) \cdot \|MHL(j) - 48\|^4 \cdot k_3 \\ & \left. + \delta_2(\|MHL(j) - 75\|) \cdot \|MHL(j) - 75\|^4 \cdot k_4 \right) \end{aligned}$$

where $k_i = 0.0001$ are weights that penalize the proximity of the output constraints.

The total operation cost is a weighted sum of these three cost:

$$h_{op}(\mathbf{y}, \mathbf{u}) = \lambda_1 J_{SM} + \lambda_2 J_{DZ} + \lambda_3 J_{RB}$$

where λ_i are technologic-economic weights which designate the influence of each operational cost in the global economic function.

4.3 Simulation results

In this section two main scenarios are proposed. In the first scenario, the convergence of the controlled system to the optimal operation trajectory is demonstrated. In the second scenario, the capability of the controller to operate the plant in presence of abrupt changes in the cost parameters is shown. All the simulations have been carried out using the high order nonlinear model presented in (Valverde et al., 2013b).

The simulations were made in *Matlab 2013a* in a computer with i7-4700 processor and 16 GB of RAM. The controller implemented was defined by the optimization problem (3.6) presented in chapter 3. Although the system is linear, the resulting optimization problem is non linear because the complexity of the optimization problem would be much higher if a nonlinear model was used for the system. This difference is more important in the case of periodic operation because the prediction horizon (at least for the artificial trajectory) must be equal to the period, and hence leads to optimization problems with a large number of optimization variables.

The optimization problem was solved using a sequential quadratic programming algorithm implemented in the function *fmincon* provided by Matlab. The solver used was *fmincon* with the *sqp* algorithm. The period of the problem was $T = 48$ and the prediction horizon was $N = 24$. Thus the number of decision variables needed to solve the optimization problem was $4T + 4N = 288$. The average time needed to solve the optimization problem was about 190-240 seconds, which is lower than the sampling time of 1800 seconds.

The renewable generation power of PV system has been obtained using a sunny day profile shown in figure 4.4(a). The internal demand of the microgrid is shown in figure 4.4(b). This demand profile correspond to the standard demand of a house in a 24h. period. The known and periodic disturbances are obtained subtracting the demand profile to the generation profile and it is shown in figure 4.4(c). These profiles are assumed to be periodic with a period of 24h.

The prices of intraday market used in this chapter are taken from the OMI-Polo Español S.A. (OMIE) web page (www.omel.es). These data correspond to June 24, 2014. The price curve and the power agreed with the EU are shown in figure 4.4. The weighting terms of the economic cost function have been taken as $\beta_1 = 10$ and $\beta_2 = 0.2$ to balance the unitary cost of operating the plant with the unitary cost of the energy dispatch.

This approach can be applied to others microgrids with for example distributed generators or shiftable loads taking into account appropriate changes in the cost function, in particular, in the degradation cost of equipments. The generation power and internal loads are assumed to be known and are considered in the controller as disturbances of the system. A change in the generation systems or in the loads are traduced as a change in the disturbances. The proposed controller has a certain degree of robustness (inherited from the receding horizon scheme) to disturbance changes.

4.3.1 First scenario: convergence.

In this scenario, the microgrid is only allowed to sell power to the EU using the prices of the figure 4.4 between 07:00 and 16:00. The price to buy energy is 0.12 e.u.

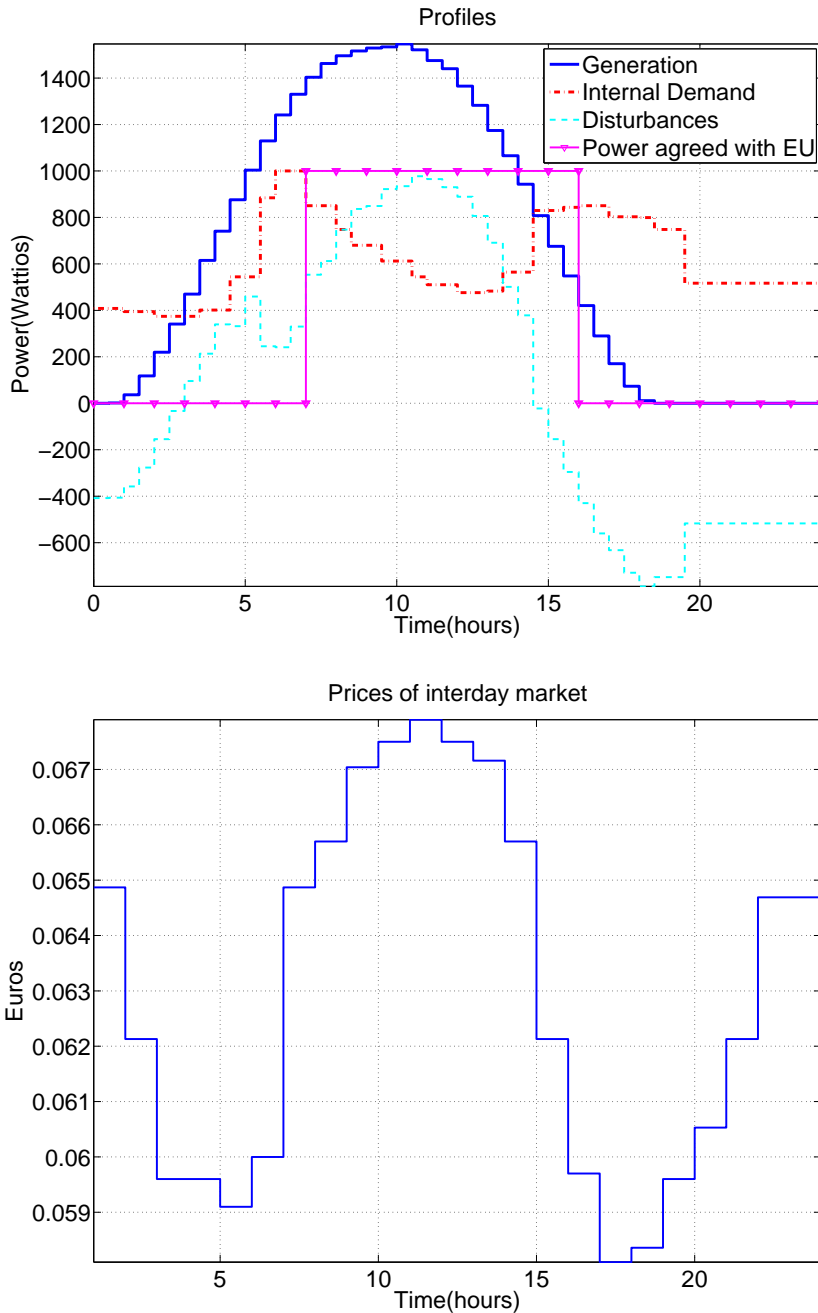


Figure 4.4 (a) Power profiles:(continuous) generation profile, (dash-dot) demand profile, (discontinues) disturbances obtained from generation and demand profile (generation minus demand) and (market continuous) power agreed with the EU; (b) prices profile: prices of intraday market.

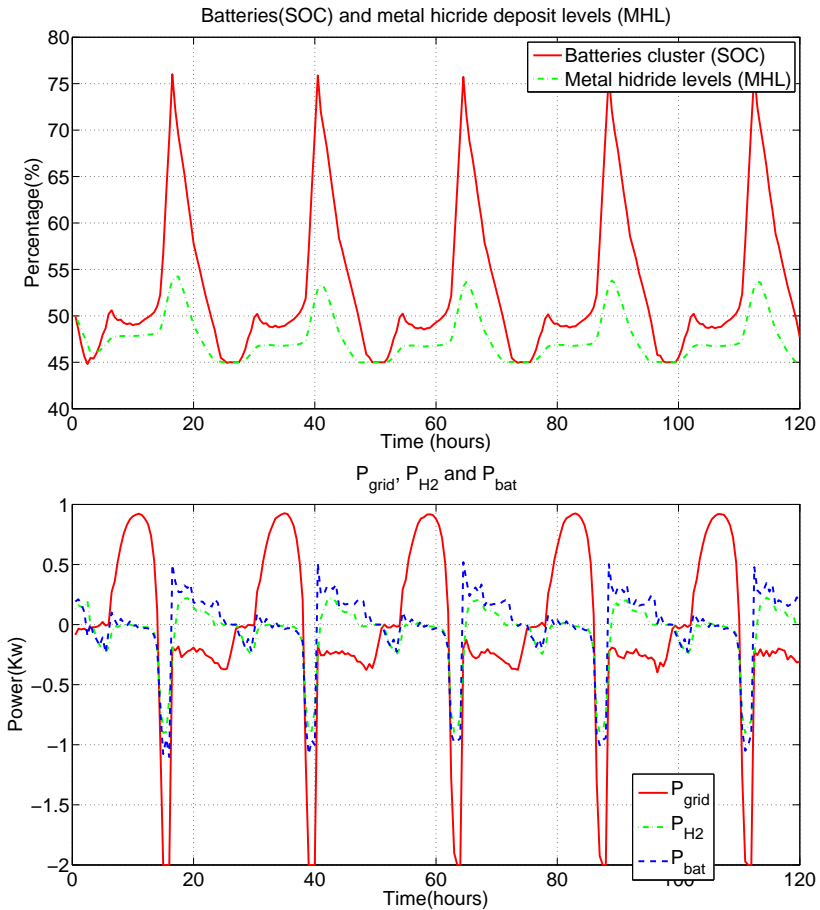


Figure 4.5 (a) Batteries and metal hidride levels, (b) power profiles P_{grid} , P_{H2} and P_{bat} for scenario 1.

Figure 4.5(a) shows the evolution of the batteries and metal hydride levels SOC and MHL. Figure 4.5(b) shows the power profiles P_{grid} , P_{H2} and P_{bat} . As shown in these 4.5, the controller tries to buy only the energy needed to maintain the SOC and MHL minimum levels. Between 07:00 and 16:00, the controller sells all the energy generated by the PV to the EU. Note that the controller buys energy when the selling price is lower. The evolution of the SOC is stabilized following a periodic trajectory near to its lower limit because during the transient, the energy extracted from the storage systems in a period of 24 hours is greater than the energy injected.

Figure 4.6(a) shows the sampling time cost of the economic function. Figure 4.6(b) shows the accumulated cost of the economic function. These figures show that the economic cost decreases when the microgrid sells energy to the EU and that it converges to a periodic trajectory which is optimal from an economic point of view.

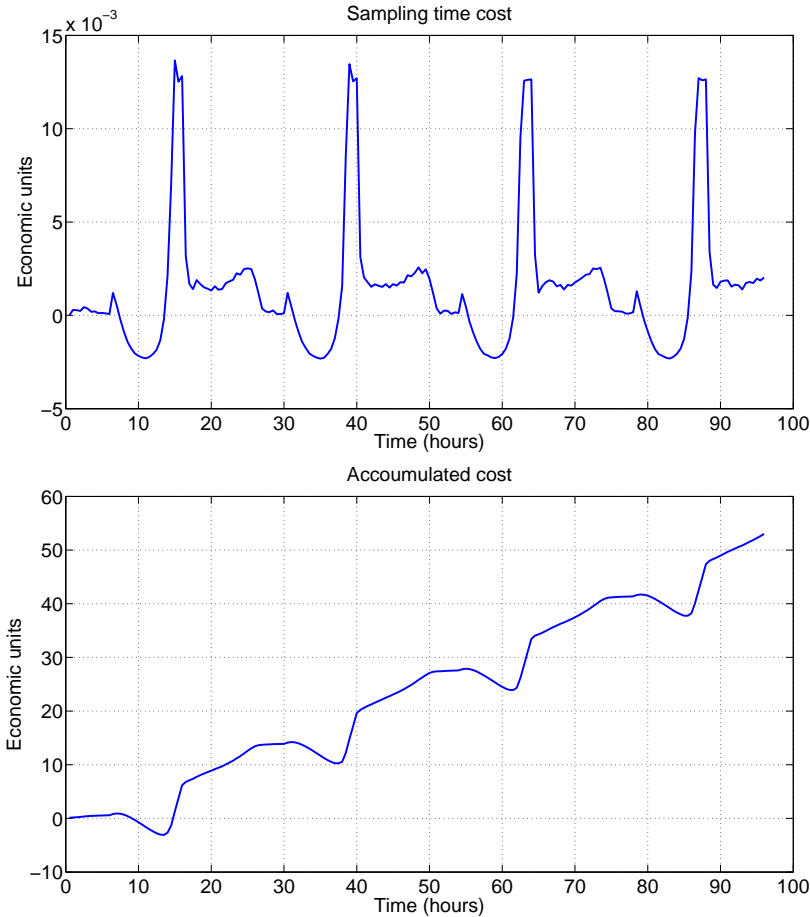


Figure 4.6 Sampling time cost and accumulated cost for scenario 1.

4.3.2 Second scenario: changing the economic cost

In the second scenario, after 24 hours the variable P_{of} becomes zero and the microgrid can't sell energy. This implies a sudden change in the economic objective function, which modifies the optimal periodic trajectory. In two stage controllers, this sudden change may lead to a loss of feasibility. In the controller used however, the constraints of the MPC problem do not depend on the economic cost function, and hence recursive feasibility is guaranteed by design.

Figure 4.7(a) shows the evolution of the batteries and metal hydride levels SOC and MHL. Figure 4.7(b) shows the power profiles P_{grid} , P_{H2} and P_{bat} . These figures show the change in the behavior of the storage systems after the cost function changes and how the controller maintains recursively feasibility. In this scenario the storage systems reaches its steady state near to the upper constraint because it cannot sell the excess of energy.

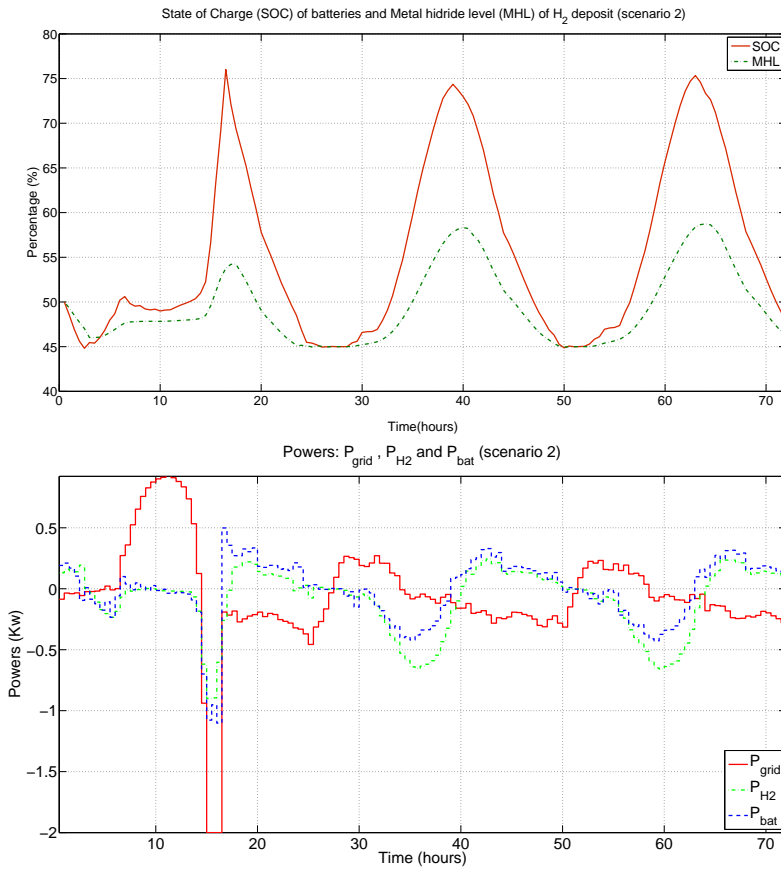


Figure 4.7 (a) Batteries and metal hydride levels and (b) power profiles P_{grid} , P_{H_2} and P_{bat} for scenario 2.

The simulation results was obtained using a high order model of a microgrid and was demonstrated that periodic economic MPC is an appropriate approach to control this class of systems to guarantee optimal performance from an economic point of view in the presence of sudden changes on the economic criterion.

5 Robust model predictive controller for tracking periodic signals

Any statement about "robustness" of a particular control algorithm must make reference to a specific uncertainty range as well as specific stability and performance criteria

ALBERT BEMPORAD AND MANFRED MORARI, 1999

The controllers presented in the previous chapters have demonstrated to be good control solutions to the problem of controlling periodic systems under the assumption that there are not mismatches between the prediction model and the real plant model. It has also shown that these controllers are inherently robust and can successfully control the plant if the model mismatches are small enough. However, if there exists model mismatches, the stability property can be ensured if these mismatches are taken into account in the design of the controller. This leads to the design of robust controllers.

This chapter presents a novel robust model predictive control for tracking periodic signals formulation based on nominal predictions and constraint tightening. The control scheme proposed in chapter 2 is extended to take into account bounded additive uncertainties following the constraint tightening method proposed in Alvarado et al. (2010a). The proposed controller joins robust dynamic trajectory planning and a robust MPC for tracking in a single optimization problem, see figure 5.1. It guarantees that the perturbed closed-loop system converges asymptotically to a neighborhood of an optimal reachable periodic trajectory while satisfying the state and input constraints for all possible uncertainties. In addition, recursive feasibility is ensured even in the presence of sudden changes in the target reference.

Two design procedures are presented: (i) based on a robust positive invariant terminal region, (ii) based on an equality terminal constraint. The properties of the proposed controller are demonstrated with a simulation in a illustrative example of a ball and plate

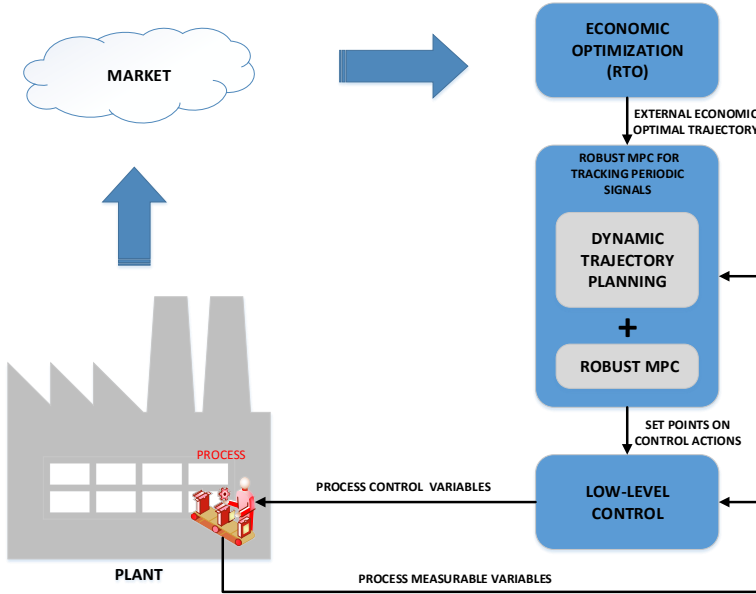


Figure 5.1 Hierarchical control structure of the robust model predictive control for tracking periodic signals.

system. The results of this chapter have been submitted as regular paper to the *IEEE Trans. Aut. Control* and a technical report of this work can be found in Pereira et al. (2015b).

5.1 Problem formulation

In this chapter, we consider the following class of discrete time linear systems subject to bounded additive uncertainties

$$x(k+1) = Ax(k) + Bu(k) + w(k) \tag{5.1a}$$

$$y(k) = Cx(k) + Du(k) \tag{5.1b}$$

where $x(k) \in \mathbb{R}^n$, $u(k) \in \mathbb{R}^m$ and $w(k) \in \mathbb{R}^n$ are the state, the input and the uncertainty at sampling time k respectively. The uncertainty is known to be confined in the convex compact polytope containing the origin in its interior \mathcal{W} . We denote as nominal model system (5.1) with $w(k)$ null.

The state and input trajectories must satisfy the $x(k) \in \mathcal{X}$ and $u(k) \in \mathcal{U}$ for all sampling times k where the set \mathcal{U} is a convex, compact polytope containing the origin in its interior and the set \mathcal{X} is a convex closed polyhedron.

The control objective is to steer the output of the system as close as possible to an exogenous periodic target reference with period T defined as \mathbf{r} . It is important to remark

that no assumption is considered in the provided reference beyond its periodicity; that is, there may not exist a control law capable of steering the system to this reference signal (even for the nominal system) or it may not satisfy the system constraints. In any case the controller must converge to a periodic trajectory that optimizes a certain criterion while satisfying the constraints for all possible uncertainties.

In addition, the reference can be subject to sudden changes. For this reason, the reference is included as one of the input parameters of the controller in addition to the state measurement. Standard tracking schemes are usually based on a hierarchical architecture in which a trajectory planner computes the optimal reachable trajectory which is then used by a MPC as a target reference. This implies that the MPC controller depends on this optimal trajectory and that two different optimization problems have to be solved. In addition, standard MPC methods for tracking are generally based on optimization problems whose feasible region depends on the reference signal. This implies that feasibility can be lost if a sudden change in the reference takes place as mentioned before. As it will be demonstrated later on, the proposed control law will deal with the case that the periodic reference signal is suddenly changed and this may differ from the previous sample time without having to redesign the parameters or loosing feasibility.

For the sake of clarity of presentation, the results are shown for the case in which the system to be controlled is modeled as a linear time invariant system subject to global uncertainty of the form (5.1). However, these results can be extended to more complex models that takes into account periodic dynamics and constraints, measurable disturbances and/or algebraic equations. In Pereira et al. (2015b) this controller has been applied to a system modeled with an differential-algebraic model subject to a measurable periodic disturbances.

5.2 Controller formulation

The proposed robust controller is based on the MPC for tracking periodic references presented in chapter 2 but extended to cope with the uncertainty using the ideas of Alvarado et al. (2010a). The controller is based on augmenting the decision variables with a set of auxiliary variables that describe a future, periodic and admissible artificial reference $\mathbf{x}^r, \mathbf{u}^r$ and taking into account in the control decision both the deviation of the predicted trajectory to the artificial reference, and the deviation of the artificial reference the target periodic reference.

To this end, the predictive control law is derived from the solution of an optimization problem that minimizes a cost function $V_N(\cdot)$ that includes two terms. The first term $V_l(\cdot)$ penalizes the deviation of a N step predicted trajectory starting from the current state, from the artificial reference. The second term $V_p(\cdot)$ penalizes the deviation of the artificial reference from the target reference over a period. The cost function is defined as follows:

$$V_N(x, \mathbf{r}; \mathbf{x}, \mathbf{u}, \mathbf{x}^r, \mathbf{u}^r) = V_l(x; \mathbf{x}, \mathbf{u}, \mathbf{x}^r, \mathbf{u}^r) + V_p(\mathbf{r}; \mathbf{x}^r, \mathbf{u}^r)$$

with

$$V_l(x; \mathbf{x}_N, \mathbf{u}_N, \mathbf{x}^r, \mathbf{u}^r) = \sum_{i=0}^{N-1} \|x(i) - x^r(i)\|_Q^2 + \|u(i) - u^r(i)\|_R^2 + \|x(N) - x^r(N)\|_P^2$$

$$V_p(\mathbf{r}; \mathbf{x}^r, \mathbf{u}^r) = \sum_{i=0}^{T-1} \|y^r(i) - r(i)\|_S^2$$

where Q, R, P and S are suitable positive definite matrices and

$$y^r(i) = Cx^r(i) + Du^r(i)$$

The optimization variables $(\mathbf{x}, \mathbf{u}, \mathbf{x}^r, \mathbf{u}^r)$ are the predicted sequences of states and inputs of the system trajectory and the artificial trajectory respectively. These are defined by the as follows:

$$\mathbf{x}_N = \begin{bmatrix} x(0) \\ \vdots \\ x(N) \end{bmatrix}, \mathbf{u}_N = \begin{bmatrix} u(0) \\ \vdots \\ u(N-1) \end{bmatrix}, \mathbf{x}^r = \begin{bmatrix} x^r(0) \\ \vdots \\ x^r(T) \end{bmatrix}, \mathbf{u}^r = \begin{bmatrix} u^r(0) \\ \vdots \\ u^r(T-1) \end{bmatrix}$$

Following Alvarado et al. (2010a), the proposed robust controller requires the design of a local robustly stabilizing control gain K such that $(A + BK)$ has all its eigenvalues in the interior of the unitary circle. Based on this gain, the following sets are defined:

$$\mathcal{X}(i) = \mathcal{X} \ominus \left\{ \bigoplus_{j=0}^{i-1} (A + BK)^j \mathcal{W} \right\} \quad (5.2)$$

$$\mathcal{U}(i) = \mathcal{U} \ominus \left\{ K \bigoplus_{j=0}^{i-1} (A + BK)^j \mathcal{W} \right\} \quad (5.3)$$

where \oplus stands for the Minkowski addition of sets and \ominus stands for the Pontryagin difference of sets. The sets $\mathcal{X}(i)$ and $\mathcal{U}(i)$ are tightened versions of the set of constraints \mathcal{X} and \mathcal{U} . These sets depend both on the size of the uncertainty set W and the local control law K . These conservative sets will be considered as set of constraints of the predicted trajectories in order to ensure robust constraint satisfaction, as it will be proved in the next section. It is important to remark that the local control gain K must be designed in a way such that these sets are not empty. There is a trade-off between perturbation rejection (which affects the size of $\mathcal{X}(i)$) and the amount of control effort used (which affects the size of $\mathcal{U}(i)$). This design challenge is inherent to semi-feedback prediction schemes, see for example Alvarado et al. (2010a) and Mayne et al. (2005).

In order to derive a stabilizing constraint, a suitable terminal control gain K_f and a suitable (robust) invariant set Ω is computed. Thus, the terminal region is given by

$$X_f = \Omega \ominus (A + BK)^{N-1} \mathcal{W} \quad (5.4)$$

Similarly to the set of constraints, the terminal region X_f is a (robust invariant) set Ω

tightened by a measure of the effect of the uncertainty in the predicted terminal state. On the other hand, the artificial trajectory is also subject to tighter constraints given by the sets

$$\mathcal{X}^r = \mathcal{X}(N) \ominus X_f \quad (5.5)$$

$$\mathcal{U}^r = \mathcal{U}(N-1) \ominus K_f \Omega \quad (5.6)$$

In the following section the design assumptions that these ingredients must satisfy to guarantee some closed-loop properties are defined.

The proposed robust model predictive for tracking periodic references is derived from the solution of the following optimization problem

$$\min_{\mathbf{x}_N, \mathbf{u}_N, \mathbf{x}^r, \mathbf{u}^r} V_N(x, \mathbf{r}; \mathbf{x}_N, \mathbf{u}_N, \mathbf{x}^r, \mathbf{u}^r) \quad (5.7a)$$

$$s.t. \quad x(0) = x \quad (5.7b)$$

$$x(i+1) = Ax(i) + Bu(i) \quad i \in \{0, 1, \dots, N-1\} \quad (5.7c)$$

$$x(i) \in \mathcal{X}(i) \quad i \in \{0, \dots, N\} \quad (5.7d)$$

$$u(i) \in \mathcal{U}(i) \quad i \in \{0, \dots, N-1\} \quad (5.7e)$$

$$x(N) - x^r(N) \in X_f \quad (5.7f)$$

$$x^r(i+1) = Ax^r(i) + Bu^r(i) \quad i \in \{0, 1, \dots, T-1\} \quad (5.7g)$$

$$x^r(i) \in \mathcal{X}^r \quad i \in \{0, \dots, T\} \quad (5.7h)$$

$$u^r(i) \in \mathcal{U}^r \quad i \in \{0, \dots, T-1\} \quad (5.7i)$$

$$x^r(T) = x^r(0) \quad (5.7j)$$

The optimal solution of this optimization problem is denoted as $(\mathbf{x}_N^*, \mathbf{u}_N^*, \mathbf{x}^{r*}, \mathbf{u}^{r*})$ and its a functions of x and \mathbf{r} . Analogously, the optimal cost function is denoted as $V_N^*(x, \mathbf{r})$.

Constraints (5.7b-5.7c) define the predicted trajectories of the system starting from the current state. Constraints (5.7g) and (5.7j) define the planned periodic reachable reference starting from the free initial state $x^r(0)$. Constraints (5.7d) and (5.7e) include the state and input constraints for the predicted states and inputs. These constraints depend on the tightened sets defined above and are different for each prediction step i . Constraints (5.7h) and (5.7i) include the state and input constraints for the artificial reference. These constraints depend on the tightened sets defined above but are constant for all prediction steps i . In addition, a terminal constraints are included to guarantee closed-loop convergence to the optimal reachable trajectory. Constraint (5.7f) guarantees that the terminal state of the predicted trajectory of the plant reaches a neighborhood of the planned reachable trajectory at the end of the prediction horizon. These constraints are designed to guarantee recursive feasibility of the close-loop system; that is, starting from an initial state inside the feasibility region of the optimization problem denoted domain of attraction, it is guaranteed that the closed-loop system will remain inside this region for all possible uncertainties.

It is important to point out that the set of constraints of this optimization problem does not depend on the reference signal \mathbf{r} . This implies that the sets of states where the optimization problem is feasible does not depend on \mathbf{r} . This set is denoted as \mathcal{X}_N and can

be defined as the set of states that can admissibly reach any reachable periodic trajectory in N steps. In general this set is large if compared with the set of states that can admissibly reach a particular reachable periodic trajectory.

At each time step k , the periodic reference signal $\mathbf{r}(k)$ used to define the controller is different because the initial time of the sequence changes. With a slight abuse of notation, we define \mathbf{r} as the target periodic reference, and $\mathbf{r}(k)$ the reference fed to the controller which takes into account the time shift. The control law is given by the first input of the optimal reachable predicted trajectory,

$$\kappa_N(x(k), \mathbf{r}(k)) = u_N^*(0; x(k), \mathbf{r}(k)) \quad (5.8)$$

In the following section is studied the stabilizing design of the proposed controller and the robust stability of the controlled system is proved.

5.3 Robust stability of the controlled system

In this section we study the closed-loop properties of the proposed controller. We prove that the closed-loop system converges asymptotically robustly satisfying the constraints to a neighborhood of an optimal reachable trajectory which can be obtained solving an optimization problem. To this end we prove that the deviation of the system from the optimal reachable trajectory is input-to-state stable with respect to the uncertainty, that is, the size of the region in which the deviation is bounded has an explicit dependence with the size of the region in which the uncertainty is bounded. The controller maintains feasibility and convergence even in the presence of sudden changes in the target reference.

In order to guarantee these properties, the controller must be designed appropriately. In particular, the following design assumptions must hold:

Assumption 5.3.1 *The weighting matrices Q , R , P and S , the controller gains K , K_f and the set Ω satisfy the following conditions:*

1. *System 5.1 is controllable.*
2. *Matrices Q , R and S are positive definite.*
3. *The eigenvalues of the matrices $(A + BK)$ and $(A + BK_f)$ are in the interior of the unitary circle.*
4. $(A + BK_f)^T P (A + BK_f) - P = -(Q + K_f^T R K_f)$
5. *The set Ω is compact polytope (as small as possible) such that*

$$(A + BK_f)\Omega \subseteq \Omega \ominus (A + BK)^{N-1} \mathcal{W}$$

6. *The sets $\mathcal{X}(i)$ and $\mathcal{U}(i)$ are non-empty for $i = 0, \dots, N - 2$.*
7. *The sets \mathcal{X}^r and \mathcal{U}^r are non-empty.*
8. *The optimization problem (5.7) is strictly convex.*

Note that under this assumption, the terminal set X_f defined in (5.4) is non-empty by definition.

The optimal reachable trajectory of the plant $(\mathbf{x}^\circ, \mathbf{u}^\circ)$ is the nominal trajectory that minimizes the following optimization problem

$$(\mathbf{x}^\circ, \mathbf{u}^\circ) = \arg \min_{\mathbf{x}^r, \mathbf{u}^r} V_p(\mathbf{r}; \mathbf{x}^r, \mathbf{u}^r) \quad (5.9a)$$

$$s.t. \quad x^r(i+1) = Ax^r(i) + Bu^r(i) \quad i \in \{0, 1, \dots, T-1\} \quad (5.9b)$$

$$x^r(i) \in \mathcal{X}^r \quad i \in \{1, \dots, T\} \quad (5.9c)$$

$$u^r(i) \in \mathcal{U}^r \quad i \in \{0, \dots, T-1\} \quad (5.9d)$$

$$x^r(T) = x^r(0) \quad (5.9e)$$

This is the admissible trajectory (according to the tighter set of constraints) that minimizes the cost function $V_p(\cdot)$ which measures the distance to the reference \mathbf{r} . It is important to remark that this trajectory is uniquely defined since from the Assumption 5.3.1 we derive that the optimization problem (5.9) is feasible and strictly convex. Note that in order to implement the proposed controller the optimal periodic trajectory is not needed. This implies that the closed-loop system reacts automatically to a sudden change in the reference or in the cost weights converging to the new optimal trajectory without having to modify the MPC design.

It can be seen that the optimization problem is similar to the MPC optimization problem, but optimizing only the artificial reference to minimize the tracking cost while satisfying the tightened set of constraints. Note that the constraints (5.7h) and (5.7i) of the optimization problem depends on the prediction horizon of the corresponding controller N . In the nominal case the optimal periodic trajectory is independent of the prediction horizon of the MPC controller.

We will prove that the optimal admissible trajectory is a robustly stable trajectory of the system in the input-to-state stability sense, which is defined as follows.

Definition 5.3.1 The periodic trajectory \mathbf{x}° is an input-to-state stable trajectory for the controlled system with a domain of attraction X_N if for all $x(0) \in X_N$, then $x(k) \in X_N$ and there exists a \mathcal{KL} function $\beta(\cdot)$ and a \mathcal{K} function $\sigma(\cdot)$ such that

$$\|x(k) - x^\circ(k)\| \leq \beta(\|x(0) - x^\circ(0)\|, k) + \sigma(\|\mathbf{w}_k\|_\infty)$$

for all $k \geq 0$. $\|\mathbf{w}_k\|_\infty$ denotes the maximum value of $\|w(i)\|$ for all $i \in \{0, \dots, k-1\}$.

As stated in Limon et al. (2009a) (and references there in), input-to-state stability implies that the controlled system is ultimately bounded in a neighborhood of the trajectory \mathbf{x}° and that the system converges asymptotically to the trajectory if the uncertainty is vanishing. Besides, if the uncertainty signal is a function of the state of the plant (i.e. parametric uncertainty) and this is bounded by a certain stability margin function, then the controlled system converges asymptotically to the trajectory \mathbf{x}° .

In the following theorem it is stated the input-to-state stability of the trajectory \mathbf{x}° which is the main result of the chapter.

Theorem 5.3.1 *Assume that conditions given in Assumption 5.3.1 hold. Then system (5.1) controlled by the proposed control law $u(k) = \kappa_N(x(k), \mathbf{r}(k))$ is recursively feasible and the optimal periodic reachable trajectory \mathbf{x}° is input-to-state stable with a region of attraction \mathcal{X}_N , i.e. the closed loop system is stable and $x(k)$ converges asymptotically to a neighborhood of $\mathbf{x}^\circ(k)$ for all $x(0) \in \mathcal{X}_N$.*

Proof. In order to prove the theorem, we first prove that if the initial state is inside the feasibility region of the optimization problem, the closed-loop system will remain inside this region; i.e. the closed-loop system is recursively feasible. Then, asymptotic stability will be proved by demonstrating that for the system that models the error between the state of the reachable optimal trajectory and the closed loop trajectory of the system the function

$$W(x(k) - x^\circ(k)) = V_N^*(x(k), \mathbf{r}(k)) - V_p^\circ(\mathbf{r}) \quad (5.10)$$

is an input-to-state Lyapunov function Limon et al. (2009a). This function is defined as the difference between the optimal cost of the MPC problem at time k and the cost value of the optimal reachable trajectory.

The proof is divided into two parts: first recursive feasibility of the optimization problem is demonstrated and then, input-to-state stability of the optimal reachable trajectory is proved.

Recursive feasibility

We define next the shifted solution at time $k + 1$ obtained from the optimal solution at time k and some corrections provided by the feedback policy K as proposed in Alvarado et al. (2010a). We use the notation $(i|k)$ to denote the time step to which a given variable is referred.

$$\begin{aligned} u^{rs}(i|k+1) &= u^{r*}(i+1|k), \quad i = 0, \dots, T-2 \\ u^{rs}(T-1|k+1) &= u^{r*}(0|k) \\ x^{rs}(i|k+1) &= x^{r*}(i+1|k), \quad i = 0, \dots, T-1 \\ x^{rs}(T|k+1) &= x^{r*}(1|k) \\ u^s(i|k+1) &= u^*(i+1|k) + K(x^s(i|k+1) - x^*(i+1|k)), \quad i = 0, \dots, N-2 \\ u^s(N-1|k+1) &= u^{rs}(N-1|k+1) + K_f(x^s(N-1|k+1) - x^{rs}(N-1|k+1)) \\ x^s(0|k+1) &= x(k+1) = Ax(k) + Bu^*(0|k) + w(k) \\ x^s(i+1|k+1) &= Ax^s(i|k+1) + Bu^s(i|k+1), \quad i = 0, \dots, N-1 \end{aligned}$$

Since $x^*(0|k) = x(k)$, we have that

$$x^s(0|k+1) - x^*(1|k) = w(k)$$

As it has been proved in Alvarado et al. (2010a) the error between the optimal trajectory at k and the shifted one is given by

$$x^s(i+1|k+1) - x^*(i+2|k) = (A + BK)(x^s(i|k+1) - x^*(i+1|k))$$

for $i = 0, \dots, N-1$. Since $w(k) \in \mathcal{W}$, the following condition holds

$$x^s(i|k+1) - x^*(i+1|k) \in (A+BK)^i \mathcal{W} \quad (5.12)$$

Proceeding similarly for the shifted input, the following inequalities hold for $i = 0, \dots, N-2$

$$u^s(i|k+1) - u^*(i+1|k) \in K(A+BK)^i \mathcal{W}$$

Based on these results, it will be proved that the shifted solution is feasible for the optimization problem at $k+1$. It is immediate to see that the constraints (5.7b), (5.7c), and (5.7g) - (5.7j) are satisfied. The remaining constraints are proved next.

- Constraint (5.7f): The shifted solution is such that $x^s(N-1|k+1) - x^*(N|k) \in A_K^{N-1} \mathcal{W}$. Since the optimal solution at k satisfies the constraint (5.7f), we can infer that

$$\begin{aligned} \Delta x^s &= x^s(N-1|k+1) - x^{rs}(N-1|k+1) \\ &= x^s(N-1|k+1) - x^{rs}(N|k) \\ &= (x^s(N-1|k+1) - x^*(N|k)) + (x^*(N|k) - x^{rs}(N|k)) \\ &\in (A+BK)^{N-1} \mathcal{W} \oplus X_f \subseteq \Omega \end{aligned}$$

Applying the shifted input $u^s(N-1|k+1)$, then

$$x^s(N|k+1) - x^{rs}(N|k+1) = (A+BK_f)(x^s(N-1|k+1) - x^{rs}(N-1|k+1))$$

Therefore $x^s(N|k+1) - x^{rs}(N|k+1) \in (A+BK_f)\Omega \subseteq \Omega \ominus (A+BK)^{N-1} \mathcal{W} = X_f$.

- Constraint (5.7d): The optimal solution satisfies that $x^*(i+1|k) \in \mathcal{X}(i+1)$. On the other hand

$$x^s(i|k+1) - x^*(i+1|k) \in (A+BK)^i \mathcal{W}$$

and then

$$x^s(i|k+1) = x^*(i+1|k) + (x^s(i|k+1) - x^*(i+1|k)) \in \mathcal{X}(i+1) \oplus (A+BK)^i \mathcal{W} \subseteq \mathcal{X}(i)$$

for all $i = 0, \dots, N-1$. For $i = N$, we have proved that

$$x^s(N|k+1) - x^{rs}(N|k+1) \in X_f$$

As $x^{rs}(N|k+1) = x^{r*}(N+1|k) \in \mathcal{X}^r = \mathcal{X}(N) \ominus X_f$, then $x^s(N|k+1) \in \mathcal{X}(N) \ominus X_f \oplus X_f \subseteq \mathcal{X}(N)$.

- Constraint (5.7e): The optimal solution satisfies that $u^*(i+1|k) \in \mathcal{U}(i+1)$. On the other hand

$$x^s(i|k+1) - x^*(i+1|k) \in (A+BK)^i \mathcal{W}$$

and then

$$\begin{aligned} u^s(i|k+1) &= u^*(i+1|k) + K(x^s(i|k+1) - x^*(i+1|k)) \\ &\in \mathcal{U}(i+1) \oplus K(A+BK)^i \mathcal{W} \subseteq \mathcal{U}(i) \end{aligned}$$

for all $i = 0, \dots, N-2$. For $i = N-1$, since $x^s(N-1|k+1) - x^{rs}(N-1|k+1) \in \Omega$ and $u^{rs}(N-1|k+1) = u^{rs}(N|k) \in \mathcal{U}^r = \mathcal{U}(N-1) \ominus K_f \Omega$, we have that

$$\begin{aligned} u^s(N-1|k+1) &= u^{rs}(N-1|k+1) + K_f(x^s(N-1|k+1) - x^{rs}(N-1|k+1)) \\ &\in \mathcal{U}(N-1) \ominus K_f \Omega \oplus K_f \Omega \subseteq \mathcal{U}(N-1) \end{aligned}$$

Figure 5.2 shows an example of one dimensional shifted state trajectories. In blue triangles the optimal artificial trajectory is shown for both time step $k = 0$ and $k = 1$. In red circles the optimal trajectory at time step $k = 0$ is shown. After four time steps (the prediction horizon), the difference between the artificial reference and the optimal trajectory is inside the terminal region denoted with a magenta ellipsoid¹. In green squares the shifted trajectory at time step $k = 1$ is shown. It can be seen that it deviates from the previous optimal trajectory because of the uncertainty. However, the deviation is corrected in the predictions by the local controller K , and this deviation converges asymptotically to zero as $(A+BK)^i w(0)$. The shifted trajectory last input is defined by the artificial reference, so it follows the blue trajectory. Although there is a difference between the shifted trajectory and the artificial reference, is inside the robust positive invariant of the local controller K_f for an uncertainty bounded in $(A+BK)^N \mathcal{W}$, so it is guaranteed that the nominal prediction lies inside X_f .

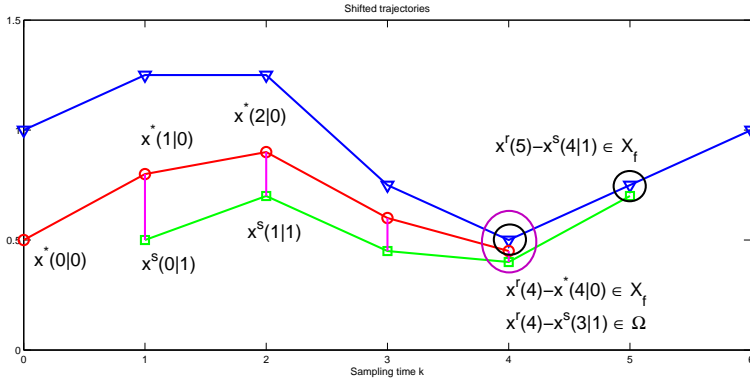


Figure 5.2 Example of shifted state trajectories considering a terminal region and a terminal controller..

Stability

¹ The terminal regions are shown as ellipsoids for aesthetic reasons, although they should be a segment because the state has dimension one.

Stability is proved by demonstrating that the function

$$W(x - x^\circ) = V_N^*(x, \mathbf{r}) - V_p(\mathbf{r}; \mathbf{x}^\circ, \mathbf{u}^\circ)$$

is an ISS Lyapunov function (Limon et al. (2009a)). Using similar arguments to the stability proof of the nominal case (Limon et al. (2015)), we have that there exists positive constants α_1 , α_2 and α_3 such that

$$\alpha_1 \|x(k) - x^\circ(k)\|^2 \leq W(x(k) - x^\circ(k)) \leq \alpha_2 \|x(k) - x^\circ(k)\|^2 \quad (5.13)$$

$$W(x(1|k) - x^\circ(k+1)) - W(x(k) - x^\circ(k)) \leq -\alpha_3 \|x(k) - x^\circ(k)\|^2 \quad (5.14)$$

On the other hand, we have that $x(k+1) = x(1|k) + w(k)$. Since the optimal cost function $V_N^*(x, \mathbf{r})$ is a convex function of x defined in a compact set, then it is Lipschitz continuous. This means that there exists a positive constant γ such that

$$W(x(k+1) - x^\circ(k+1)) - W(x(1|k) - x^\circ(k+1)) \leq \gamma \|w(k)\|$$

Therefore, we have that

$$\begin{aligned} \Delta W &= W(x(k+1) - x^\circ(k+1)) - W(x(k) - x^\circ(k)) \\ &\quad - W(x(k+1) - x^\circ(k+1)) \\ &\quad - W(x(1|k) - x^\circ(k+1)) + W(x(1|k) - x^\circ(k+1)) \\ &\quad - W(x(k) - x^\circ(k)) \\ &\leq \gamma \|w(k)\| - \alpha_3 \|x(k) - x^\circ(k)\|^2 \end{aligned}$$

and then $W(\cdot)$ is an ISS Lyapunov function which completes the proof ■

A relevant property of the proposed controller is that the recursive feasibility has been proved irrespective of the actual value of the reference \mathbf{r} since the set of constraints in the optimization problem does not depend on this. Therefore this implies that a sudden change of r does not affect the recursive feasibility property of the closed-loop system. Besides, if the reference remains the same for a sufficient period of time, the system converge to a neighborhood of the new optimal reachable trajectory.

The proposed controller requires the calculation of the terminal ingredients: a stabilizing gain K_f and a small robust positively invariant set Ω . There exists efficient algorithms to compute these ingredients, but their complexity grows exponentially with the dimension of the system to be controlled. Then, from a practical point of view, it is very interesting to take K such that the eigenvalues $\lambda_i(A + BK) = 0$, since in this case $(A + BK)^{N-1} \mathscr{W}$ is $\{0\}$ and then the stabilizing terminal ingredients can be chosen as $K_f = 0$, $P = 0$ and $X_f = \{0\}$. This is equivalent to consider a terminal equality constraint $x(N) = x^r(N)$. In figure 5.3, it is illustrated the different trajectories in the case of using a terminal equality constraint.

It's worth remarking that in practice it suffices to design a K such that $\sigma = \max_{w \in \mathscr{W}} \|(A + BK)^{N-1} w\|$ is sufficiently small w.r.t. to the precision of the optimization solver. For

instance if the set \mathcal{W} is the unitary ball and $N = 30$, then taking a control gain K such that $\|A + BK\| \leq 0.28$, then the value of σ is lower than 10^{-16} and if $\|A + BK\| \leq 0.57$ then σ is lower than $\leq 10^{-7}$. These values of σ are smaller than the matlab spacing for double and single precision respectively. Therefore, introducing this practical relaxation makes the design more flexible since it is not necessary to guarantee that $\lambda_i(A + BK) = 0$. In Pereira et al. (2015b) this controller design has been applied to a drinking water network which accounts for 17 states (the level of the tanks) and 61 inputs (manipulable flows). In the example section, this design procedure has been used to carry out the simulations.

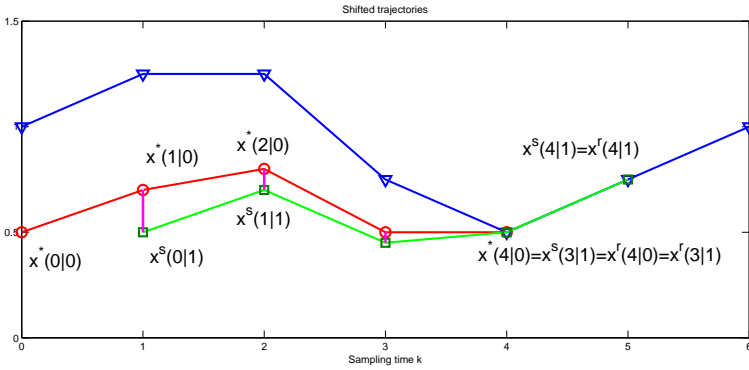


Figure 5.3 Example of shifted state trajectories considering an equality terminal constraint.

5.4 Application to a ball and plate system

In this section we apply the proposed controller to a linear approximation of the same ball and plate system used in one of the examples of chapter 2, but including bounded disturbances. Figure 2.2 shows a schematic of the system.

To carry out the simulations, the same nonlinear model presented in Section 2.5 is used, but including an unknown but bounded perturbation in the acceleration of the ball denoted as

$$w_e(t) = [w_{e1}, w_{e2}]$$

. This perturbation is supposed to satisfy $\|w_e\|_\infty \leq 0.2m/s^2$. The state $x \in \mathbb{R}^8$ is defined as follows

$$x^T = [z_1, \dot{z}_1, \theta_1, \dot{\theta}_1, z_2, \dot{z}_2, \theta_2, \dot{\theta}_2]^T$$

We consider the following constraints in the position, angles and inputs:

$$\begin{aligned} |z_i| &\leq 0.06 \quad m, i = 1, 2 \\ |\theta_i| &\leq \frac{\pi}{2} \quad rad, i = 1, 2 \\ |u_i| &\leq 110 \quad rad/s^2, i = 1, 2 \end{aligned}$$

To apply the proposed MPC control scheme, a discrete time linear system is obtained taking as equilibrium point the origin for all the states and inputs and a sampling time of 0.05 seconds. The matrices that define system (5.1) are the following

$$A = \begin{pmatrix} 1 & 0.05 & 0.0088 & 0.0001 & 0 & 0 & 0 & 0 \\ 0 & 1 & 0.35 & 0.0088 & 0 & 0 & 0 & 0 \\ 0 & 0 & 1 & 0.05 & 0 & 0 & 0 & 0 \\ 0 & 0 & 0 & 1 & 0 & 0 & 0 & 0 \\ 0 & 0 & 0 & 0 & 1 & 0.05 & 0.0088 & 0.0001 \\ 0 & 0 & 0 & 0 & 0 & 1 & 0.35 & 0.0088 \\ 0 & 0 & 0 & 0 & 0 & 0 & 1 & 0.05 \\ 0 & 0 & 0 & 0 & 0 & 0 & 0 & 1 \end{pmatrix}$$

$$B = \begin{pmatrix} 0 & 0 \\ 0.0001 & 0 \\ 0.0013 & 0 \\ 0.05 & 0 \\ 0 & 0 \\ 0 & 0.0001 \\ 0 & 0.0013 \\ 0 & 0.05 \end{pmatrix} \quad C = \begin{pmatrix} 1 & 0 & 0 & 0 & 0 & 0 & 0 & 0 \\ 0 & 0 & 0 & 0 & 1 & 0 & 0 & 0 \end{pmatrix}$$

The set of uncertainty in the discrete time system is given by

$$\mathcal{W} = \{w \in \mathbb{R}^8 : w = B_d w_e, \|w_e\|_\infty \leq 0.2\}$$

where

$$B_d = \begin{pmatrix} 0.0013 & 0 \\ 0.05 & 0 \\ 0 & 0 \\ 0 & 0 \\ 0 & 0.0013 \\ 0 & 0.05 \\ 0 & 0 \\ 0 & 0 \end{pmatrix}$$

It is important to remark that the dynamics of variables z_1 and z_2 are decoupled. This model is used both to design the controller and to carry out the simulations. To demonstrate the main properties of the proposed controller we consider only one scenario. The

weighting matrices of the controller are $R = 10 \cdot I^2$, $Q = 100 \cdot I^8$, $S = 7000 \cdot I^2$ where I is the identity matrix of appropriate dimension. The simulations were done in Matlab 2013a using the solver quadprog.

In the proposed scenario the prediction horizon is $N = 28$. The number of decision variables of the optimization problem posed in sequential formulation are $n_u \cdot (N + T) + n_x = 120$. In addition, in order to prove that recursive feasibility is not lost even in the presence of a sudden change in the target reference, in this scenario the reference switches between two geometric figures. First the ball must draw a rectangle of size $6 \times 4\text{cm}$ and is centred in $(4,5)\text{cm}$ with a speed of $11.43 \frac{\text{cm}}{\text{s}}$. At time 3.5 seconds the reference changes in order to draw a circumference with center on $(-4, -4)\text{cm}$ and a radius of 1 cm. The target speed of the second trajectory is $2.3 \frac{\text{cm}}{\text{s}}$. The period length of both references is the same, that is $T = 28$. The initial state of this scenario is the ball in equilibrium at $\{z_1, z_2\} = \{-5, 5\}\text{cm}$.

The local control feedback K used to obtain the reduced set of constraints that guarantee both robust constraint satisfaction and recursive feasibility of the closed-loop controller has been designed using the LMI based procedure presented in D. Limon et al. (2008) with $\lambda = 0.5$ and $\rho = 0.8$. This design procedure provides a tuning parameter to obtain a trade-off between the disturbance rejection and the size of the resulting tightened constraint sets. The controller is the following

$$K = \begin{bmatrix} K_1 & 0 \\ 0 & K_1 \end{bmatrix}$$

where $K_1 = 10^3[-7.2087, -1.3139, -0.7509, -0.0349]$. This local control gain obtained by the previous LMI based procedure D. Limon et al. (2008) satisfies that

$$\max_{w \in \mathcal{W}} \|(A + BK)^{N-1} B_d w\| \leq 2.8475 \cdot 10^{-11}$$

This value is lower than the tolerance of the optimization solver used.

The proposed robust controller has been designed using a terminal equality constraint, as suggested in section 5.3. This avoids the calculation of the robust invariant set Ω , which in this case is a cumbersome procedure. In order to guarantee recursive feasibility and convergence, the local controller must guarantee that any possible perturbation is rejected in N time steps.

The simulations have been executed for the uncertainty trajectory $w_{e1}(k) = w_{e2}(k)$ shown in figure 5.4. This uncertainty realization is divided into two stages. During the first stage (the first 3.5 seconds while the ball follows the rectangle), the uncertainty switches between the extreme values every 0.5 seconds. This extreme uncertainty realization aims to demonstrate that the controller is robust to any possible uncertainty included in the set \mathcal{W} . During the second state (the last 3.5 seconds while the ball follows the circle), the uncertainty vanishes exponentially, demonstrating that in this case, the closed-loop system will converge to the optimal reachable trajectory with zero error.

The trajectory of the ball converges to a neighborhood new optimal reachable trajectory satisfying the constraints and without losing feasibility even when the prediction horizon is much lower than the period. Figure 5.5 shows the trajectories of (z_1, z_2) for the closed

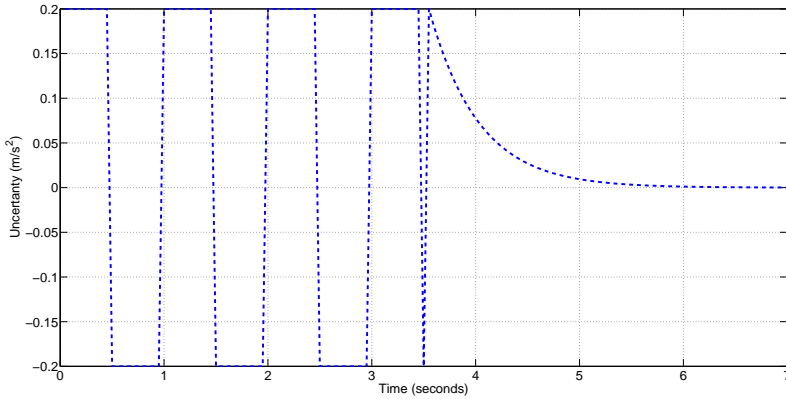


Figure 5.4 Uncertainty trajectory..

loop system (dash-dot blue), the trajectory planner (discontinuous green and black) and the target reference (discontinuous red) in the z_1, z_2 plane. Figures 5.6 and 5.7 show the trajectory of the ball on each axis. Figures 5.8 and 5.9 show the temporal evolution of the accelerations and that the constraints on the input were satisfied at all times. It can be seen that there exists a deviation between the trajectory of the planner and the target reference for the rectangle, because one of the sides of the rectangles lies outside the position limits. The robust planner trajectory tries to get as close as possible to the target reference, but maintains a safe distance from the positions limits to guarantee that the constraint are satisfied for all possible uncertainties.

The constraints are robustly satisfied for all times, in particular during stage 1, in which the uncertainty takes extreme values and the target trajectory is close to the physical limits. During this stage, the closed-loop trajectories are close to the optimal reachable trajectory \mathbf{x}° . In stage 2, it can be seen that the trajectory of the closed-loop system converges to the optimal reachable tightened reference trajectory with zero error as the perturbation vanishes with time and how the planner reachable trajectory converges to the target when the target is a robust reachable reference.

Figures 5.6,5.7 show that the optimal trajectory maintains a safe distance from the constraints.

Figure 5.10 shows the trajectories of the optimal cost V_N^* (discontinuous blue) and trajectory planner cost V_p^o (discontinuous green). The simulations include a sudden change in the reference when it switches from the rectangle to the circle which as a clear effect on the optimal costs, in particular the difference between both values increases suddenly when the reference changes, but then it converges again to the new optimal trajectory planner cost. The cost evolution is non-strictly decreasing during stage 1 because of the effect of the uncertainties of the closed-loop system. The cost of the proposed controller converges to the cost of the trajectory planners in a non-increasing manner in stage 2, demonstrating that the optimal trajectory is input-to-state stable, so as the uncertainties vanish, the closed-loop system converges asymptotically with zero error.

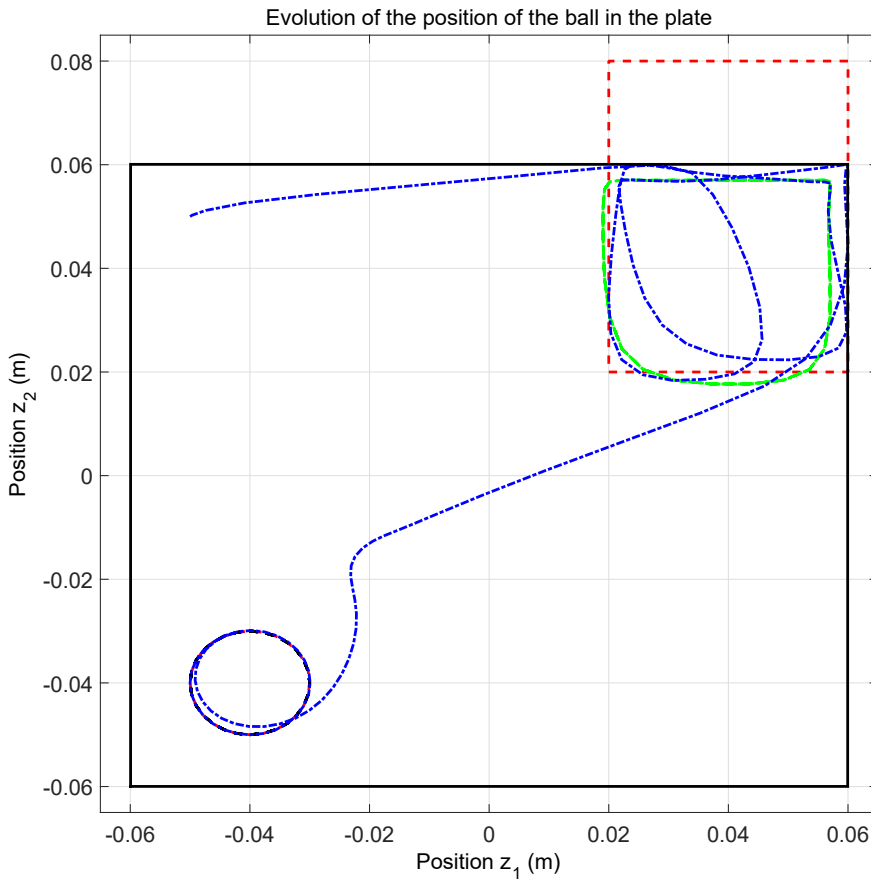


Figure 5.5 Trajectories of z_1, z_2 for the closed loop system (dash-dot blue), the trajectory planners (discontinuous green and black), the target reference (discontinuous red) and the limit of the plate (dot black).

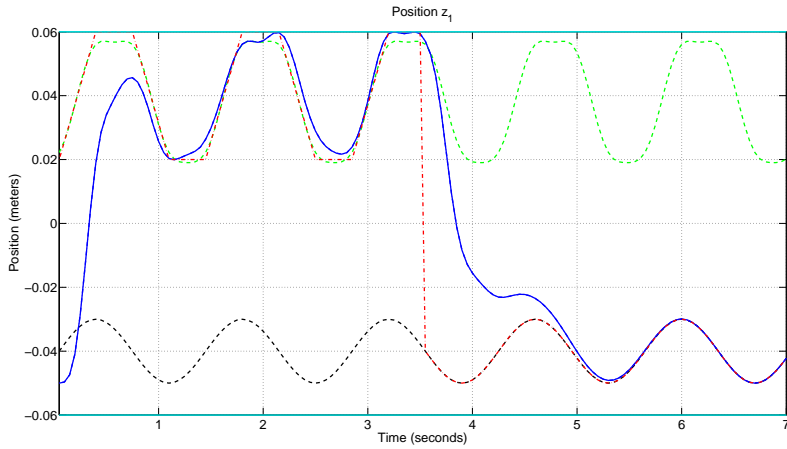


Figure 5.6 Trajectories of z_1 for the closed loop system (continuous blue), the trajectory planners (discontinuous green and black) and the target reference (discontinuous red).

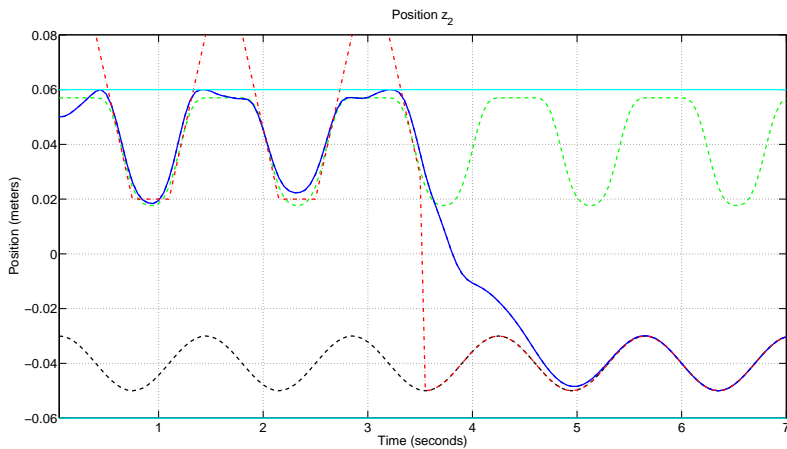


Figure 5.7 Trajectories of z_2 for the closed loop system (continuous blue), the trajectory planners (discontinuous green and black) and the target reference (discontinuous red).

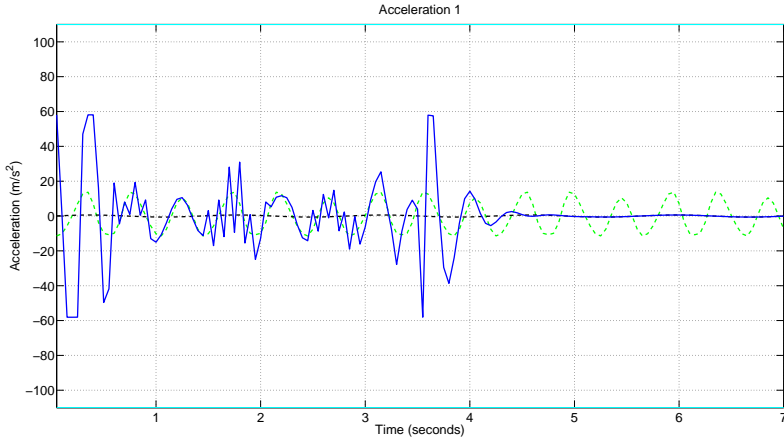


Figure 5.8 Trajectories of $\ddot{\theta}_1$ for the closed loop system (blue), the trajectory planners (discontinuous green and black) and the constraints are shown in cyan (scenario 2).

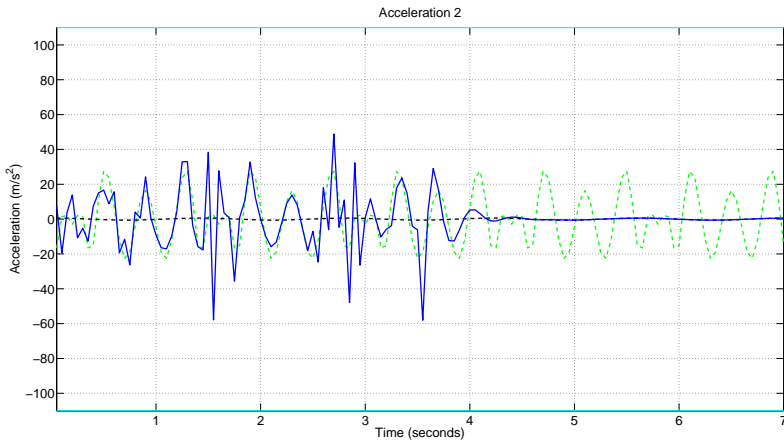


Figure 5.9 Trajectories of $\ddot{\theta}_2$ for the closed loop system (blue), the trajectory planners (discontinuous green and black) and the constraints are shown in cyan (scenario 2).

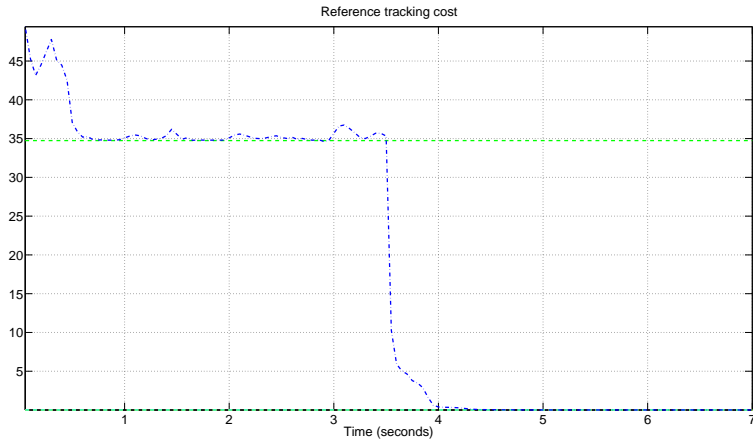


Figure 5.10 Trajectories of the optimal cost V_N^* (discontinuous blue) and trajectory planner cost V_p^o (discontinuous green).

6 Application to a large-scale DWN of robust MPC for tracking periodic references

Drinking water network (DWN) are large-scale systems subject to a set of operating, safety and quality-of-service constraints. The dynamics of these type of systems is usually affected by stochastic disturbances as is shown in Grosso et al. (2013). Thus, an interesting research focus is the improvement of the management of the DWN guaranteeing the water supply when exists error in the demand forecasting as Barcelli et al. (2010) and Ocampo-Martínez et al. (2012) have pointed out. Examples of this interest are Sampathirao et al. (2014) where various methods for demand forecasting were studied, such as seasonal ARIMA, BATS and support vector machine presenting a set of statically validated time series models; Agudelo-Vera et al. (2014) where a methodology to determine the robustness of the water drinking distribution systems was developed testing the performance of three networks under three future demand scenarios using head loss and resident time as indicators; and Le Quiniou et al. (2014) where off-line support tools to optimize the procurement management of water reducing the energy costs where developed and applied to a DWN in France.

Recently, model predictive control (MPC), has been applied to improve the management of DWN. In Fiorelli et al. (2011) MPC was used to manage the water storage in a small DWN in Luxemburg. In Ocampo-Martínez et al. (2011) a decentralized MPC over a partitioned model of the Barcelona drinking water network was presented. In Grosso et al. (2014a) a chance-constrained MPC strategy based on a finite horizon stochastic optimization problem with joint probabilistic constraints was proposed. In Pascual et al. (2013) some model predictive control techniques are applied to the supervisory flow management in large-scale DWNs. In this case, MPC was used to generate the set-points for the regulatory controller (low level layer). In Grosso et al. (2012) a model predictive control strategy to assure reliability of the DWN given a customer service level and a forecasting demand was presented. In Grosso et al. (2014b) a multi-objective cost function

using an economically oriented model predictive control strategy was studied.

The operation of DWNs is strongly conditioned by the uncertainties in the forecast water demand and the possibly time varying costs, see Quevedo et al. (2006). In addition, the demand and economic criterions present almost periodic trajectories. This implies that the controller presented in chapter 5 is appropriate to tackle this class of systems. This chapter presents the application of the previous novel robust predictive controller for tracking periodic references to an uncertain discrete time algebraic-differential linear model of a large scale drinking water network presented in Sampathirao et al. (2014). The system considered has been obtained from the water balance equations of a section of Barcelona’s drinking water network taking into account bounded additive variations on the demands, see figure 6.1.

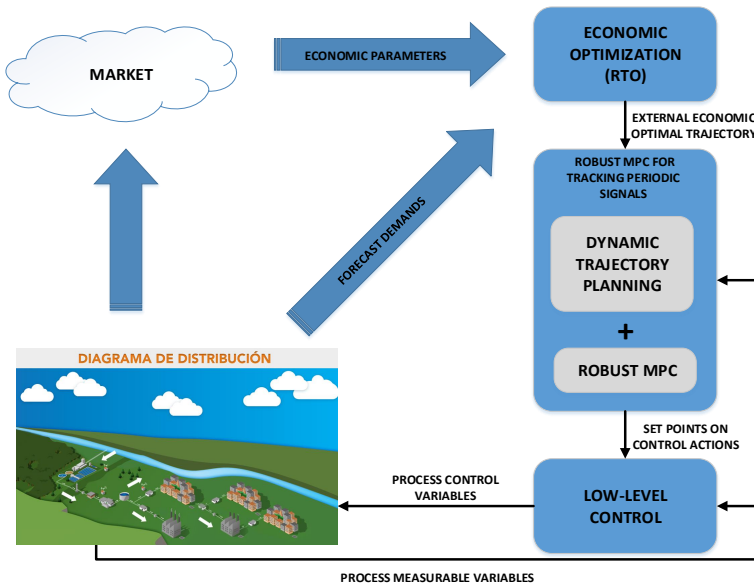


Figure 6.1 Hierarchical control structure.

In this model, we assume that a prediction of the water demand is available and that the prediction error is bounded. In this application we use a MPC design based on an equality terminal constraint to avoid the computation of the minimal robust positive invariant set to calculate the problem constraints, which is a relevant property that allows this controller to be used in large scale applications. The results of this chapter have been submitted in the journal *Control Engineering Practice* as full paper. A technical report of this work can be found in Pereira et al. (2015b).

6.1 Application to a drinking water network

In this chapter we consider a section of Barcelona's drinking water network (DWN), see Sampathirao et al. (2014). Figure A.1 shows an schematic of the topology of the network which consists of seventeen water tanks connected to twenty five demand points from which water is consumed and nine water supply points from which water is obtained. The water flow in the network is controlled with sixty one manipulable inputs composed of a set of valves and water pumps which we will denote as network actuators.

The network is modeled from the water balance equation at each of the network nodes. Each water tank is modeled using a single integrator with a time derivative that depends on the input and output flows, see Grosso et al. (2013); Limon et al. (2014). Equation (6.3a) models the water balance equations of the tanks and equation (6.3b) models the water balance equations at those nodes of the network which are not included in equation (6.3a). The water balance equations of the tanks are the following:

$$\dot{x}_1(t) = u_3(t) + u_4(t) - d_1(t) \quad (6.1a)$$

$$\dot{x}_2(t) = u_5(t) - d_3(t) \quad (6.1b)$$

$$\dot{x}_3(t) = u_7(t) - u_8(t) + u_{10}(t) + u_{11}(t) - d_4(t) \quad (6.1c)$$

$$\dot{x}_4(t) = u_8(t) + u_9(t) - u_{10}(t) - u_{11}(t) + u_{13}(t) - u_{14}(t) + u_{19}(t) \quad (6.1d)$$

$$\dot{x}_5(t) = u_{12}(t) - u_{15}(t) + u_{16}(t) - u_{20}(t) - u_{21}(k) \quad (6.1e)$$

$$\dot{x}_6(t) = u_6(t) + u_{20}(t) - u_{23}(t) + u_{27}(t) \quad (6.1f)$$

$$\begin{aligned} \dot{x}_7(t) = & u_{17}(t) - u_{18}(t) - u_{22}(t) + u_{23}(t) + u_{24}(t) - u_{31}(t) - u_{32}(t) \\ & + u_{37}(t) - u_{38}(t) - d_{13}(t) \end{aligned} \quad (6.1g)$$

$$\dot{x}_8(t) = u_{21}(t) - u_{24}(t) - u_{27}(t) - u_{33}(t) - u_{34}(t) - d_{10}(t) \quad (6.1h)$$

$$\dot{x}_9(t) = -u_{28}(t) + u_{29}(t) + u_{33}(t) - d_8(t) \quad (6.1i)$$

$$\begin{aligned} \dot{x}_{10}(t) = & -u_{29}(t) + u_{30}(t) - u_{36}(t) - u_{37}(t) + u_{38}(t) - u_{42}(k) \\ & + u_{45}(t) + u_{51}(t) + u_{52}(t) - d_{12}(t) \end{aligned} \quad (6.1j)$$

$$\dot{x}_{11}(t) = u_{35}(t) + u_{36}(t) - d_{11}(t) \quad (6.1k)$$

$$\dot{x}_{12}(t) = u_{41}(t) + u_{47}(t) - u_{48}(t) + u_{56}(t) - d_{18}(t) \quad (6.1l)$$

$$\dot{x}_{13}(t) = u_{42}(t) - u_{44}(t) - d_{19}(t) \quad (6.1m)$$

$$\dot{x}_{14}(t) = -u_{46}(t) - u_{53}(t) - u_{54}(t) + u_{55}(t) + u_{57}(t) + u_{58}(t) - d_{21}(t) \quad (6.1n)$$

$$\dot{x}_{15}(t) = -u_{49}(t) + u_{50}(t) + u_{53}(t) - d_{23}(t) \quad (6.1o)$$

$$\dot{x}_{16}(t) = u_{54}(t) + u_{59}(t) - d_{24}(t) \quad (6.1p)$$

$$\dot{x}_{17}(t) = u_{48}(t) + u_{60}(t) - d_{22}(t) \quad (6.1q)$$

where $x_i(t) \in \mathbb{R}$ denotes the volumes in storage tank i in m^3 , $u_i(t) \in \mathbb{R}$ denotes water flows through actuator i given in $\frac{m^3}{s}$ and $d_i(t) \in \mathbb{R}^{25}$ denotes the network water flow demand i in $\frac{m^3}{s}$. Note that the water balance equations at each tank include some of the demands, which implies that the controller has to account for the uncertainty in order to maintain the tanks between the maximum and minimum values for all possible cases.

The water balance equations of the rest of the nodes are the following:

$$0 = u_1(t) - u_2(t) - u_5(t) - u_6(t) \quad (6.2a)$$

$$d_2(t) = u_2(t) - u_3(t) \quad (6.2b)$$

$$d_5(t) = u_{18}(t) - u_{13}(t) \quad (6.2c)$$

$$d_7(t) = u_{14}(t) + u_{15}(t) - u_{19}(t) - u_{25}(t) + u_{26}(t) \quad (6.2d)$$

$$d_9(t) = u_{22}(t) - u_{30}(t) \quad (6.2e)$$

$$d_{14}(t) = u_{32}(t) - u_{39}(t) - u_{40}(t) \quad (6.2f)$$

$$d_{15}(t) = u_{25}(t) - u_{26}(t) + u_{32}(t) + u_{34}(t) + u_{40}(t) - u_{41}(t) \quad (6.2g)$$

$$d_{17}(t) = u_{39}(t) - u_{45}(t) + u_{46}(t) - u_{47}(t) \quad (6.2h)$$

$$d_{16}(t) = u_{28}(t) - u_{35}(t) - u_{43}(t) + u_{49}(t) \quad (6.2i)$$

$$d_{20}(t) = u_{43}(t) + u_{44}(t) \quad (6.2j)$$

$$d_{25}(t) = u_{61}(t) - u_{50}(t) - u_{51}(t) - u_{52}(t) - u_{56}(t) \\ - u_{57}(t) - u_{58}(t) - u_{59}(t) - u_{60}(t) \quad (6.2k)$$

We consider constraints which limit the maximum volume of each tank and the maximum water flow of each actuator (the flows of the network are one directional and cannot be reversed). In particular we assume that $0 \leq x_i(t) \leq x_i^{max}$ and $0 \leq u_i(t) \leq u_i^{max}$ for all tanks and actuators. The maximum values for each tank and actuator are defined in Tables A.1 and A.2 respectively. In Table A.2 it can be seen that there are large differences between the maximum flow values of each of the actuators. For example actuator 50 has a maximum value of $15 \frac{m^3}{s}$, while actuators 8 or 9 have minimum values of $0.03 \frac{m^3}{s}$ or $0.0056 \frac{m^3}{s}$ respectively. It is worth to note that one of the actuators is assumed to be zero for operating reasons, in particular actuator 7, which has a maximum flow of $10^{-5} \frac{m^3}{s}$. These differences must be taken into account in the controller design to avoid feasibility and constraint satisfaction issues in the presence of uncertainty in the demand.

In order to design the proposed controller, the following uncertain discrete time algebraic-difference linear model is obtained from equations (6.2) and (6.1) using the Euler approximation and a sampling time of one hour:

$$x(k+1) = Ax(k) + Bu(k) + B_d(d(k) + w(k)) \quad (6.3a)$$

$$0 = E_u u(k) + E_d(d(k) + w(k)) \quad (6.3b)$$

where $x(k) \in \mathbb{R}^{17} \in \mathcal{X}$ denotes vector of the level of the tanks in m^3 , $u(k) \in \mathbb{R}^{61} \in \mathcal{U}$ denotes de vector of water flows through the sixty one actuators given in $\frac{m^3}{s}$, vector $d(k) \in \mathbb{R}^{25}$ denotes the known predicted demands in $\frac{m^3}{s}$ and vector $w(k) \in \mathbb{R}^{25}$ denotes the prediction error in these demands. Sets \mathcal{X} and \mathcal{U} are defined from the values of the Tables A.1 and A.2.

The predicted demand $d(k)$ that will be used in the simulations is shown in Tables A.3,A.4 and A.5. This demand has been obtained from historic data. The prediction error

is assumed to be bounded in the set \mathcal{W} defined as follows:

$$w(k) \in \mathcal{W} \triangleq \{w \in \mathbb{R}^{25} : |w_i| \leq w_i^{max}, \forall i = 1, \dots, 25\} \quad (6.4)$$

In the simulations, the robust MPC for tracking is designed assuming that the maximum prediction error is equal to 5% of its maximum daily value, that is, $w_i^{max} = 0.05 \max_k d(k)$.

The control objective is to drive the system as close as possible to an arbitrary state and input periodic target reference. For this case study, the target trajectories of the tank levels $x_i^t(k)$ are given in Tables A.6, A.7 and A.8. The value of the actuator water flow references $u_i^t(k)$ have been obtained from the solution in the least squares sense to the under determined system of equations obtained from the dynamic model and the predicted values of the demand. Figure (6.2) shows the level trajectories for tanks 10 and 11. Figure (6.3) shows the water flow trajectories for actuators 15, 18. It can be seen that the target trajectories do not satisfy the constraints. The target level of the tanks is greater than the maximum allowed value. These target trajectories have been chosen on purpose to demonstrate that the robust MPC for tracking will drive the system to the closest (in a sense) trajectory to the target trajectory that guarantees robust constraint satisfaction.

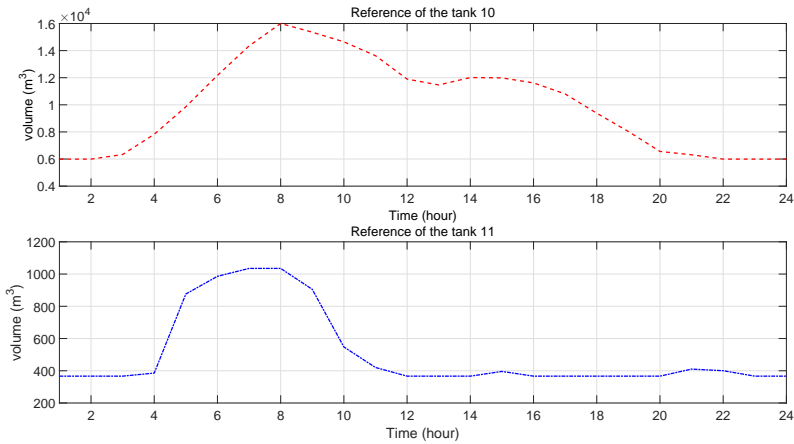


Figure 6.2 Target trajectories of tanks 10 and 11.

To design a robust controller, an auxiliary control input is introduced from the explicit solution of equation (6.3b) in order to satisfy the water balance equations for any demand prediction error. Note that it is not possible to formulate a robust model predictive control optimization problem based on a differential-algebraic equation using as optimization variables the actuator flows because it would not be possible to satisfy the water balance equality constraints for all possible uncertainties. The value of the water flows $u(k)$ that satisfy the water balance equations are given by

$$u(k) = M_1 d(k) + M_2 v(k) \quad (6.5)$$

where $v(k) \in \mathbb{R}^{50}$ denotes the new set of control inputs which guarantee the water balance

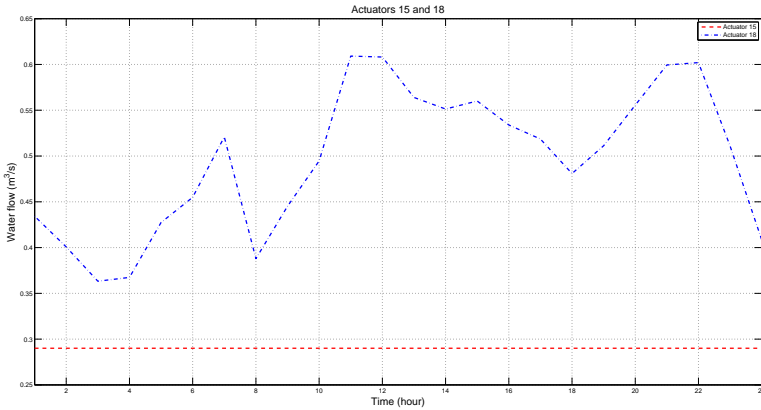


Figure 6.3 Target trajectories of actuators 15 and 18.

equations in the eleven nodes that do not have a tank. Matrices $M_1 \in \mathbb{R}^{61 \times 25}$ and $M_2 \in \mathbb{R}^{61 \times 50}$ are obtained from the solution of (6.3b). Matrix M_2 is an orthonormal basis for the null space of E_u obtained from the singular value decomposition. Matrix M_1 provides a particular solution to the equation that depends on $d(k)$. There are infinite solutions which provide different ways of distributing the flow to satisfy the balance equations for a given demand. An inappropriate selection of matrix M_1 may lead to optimization problems with a reduced feasibility region, in particular if matrix M_1 distributes the demand in a way such that the actuators with a lower maximum value are saturated. In order to distribute the demand taking into account that each flow has a different maximum value, matrix M_1 has been chosen in a way such that minimizes the norm of the matrix $M_1^T G M_1$ where G is a diagonal matrix that weights each actuator u_i inversely to the square of its maximum value.

The real water demand must always be satisfied, to this end at each sampling time, the MPC controller will decide the optimal value for the auxiliary control input $v^*(k)$, which is designed to satisfy the predicted demand $d(k)$, however, the real value of the actuators $u^*(k)$ are obtained both from $v^*(k)$ and the real demand which is available instantaneously; that is, taking into account the prediction error $w(k)$:

$$u^*(k) = M_1(d(k) + w(k)) + M_2 v^*(k)$$

In order to design the proposed robust MPC for tracking periodic references, a local control law aimed at reducing the effect of the uncertainty in the predictions is needed. In the water distribution control problem considered, this local control law decides the value of the auxiliary control inputs $v(k)$ on behalf of the deviation of the perturbed predictions from the nominal predictions obtained the previous sampling time $e(k)$. The objective of this control law is to reject the uncertainty. To this end, a linear control law, that is

$v(k) = Ke(k)$ is designed for the system

$$e(k+1) = Ae(k) + BM_1v(k)$$

where $e(k)$ in the aforementioned deviation. This system is obtained taking into account the definition of the auxiliary control variable and ignoring the effect of the predicted demand in system (6.3).

The local controller is used to design the reduced set of constraints that guarantee both robust constraint satisfaction and recursive feasibility of the controller in closed-loop. In order to guarantee recursive feasibility and hence, closed-loop convergence to the optimal feasible periodic trajectory, the local control gain must satisfy

$$\max_{w \in \mathcal{W}} \|(A + BM_1K)^{N-1}w\| \leq \sigma$$

where σ is the tolerance of the optimization problem solver. This implies that the local controller is able to eliminate the effect of any uncertainty after $N - 1$ time steps. Although in principle any stabilizing linear gain that guarantees disturbance rejection in N steps could be used, an inappropriate design of this controller may result in empty feasibility regions of the MPC optimization problems. To avoid this issue, the controller has to be designed taking into account the constraints on the tanks and the actuators, and more precisely, it has to take into account the difference in the state and actuators ranges. Design procedures to guarantee that the resulting optimization problem has a non-empty feasibility region are out-side the scope of this work. The reader can refer to Alvarado et al. (2010b) for an LMI based design procedure for this problem.

In the WDN considered, a LQR control law has been designed by trial and error using weight matrices that depend on the maximum tank and water flow levels. In particular, the weighting matrices Q_K and R_K are defined as follows

$$\begin{aligned} Q_K &= \text{diag}(1/x_i^{\max}) \\ R_K &= pM_2^T \text{diag}(1/u_i^{\max})M_2 \end{aligned} \quad (6.6)$$

where p weights the input cost with respect to the state cost. The value $p = 10$ was chosen by trial and error.

The control gain obtained using these weights satisfies the uncertainty rejection assumption and yields a MPC optimization problem with a nonempty feasibility region. In particular, the maximum eigenvalue of the matrix $(A + BM_1K)^{23}$ is $1.6483 \cdot 10^{-34}$ thus $\sigma = 2.7157 \cdot 10^{-30}$ is lower than the precision of the simulations carried out with Matlab.

6.1.1 Proposed robust MPC controller

The cost function¹ of the proposed controller is defined as follows:

$$V_N(x, \mathbf{x}', \mathbf{u}', \mathbf{d}; x_0', \mathbf{v}', \mathbf{v}) = V_t(x, \mathbf{d}; x_0', \mathbf{v}', \mathbf{v}) + V_p(\mathbf{x}', \mathbf{u}', \mathbf{d}; x_0', \mathbf{v}')$$

¹ Bold letters denote trajectories of signals over the prediction horizon/period.

where

$$V_t(x, \mathbf{d}; x_0^r, \mathbf{v}^r, \mathbf{v}) = \sum_{i=0}^{N-1} \|x(i) - x^r(i)\|_Q^2 + \|u(i) - u^r(i)\|_R^2$$

$$V_p(\mathbf{x}^t, \mathbf{u}^t, \mathbf{d}; x_0^r, \mathbf{v}^r) = \sum_{i=0}^{T-1} \|x^r(i) - x^t(i)\|_S^2 + \|u^r(i) - u^t(i)\|_W^2$$

The parameters that define the optimization problem at time step k are the current state x , the future state and actuator trajectories given by vectors $\mathbf{x}^t, \mathbf{u}^t$ respectively and the predicted demand given by vector \mathbf{d} . The optimization variables are the the auxiliary reference defined by its initial state x_0^r and future T -step (one period) auxiliary control input trajectory \mathbf{v}^r , and the predicted N -step auxiliary control input trajectory \mathbf{v}^r .

The term $V_t(x, \mathbf{d}; x_0^r, \mathbf{v}^r, \mathbf{v})$ penalizes the tracking error of the open-loop predicted trajectories with respect to the planned reachable reference along the prediction horizon N . The term $V_p(\mathbf{x}^t, \mathbf{u}^t, \mathbf{d}; x_0^r, \mathbf{v}^r)$ penalizes the error between the artificial reference trajectory and the target reference trajectory along one period of length T time steps.

The optimal trajectories of the proposed robust MPC for tracking periodic signals can be obtained from the solution of the following finite horizon optimal control problem $\mathcal{P}_N(x, \mathbf{x}^t, \mathbf{u}^t)$

$$\begin{aligned} & \min_{x_0^r, \mathbf{v}^r, \mathbf{v}} V_N(x, \mathbf{x}^t, \mathbf{u}^t, \mathbf{d}; x_0^r, \mathbf{v}^r, \mathbf{v}) \\ \text{s.t.} \quad & x(0) = x & (6.7a) \\ & x(i+1) = Ax(i) + B_u u(i) + B_d d(i) \quad i \in \mathbb{Z}_N & (6.7b) \\ & u(i) = M_1 d(i) + M_2 v(i) \quad i \in \mathbb{Z}_N & (6.7c) \\ & x(i) \in \mathcal{X}_i \quad i \in \{1, \dots, N\} & (6.7d) \\ & u(i) \in \mathcal{U}_i \quad i \in \{0, \dots, N-1\} & (6.7e) \\ & x(N) = x^r(N) & (6.7f) \\ & x^r(i+1) = Ax^r(i) + B_u u^r(i) + B_d d(i) \quad i \in \mathbb{Z}_T & (6.7g) \\ & u^r(i) = M_1 d(i) + M_2 v^r(i) \quad i \in \mathbb{Z}_N & (6.7h) \\ & x^r(i) \in \mathcal{X}_N^r \quad i \in \{0, \dots, T\} & (6.7i) \\ & u^r(i) \in \mathcal{U}_{N-1}^r \quad i \in \{0, \dots, T-1\} & (6.7j) \\ & x^r(T) = x^r(0) = x_0^r & (6.7k) \end{aligned}$$

where the sets \mathcal{X}_i and \mathcal{U}_i are defined as follows

$$\mathcal{X}_i = \mathcal{X} \ominus \bigoplus_{j=0}^{i-1} (A + B_u M_2 K)^j (B_d + B_u M_1) \mathcal{W}$$

$$\mathcal{U}_i = \mathcal{U} \ominus M_1 \mathcal{W} \ominus M_2 K \bigoplus_{j=0}^{i-1} (A + B_u M_2 K)^j (B_d + B_u M_1) \mathcal{W}$$

It is important to remark that the calculation of these sets is trivial, even for the system of dimension seventeen considered. The calculation however of a robust positive invariant set may be in general a difficult task, precluding the application of robust scheme to large scale systems.

The optimal solution of this optimization problem at time step k is denoted $(x_0^{r*}(k), \mathbf{v}^{r*}(k), \mathbf{v}^*(k))$. The value of the water flows of each actuator depends on the solution

of this optimization problem and the demand and is obtained as follows:

$$u(k) = M_2 v^*(0|k) + M_1 (d(k) + w(k))$$

where $v^*(0|k)$ is the optimum value for the first auxiliary input at time step k . This implies that the water flows are different from the predicted in the optimization problem because they have to be modified to account for the prediction errors. For this reason, in order to guarantee robust constraint satisfaction on the constraints of the water flows, the feasible set must be reduced taking into account the possible effect of the prediction error. Constraints (6.7e) and (6.7j) reduce the feasible set of water flows \mathcal{U} by the set $M_1 \mathcal{W}$ to account for this issue.

The constraints of the optimization variables, which define maximum and minimum values of the tank levels and the network water flows, are contracted with every step of the prediction horizon. Constraints (6.7d) and (6.7e) show that as the prediction step i increases, the sets are reduced taking into account the possible effect to a perturbation on the predicted system in closed-loop with the auxiliary controller. This contraction is time invariant and can be calculated off-line. Constraints (6.7b)-(6.7c) are defined by the nominal model, that is, assuming that the prediction error is zero, and provides the predicted state and input trajectories. Constraint (6.7b) imposes that the initial state of the predicted trajectory is equal to the state of the system at time step k . Constraint (6.7f) states that the predicted state must reach the artificial reference in T steps. These constraints are used to guarantee recursive feasibility using an appropriately defined shifted solution. Constraints (6.7g)-(6.7h) are defined by the nominal model, that is, assuming the prediction error is zero, and provides the artificial references state and input trajectories. Note that the initial state of the artificial reference is a free variable, however, it is constrained to be a periodic trajectory in constraint(6.7k). The artificial references must satisfy the state and input constraints, but because in order to guarantee recursive feasibility, the artificial reference is used to define the shifted input trajectory at prediction time $N - 1$, the constraint set is contracted by the same set for all steps which depends on the prediction horizon N . In particular, the artificial references must satisfy (6.7d) and (6.7e) for $i = N - 1$.

If the controller is not designed appropriately, the admissible tank levels and actuators flow sets for the predicted trajectories may be empty for some time step i . In this case, the optimization problem is unfeasible for all states. The chosen matrix M_1 and the control law gain K for the simulations guarantee the cancelation of the effect of an uncertainty in $N - 1$ time steps and that the feasibility set is not empty.

It is important to note that the constraints of the optimization problem do not depend on the target trajectories. This implies that a sudden change in these trajectories cannot cause a loss of feasibility of the optimization problem. This will be shown in the simulation example.

For this case study, the prediction horizon is chosen equal to the period, that is $N = T = 24$. The cost matrices Q , R , S and V are defined as follows

$$\begin{aligned} Q &= 100 \cdot \mathcal{I}_{17} \\ R &= 10 \cdot \mathcal{I}_{61} \\ S &= 700 \cdot \mathcal{I}_{17} \\ V &= 700 \cdot \mathcal{I}_{61} \end{aligned} \quad (6.8)$$

where \mathcal{I}_n is the identity matrix of dimension n . These matrices define the optimal trajectories but do not affect the closed-loop properties of the controller.

The provided target trajectory may not be coherent with the dynamic model or the constraints. As proved in chapter 5, the system in closed-loop converges asymptotically to a neighborhood of the trajectory obtained minimizing $V_p(\mathbf{x}^t, \mathbf{u}^t, \mathbf{d}; x_0^t, \mathbf{v}^t)$ subject to constraints (6.7g)-(6.7k). This optimization problem is denoted the robust planner. Because the demand and the target references are periodic, and the cost function is strictly convex, the optimal periodic trajectories do not depend on the time step k in which the optimization problem is formulated. The resulting trajectory takes into account the effect of the uncertainty in the constraints in order to guarantee robust constraint satisfaction. In this case, the robust planner is not independent of the prediction horizon of the corresponding robust MPC for tracking, because the reduction of the constraint set depends on N . In the simulations we denote the optimal trajectories of this optimization problem as the robust planner trajectories. If the prediction error is assumed to be zero, the nominal planner trajectories defined in chapter 2 are obtained. It is important to remark that it is not necessary to solve the planner optimization problems to define the MPC controller. The convergence property stems directly from the controller formulation.

6.1.2 Recursive feasibility

In this section we prove that closed-loop constraint satisfaction and recursive feasibility of the optimization problem is guaranteed if the initial state is inside the feasibility region, even in the presence of sudden changes in the reference. To this end, a feasible solution for $x(k+1)$ denoted shifted solution is obtained from the optimal solution for $x(k)$. We use the notation $|k$ to denote the time step to which a given variable is referred and bold letter to denote vectors or a sequential of variables. The shifted variables are denoted with the superscript s . The shifted solution at time $k+1$ is obtained as follows:

$$x^s(0|k+1) = x(k+1) = Ax(k) + B_u u(0|k)^* + B_d d(k) + B_d w(k) \quad (6.9a)$$

$$v^{rs}(i|k+1) = v^{r*}(i+1|k), \quad i \in \mathbb{I}_{N-2} \quad (6.9b)$$

$$v^{rs}(N-1|k+1) = v^{r*}(0|k) \quad (6.9c)$$

$$v^s(i|k+1) = v^*(i+1|k) + K(x^s(i|k+1) - x^*(i+1|k)), \quad i \in \mathbb{I}_{N-2} \quad (6.9d)$$

$$v^s(N-1|k+1) = v^{r*}(0|k) \quad (6.9e)$$

Taking into account constraints (6.7b), (6.7c), (6.7g) and (6.7h) it follows for $i \in \mathbb{I}_{N-2}$ that:

$$u^{rs}(i|k+1) = u^{r*}(i+1|k) \quad (6.10a)$$

$$u^{rs}(N-1|k+1) = u^{r*}(0|k) \quad (6.10b)$$

$$u^s(i|k+1) = u^*(i+1|k) + M_2K(x^s(i|k+1) - x^*(i+1|k)) \quad (6.10c)$$

$$u^s(N-1|k+1) = u^{r*}(0|k) \quad (6.10d)$$

Taking into account that the artificial reference is a periodic trajectory, the shifted artificial reference states are the following

$$x^{rs}(i|k+1) = x^{r*}(i+1|k), \quad i \in \mathbb{I}_{N-1} \quad (6.11a)$$

$$x^{rs}(N|k+1) = x^{r*}(1|k) \quad (6.11b)$$

The shifted predicted states are obtained using the following equation

$$x^s(i+1|k+1) = Ax^s(i|k+1) + B_u u^s(i|k+1) + B_d d(i)$$

with $x^s(0|k+1) = x(k+1)$. By definition, these states satisfy

$$x^s(i|k+1) = x^*(i+1|k) + (A + B_u M_2 K)^i (B_d - B_u M_1) w(k), \quad i \in \mathbb{I}_{N-1} \quad (6.12)$$

providing a bound of the error between the state of the proposed feasible solution at time $k+1$ and the predicted state in k . In addition, if K is chosen as a $N-1$ dead-beat control law, that is, it satisfies that

$$(A + B_u M_2 K)^{N-1} = 0$$

then it follows that

$$x^s(N-1|k+1) = x^*(N|k) = x^{r*}(N|k) = x^{rs}(N-1|k+1)$$

and taking into account that

$$u^s(N-1|k+1) = u_{0|k}^{r*} = u^{rs}(N-1|k+1)$$

it follows that

$$x^s(N, k+1) = x^{rs}(N|k+1) \quad (6.13)$$

Constraints 6.7d and 6.7e are satisfied at time step $k+1$ for $i = N-1$ because the optimal artificial reference satisfies (6.7i) and (6.7j) for all future time steps and the optimal and shifted states satisfy (6.1.2). By definition the shifted trajectories satisfy the model equations so (6.7b), (6.7c), (6.7g) and (6.7h) are satisfied. Taking into account that $x(i+1|k)$ satisfies (6.7d) for $i+1$ and that (6.13) holds, it follows that $x(i|k+1)$ satisfies (6.7d) for i . The same holds true for constraint (6.7e). The terminal equality constraint (6.7f) is satisfied because the $N-1$ dead beat control law cancels the disturbance in the predicted states in $N-1$ states and the shifted trajectory follows the artificial optimal at time trajectory step k following (6.10d). Constraints (6.7i), (6.7j) and (6.7k) hold because

the optimal artificial reference at time step k is periodic and the shifted reference trajectory is not modified following (6.9b) and (6.9c). Because at time step N the artificial reference state and actuators must satisfy (6.7d) and (6.7e) for $i = N - 1$ because the shifted trajectory follows the artificial trajectory, see (6.10d), those constraints must be included along the whole prediction horizon as shown in (6.7i) and (6.7j).

6.1.3 Simulation results

To demonstrate the properties of the proposed controller different simulations scenarios have been considered. The simulations have been made with Matlab 2013a using the function *quadprog* to solve the resulting QP optimization problem. The number of decision variables is 6144 because a simultaneous formulation in which the tank levels, actuator water flows and auxiliary control input for both the predicted and the artificial reference trajectories were included as decision variables. For all the simulations, the initial volume of each tank is 60% of its corresponding maximum volume and have a duration of three days.

First, the robust MPC for tracking periodic references is compared with the nominal MPC for tracking periodic references proposed in chapters 2 and 3. The nominal MPC controller is based on the same optimization problem, but assuming that the prediction error is zero for all times. Both controllers use the same design parameters. The main difference between both controllers is that the nominal controller does not take into account the uncertainties, which may lead to constraint violation and possible loss of feasibility. The objective of the first simulation is twofold, first to compare the behavior of the nominal controller and the proposed robust controller and second to show the proposed controller converge properties. To this end, for these simulations the prediction error is assumed to be zero. For this simulation both the nominal and the robust controller closed-loop trajectories converge to their corresponding planner with zero error. The planner trajectories follow the target trajectories if possible. It can be seen that the target trajectories do not satisfy the constraints for all times.

Figures 6.4 and 6.5 show the trajectories of the tank levels 10 and 11 of the nominal (blue discontinuous) and robust (blue) controller. In this case the nominal controller drives the closed-loop system as close as possible to the target reference (red discontinuous) without violating the constraints reaching the trajectory provided by the nominal planner (note that the reference is not always feasible). The robust controller converges to the trajectory provided by the robust planner (green discontinuous), which is the best trajectory that the disturbed system can follow when the closed loop system is tracking the proposed reference without violating the constraint. The trajectory provided by the robust planner does not reach the constraint limits in order to guarantee robust constraint satisfaction in the presence of disturbances. The water flow of the actuators show similar results. Figure 6.6 shows the water flow trajectories of actuator 15. It can be seen that the nominal controller saturates the controller in certain times, while the robust controller converges to the robust planner trajectory, which has to take into account possible prediction errors and hence has to be more conservative.

It's interesting to remark that the time needed to converge to the optimal cost is about 4 hours. The cost of the robust planner is about 8.9×10^{11} and the cost of the nominal

controller is about 8.17×10^{11} . The conservativeness feature of robust controller is the cause of this mismatch between the costs.

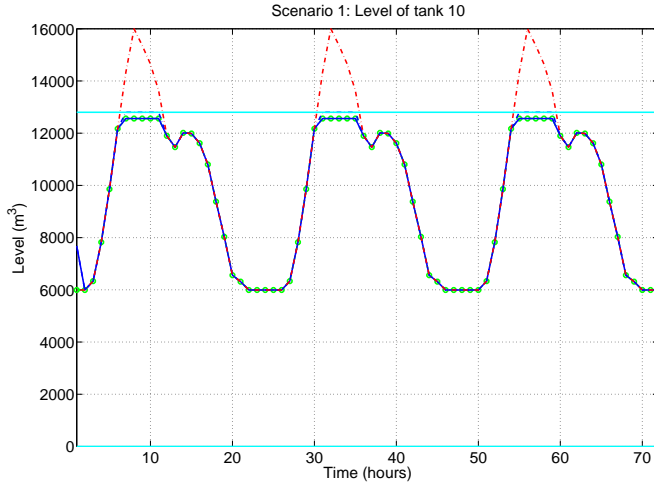


Figure 6.4 Trajectories of tank number 10 (scenario 1): nominal controller (blue discontinuous), robust controller (blue), robust planner (green discontinuous with circle), level constraints (cyan), target trajectory (red discontinuous).

In the second scenario, the same simulations are carried out assuming that the demand was always 5% lower than the predicted value, that is, $d(k) + w(k) = 0.95d(k)$ for all times. This is a worst case scenario that is included in the uncertainty bounds used to design the robust controller. This implies that even in this case, the controller guarantees robust constraint satisfaction and recursive feasibility. On the other hand, the nominal controller does not guarantee constraint satisfaction. The simulations demonstrate this issue and show that often the level of the tanks and the water flow of the actuators of the trajectories of the nominal controller were higher than the maximum levels, in particular, when the nominal planner trajectory was saturated or close to the constraints. The robust controller closed-loop trajectories satisfied the constraints for all times. Figures 6.7, 6.8 show the trajectories of the tank levels 10 and 11 of the nominal (yellow discontinuous) and robust (blue) controller. In the case of the proposed disturbed close loop system the nominal controller break the upper constraints becoming the closed loop system unfeasible but in the case of the robust controller the trajectory are near to the upper constraint without violate it. Must be remarked that the constraints are violated about 5 hours of the 24 hours of a period, that is approx the 20% of the duration of a period.

Figure 6.9 shows the evolution of actuator 15 along the three days of simulation and it can be seen how the trajectory of this water flow is equal to the trajectory of the robust planner as in the case of the evolution of the tanks. When the drinking water network is subject to prediction error in the demand the trajectory of the closed-loop system doesn't converge the robust planner but never break the constraints making the system infeasible.

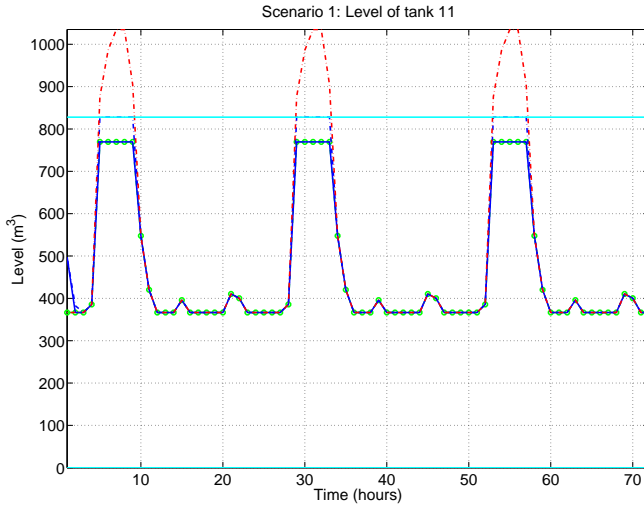


Figure 6.5 Trajectories of tank number 11 (scenario 1): nominal controller (blue discontinuous), robust controller (blue), robust planner (green discontinuous with circle), level constraints (cyan), target trajectory (red discontinuous).

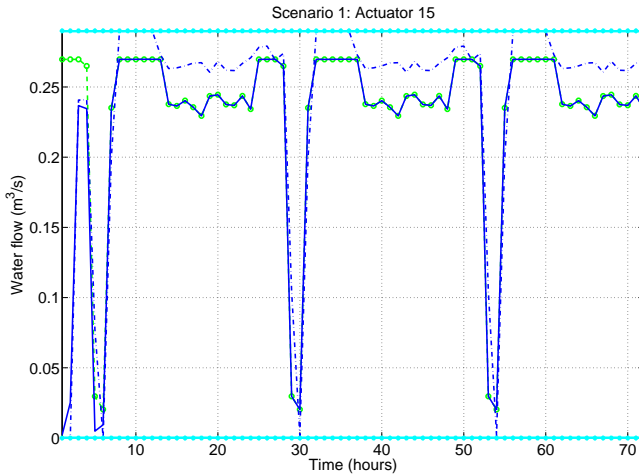


Figure 6.6 Trajectories of actuator number 15 (scenario 1): nominal controller (blue discontinuous), robust controller (blue), robust planner (green discontinuous with circle), flow constraints (cyan).

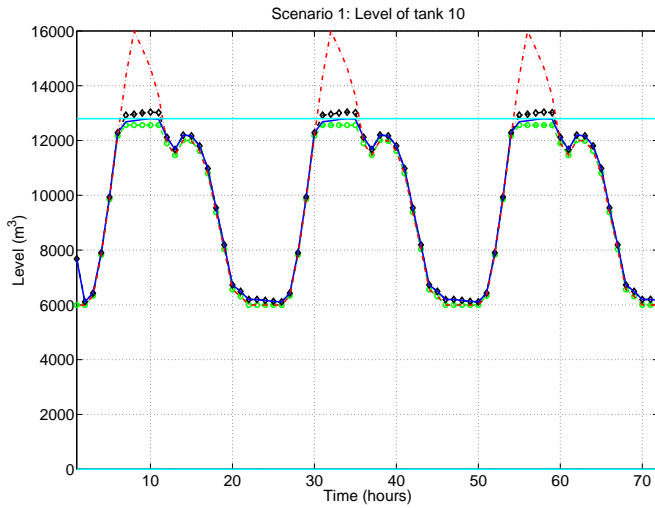


Figure 6.7 Trajectories of tank number 10 (scenario 2): nominal controller (black discontinuous with diamond), robust controller (blue), robust planner (green discontinuous with circle), level constraints (cyan), target trajectory (red discontinuous).

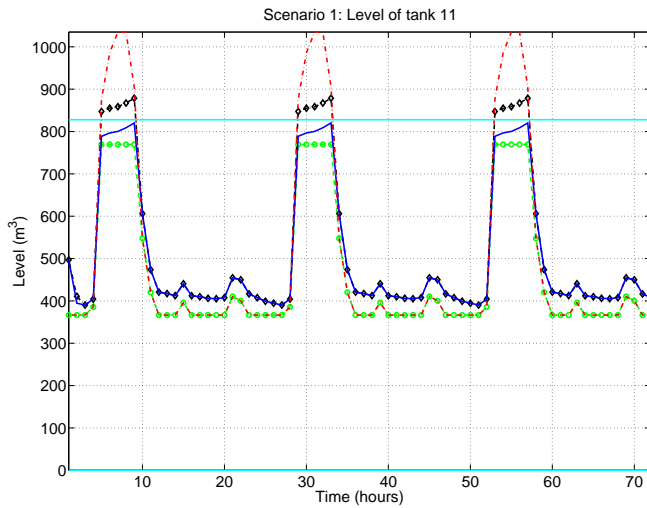


Figure 6.8 Trajectories of tank number 11 (scenario 2): nominal controller (black discontinuous with diamond), robust controller (blue), robust planner (green discontinuous with circle), level constraints (cyan), target trajectory (red discontinuous).

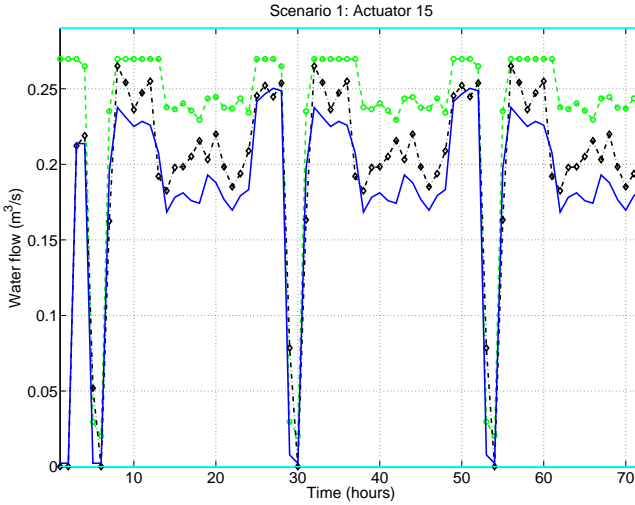


Figure 6.9 Trajectories of actuator number 15 (scenario 2): nominal controller (black discontinuous with diamond), robust controller (blue), robust planner (green discontinuous with circle), flow constraints (cyan).

In the third scenario a sudden change in the target levels and water flow trajectories is shown. The prediction error in this simulation is 5% of the maximal demand along the period but its sign is random. In this simulation the target level for each tank changes after 38 hours. The new target trajectory for each tank $\hat{x}_i^t(k)$ is obtained as $\hat{x}_i^t(k) = x_i^{max} - x_i^t(k)$. The corresponding values of the actuator references $u_i^t(k)$ are been obtained from the solution in the least squares sense to the under determined system of equations obtained from the dynamic model and the predicted values of the demand as with the original target trajectory. The trajectory of the robust planner is different for both target references. Their corresponding costs are $8.8926 \cdot 10^{11}$ and $1.0854 \cdot 10^{12}$ respectively. The simulation shows that the robust MPC optimization cost converges to a neighborhood of the cost of the original trajectory, and then changes suddenly to the cost of the modified trajectory without losing feasibility or violating any constraints.

Figures 6.10 and 6.11 show the evolution of the closed-loop system and its behavior when the tracking reference suddenly changes. In this figures it's represented the trajectory of the robust planner for the first reference (green discontinuous with circle) and for the second reference (black discontinuous with x). The evolution of the closed-loop system change its evolution from following the first reference to follow the new reference without breaking the constraints even with the disturbances. In the case of the behavior of actuator 18, the evolution of the water flow follow the same pattern of the tank level 10. It demonstrate that it robust controller (under the previous assumptions) is recursive feasible even when the references are not periodically constant and without the necessity of calculate any robust invariant set.

Figure 6.12 shows the evolution of the cost of the closed loop system (blue discontinuous

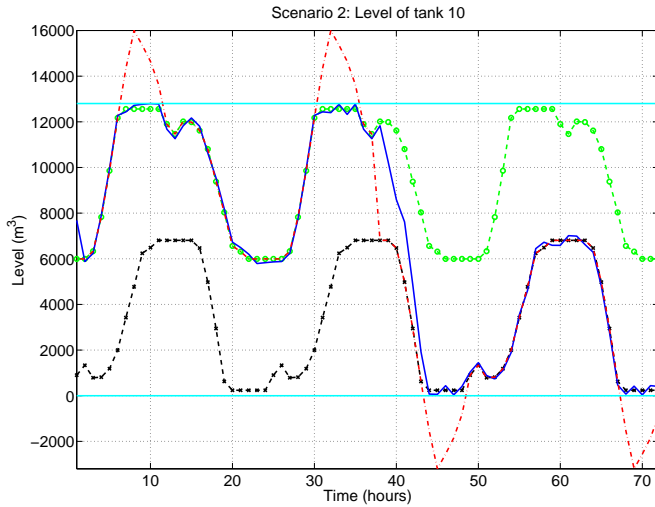


Figure 6.10 Trajectories of tank number 10 (scenario 3): Robust planner for reference 1 (green discontinuous), robust planner for reference 2 (black discontinuous with x), closed-loop trajectories (blue), target reference (red discontinuous) and constraints (cyan).

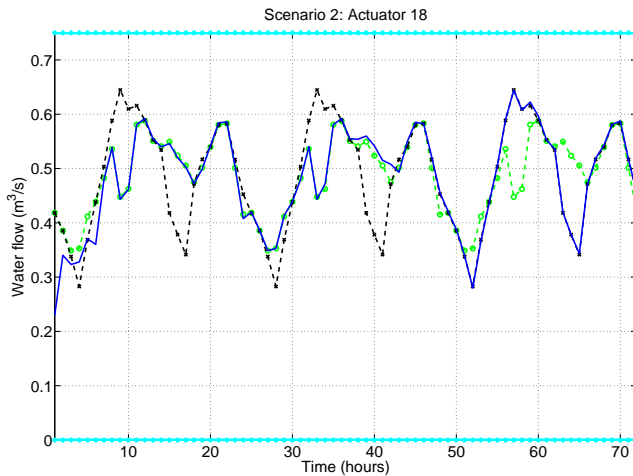


Figure 6.11 Trajectories of actuator number 18 (scenario 3): Robust planner for reference 1 (green discontinuous), robust planner for reference 2 (black discontinuous with x), closed-loop trajectories (blue) and constraints (cyan).

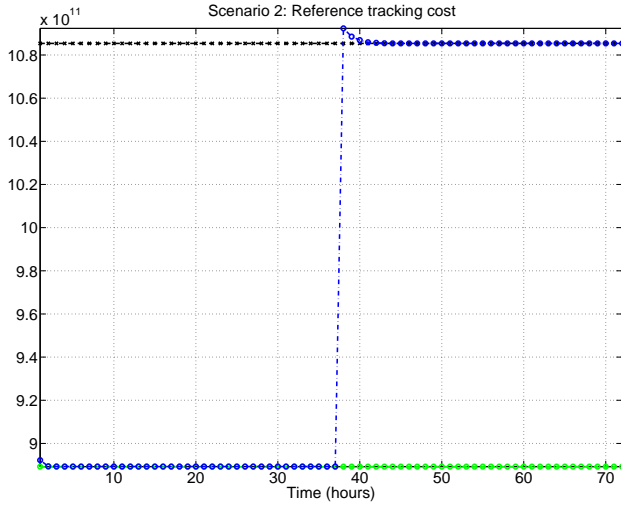


Figure 6.12 Trajectory of the optimal cost (scenario 3) of the robust controller (blue discontinuous with circle) and the robust planers for references 1 and 2 (green discontinuous with circle and black discontinuous with x respectively).

with circle) with the robust controller and how it changes at instant 38 from the previous cost value (green discontinuous with circle) to the new cost value (black discontinuous with x).

7 Conclusions and future lines

In this thesis we have studied several approaches to obtain optimal controllers for systems such as the optimal operation from an economic point of view is not to remain at a steady state, but to follow a periodic trajectory. To this end, we have developed new economic and periodic control schemes based on the extension of the ideas used in the development of the predictive controller for tracking equilibrium points. These new controllers unify a planning and control stages. This planning layer provides the best periodic reachable trajectory that can be followed by the closed-loop system. As it has been seen, this new approach provides an appropriate framework to tackle several kinds of economic control problems such as the optimal management of different critical infrastructures. Moreover, these formulations ensure a set of features such as:

- Input to state stability of the closed loop system.
- Convergence to the best periodic reachable trajectory in a economic way.
- Recursive feasibility even when the economic criteria changes without the necessity to redesign the controller.
- Robustness under bounded uncertainties.
- Scalability which allows us to apply these controllers to large scale system holding all the previous features with a relatively low computational cost comparing these methods with others recent formulations.
- General formulation which can be apply to any periodic linear system.

It is worthwhile to remark that in this thesis a great effort has been made to obtain control schemes which provide all the previous features under the only assumption of the periodicity of the optimal trajectory. No assumption is considered in the shape of the trajectories. On the other hand, there has been a price to pay in terms of computational cost because of the increase of the decision variables in the optimization problems and the general character of these formulations.

We present next the main contribution of each of the chapter of this thesis:

In chapter 2, the problem of tracking periodic references for constrained linear systems was considered. In particular, an MPC method for tracking was proposed in which an artificial reachable reference was included as a decision variable in the optimization problem solved to compute the future control inputs. The cost function penalizes the tracking error between the predicted trajectory and the reachable reference as well as the difference between this reference and the real target reference. The proposed controller guarantees an admissible evolution of the closed-loop system for any possible reference and asymptotic stability to the best periodic reachable reference.

In chapter 3 focused on periodic optimal operation of constrained linear systems. We proposed an economic model predictive controller based on a single layer that unites dynamic real time optimization and control. The proposed controller guarantees closed-loop convergence to the optimal periodic trajectory that minimizes the average operation cost for a given economic criterion. A-priori calculation of the optimal trajectory is not required and if the economic cost function is changed, recursive feasibility and convergence to the new periodic optimal trajectory was guaranteed. The results was demonstrated with two simulation examples, a four tank system, and a simplified model of a section of Barcelona's water distribution network.

Chapter 4 presented the application of a novel economic predictive control to minimize the cost of operating a non-isolated micro-grid connected to a electric utility subject to a periodic internal demand. An economic cost function that penalizes the deviation respect to the agreed power with the service provider and the degradation of the system associated with the micro-grid was proposed. One of the most interesting properties of the controller applied is that it provides a large domain of attraction and that the controller ensures closed loop stability and convergence to the periodic trajectory that provides the optimal operation of the plant. In addition, if the unitary costs are changed, this controller remains feasible and converges to the new periodic optimal trajectory. The simulation results was obtained using a high order model of a microgrid and was demonstrated that periodic economic MPC is an appropriate approach to control this class of systems to guarantee optimal performance from an economic point of view in the presence of sudden changes on the economic criterion.

Chapter 5 proposed a novel robust MPC formulation based on a constraint tightening method. This controller joins a dynamic and robust trajectory planning and a robust MPC for tracking in a single layer taking into account periodic references. The cost function penalizes both the tracking error of the predicted trajectory to the planned reachable one, and the deviation of the planned reachable trajectory to the target periodic reference but taking into account a reduction in the constraint sets and the use of a deadbeat control law to reject the effect of the disturbances in the prediction. This controller guarantees that the perturbed closed loop system is input-to-state stable, converges asymptotically to the optimal reachable periodic trajectory, robustly satisfies all the constraints and maintains feasibility even in the presence of a sudden change in the target reference. In addition, it is not necessary the computation of the minimal robust positive invariant set. These properties was demonstrated in simulation with a ball and plate system.

In chapter 6 we applied a novel robust MPC for tracking periodic references to an uncertain discrete time algebraic-differential linear model of a large scale water distribution network obtained from the water balance equations of a section of Barcelona's water

drinking network. To this end, a large scale model of the network and uncertain predictions of the demand have been considered. The control objective is to track a periodic arbitrary reference while guaranteeing robust constraint satisfaction. The proposed controller provides closed-loop robust constraint satisfaction even in the presence of sudden changes in the periodic target reference and asymptotic convergence to an optimal (in a sense) trajectory. The proposed controller is based on the solution of a single quadratic programming optimization problem. The controller is defined without the necessity of the computation of a robust positive invariant set. We consider that these features are very important in practical applications and make this controller an appropriate approach to control large scale systems.

7.1 Future work

The results on control of periodic systems studied on this thesis open new topics to be researched in, such as the following:

- Validation of the proposed controllers in real plants.
- Robust version of the nominal economic periodic approach of chapter 3. This controller is the last of the set of economic controllers for linear systems. Extension of the economic predictive controller presented in chapter 3 to deal with disturbances and uncertainties.
- The development of the equivalent economic approaches for nonlinear systems holding all the features of the previous controllers such as stability, recursive feasibility and robustness.
- Development of different methods to reduce the computational cost of these approaches and the development of tools to help in the implementation on industrial control devices such as PLCs.

Appendix A

Data about DWN example

Table A.1 Maximum volumes of the tanks.

Tank	01	02	03	04	05	06	07	08	09
$x_i^{max} (m^3)$	445	960	3870	3250	14450	3100	65200	11745	7300
Tank	10	11	12	13	14	15	16	17	
$x_i^{max} (m^3)$	16000	1035	98041	4240	37700	7300	4912	1785	

Table A.2 Maximum water flows.

	1	2	3	4	5	6	7	8	9
$u_i^{max} (\frac{m^3}{s})$	1.297	0.05	0.0317	0.015	0.022	1.2	10^{-5}	0.03	0.0056
	10	11	12	13	14	15	16	17	18
$u_i^{max} (\frac{m^3}{s})$	0.12	0.05	5.34	0.22	0.065	0.29	2.5	0.23	0.75
	19	20	21	22	23	24	25	26	27
$u_i^{max} (\frac{m^3}{s})$	0.0108	1.8	2.9	0.62	3	3.1	15	0.1594	0.6
	28	29	30	31	32	33	34	35	36
$u_i^{max} (\frac{m^3}{s})$	0.29	0.26	0.45	3.5	0.35	0.09	0.4	0.15	0.1563
	37	38	39	40	41	42	43	44	45
$u_i^{max} (\frac{m^3}{s})$	0.5249	0.85	1.2	1.3	1.2	0.425	0.15	0.15	0.005
	46	47	48	49	50	51	52	53	54
$u_i^{max} (\frac{m^3}{s})$	1.35	0.55	0.025	0.24	15	1.7	0.4051	0.1342	0.392
	55	56	57	58	59	60	61		
$u_i^{max} (\frac{m^3}{s})$	0.38	1.5001	1.7361	15	0.1852	0.035	6.2768		

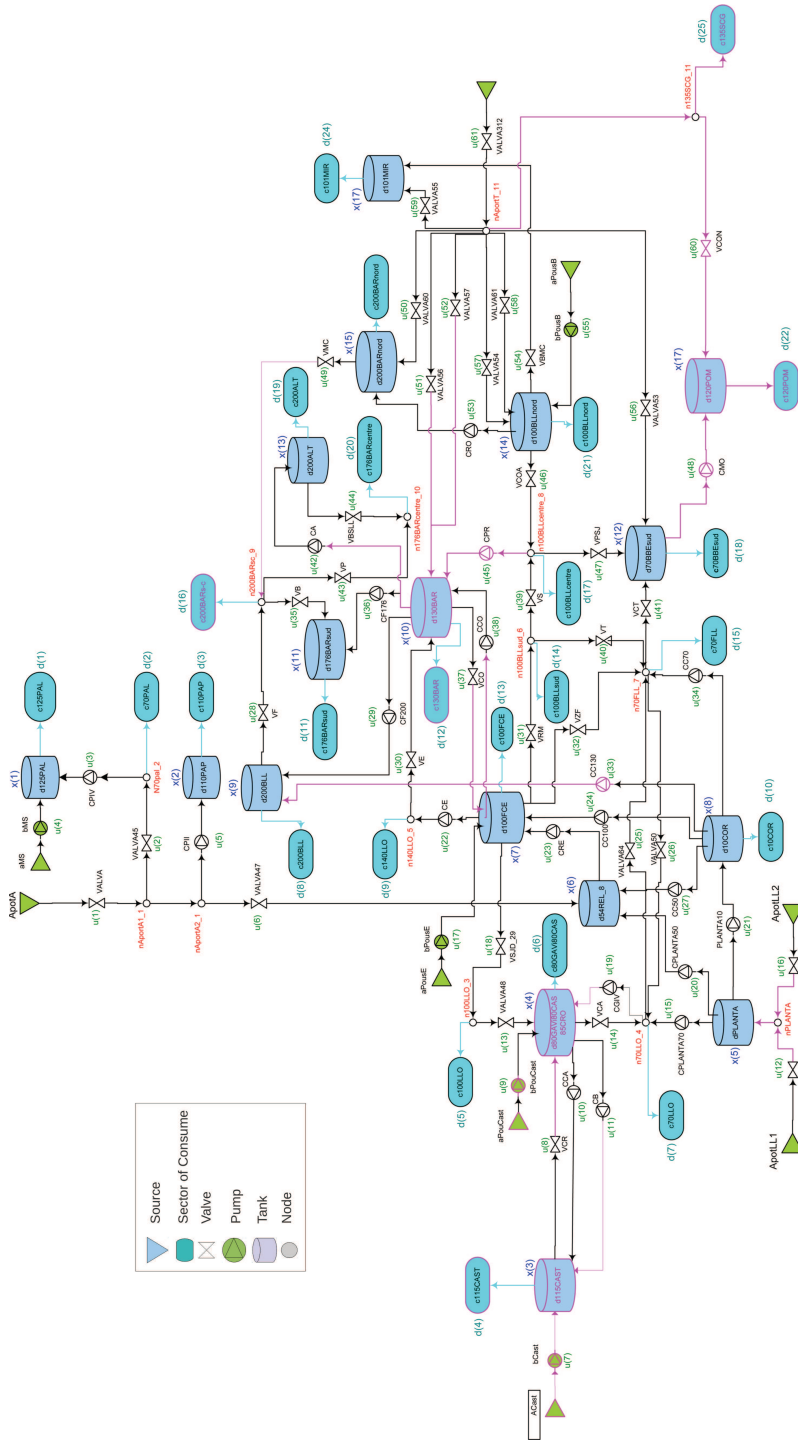


Figure A.1 Topology of the seventeen-tanks DWN example.

Table A.3 Predicted demand from 1h to 8 h.

Hours Demand	1h	2h	3h	4h	5h	6h	7h	8h
01	0.0073	0.0062	0.0049	0.0050	0.0071	0.0080	0.0103	0.0133
02	0.0047	0.0040	0.0032	0.0032	0.0046	0.0052	0.0066	0.0085
03	0.0088	0.0074	0.0059	0.0060	0.0085	0.0096	0.0123	0.0159
04	0.0088	0.0074	0.0059	0.0060	0.0085	0.0096	0.0123	0.0159
05	0.2099	0.1771	0.1404	0.1444	0.2032	0.2302	0.2949	0.3801
06	0.0916	0.0773	0.0613	0.0630	0.0887	0.1005	0.1287	0.1659
07	0.1249	0.1053	0.0835	0.0859	0.1209	0.1369	0.1754	0.2261
08	0.0113	0.0095	0.0076	0.0078	0.0109	0.0124	0.0159	0.0205
09	0.1019	0.0859	0.0681	0.0701	0.0986	0.1117	0.1431	0.1845
10	0.0007	0.0006	0.0005	0.0005	0.0007	0.0008	0.0010	0.0013
11	0.1275	0.1076	0.0853	0.0877	0.1234	0.1398	0.1791	0.2309
12	0.5952	0.5020	0.3980	0.4095	0.5761	0.6527	0.8361	1.0778
13	0.3167	0.2671	0.2118	0.2179	0.3066	0.3473	0.4449	0.5735
14	0.1059	0.0893	0.0708	0.0729	0.1025	0.1161	0.1488	0.1917
15	0.6866	0.5791	0.4591	0.4724	0.6646	0.7530	0.9645	1.2433
16	0.1942	0.1638	0.1299	0.1336	0.1880	0.2130	0.2728	0.3516
17	0.2258	0.1905	0.1510	0.1554	0.2186	0.2477	0.3173	0.4090
18	1.3719	1.1572	0.9174	0.9440	1.3280	1.5046	1.9273	2.4843
19	0.0646	0.0545	0.0432	0.0445	0.0625	0.0709	0.0908	0.1170
20	0.0487	0.0410	0.0325	0.0335	0.0471	0.0534	0.0683	0.0881
21	0.2715	0.2290	0.1816	0.1868	0.2628	0.2978	0.3815	0.4917
22	0.0070	0.0059	0.0047	0.0048	0.0067	0.0076	0.0098	0.0126
23	0.0007	0.0006	0.0005	0.0005	0.0007	0.0008	0.0010	0.0013
24	0.2979	0.2513	0.1992	0.2050	0.2884	0.3267	0.4185	0.5394
25	0.0891	0.0752	0.0596	0.0613	0.0863	0.0977	0.1252	0.1614

Table A.4 Predicted demand from 9h to 16h.

Hours Demand	9h	10h	11h	12h	13h	14h	15h	16h
01	0.0152	0.0140	0.0142	0.0133	0.0120	0.0117	0.0119	0.0113
02	0.0098	0.0090	0.0091	0.0085	0.0077	0.0075	0.0077	0.0073
03	0.0182	0.0167	0.0170	0.0159	0.0144	0.0140	0.0143	0.0135
04	0.0182	0.0168	0.0170	0.0159	0.0144	0.0140	0.0143	0.0135
05	0.4362	0.4012	0.4072	0.3804	0.3443	0.3356	0.3416	0.3237
06	0.1903	0.1751	0.1777	0.1660	0.1502	0.1465	0.1491	0.1413
07	0.2594	0.2386	0.2422	0.2263	0.2048	0.1996	0.2032	0.1926
08	0.0235	0.0216	0.0219	0.0205	0.0185	0.0181	0.0184	0.0174
09	0.2117	0.1947	0.1976	0.1846	0.1671	0.1629	0.1658	0.1571
10	0.0015	0.0014	0.0014	0.0013	0.0012	0.0012	0.0012	0.0011
11	0.2650	0.2437	0.2474	0.2311	0.2091	0.2039	0.2075	0.1967
12	1.2368	1.1375	1.1546	1.0786	0.9762	0.9517	0.9686	0.9179
13	0.6581	0.6053	0.6144	0.5739	0.5194	0.5064	0.5154	0.4885
14	0.2200	0.2024	0.2054	0.1919	0.1737	0.1693	0.1723	0.1633
15	1.4267	1.3121	1.3319	1.2442	1.1260	1.0978	1.1173	1.0589
16	0.4035	0.3711	0.3767	0.3519	0.3185	0.3105	0.3160	0.2995
17	0.4693	0.4316	0.4381	0.4093	0.3704	0.3611	0.3675	0.3483
18	2.8508	2.6219	2.6614	2.4861	2.2500	2.1936	2.2326	2.1158
19	0.1343	0.1235	0.1254	0.1171	0.1060	0.1033	0.1052	0.0997
20	0.1011	0.0930	0.0944	0.0882	0.0798	0.0778	0.0792	0.0750
21	0.5642	0.5189	0.5268	0.4921	0.4453	0.4342	0.4419	0.4188
22	0.0145	0.0133	0.0135	0.0126	0.0114	0.0111	0.0113	0.0107
23	0.0015	0.0014	0.0014	0.0013	0.0012	0.0012	0.0012	0.0011
24	0.6190	0.5693	0.5779	0.5398	0.4886	0.4763	0.4848	0.4594
25	0.1852	0.1703	0.1729	0.1615	0.1462	0.1425	0.1450	0.1374

Table A.5 Predicted demand from 17h to 24h.

Hours Demand	17h	18h	19h	20h	21h	22h	23h	24h
01	0.0104	0.0101	0.0108	0.0115	0.0130	0.0131	0.0107	0.0085
02	0.0067	0.0065	0.0069	0.0074	0.0083	0.0084	0.0069	0.0055
03	0.0124	0.0121	0.0129	0.0138	0.0155	0.0156	0.0129	0.0102
04	0.0124	0.0121	0.0129	0.0138	0.0155	0.0156	0.0129	0.0102
05	0.2969	0.2896	0.3083	0.3310	0.3718	0.3744	0.3080	0.2443
06	0.1296	0.1264	0.1345	0.1444	0.1623	0.1634	0.1344	0.1066
07	0.1766	0.1723	0.1834	0.1969	0.2212	0.2227	0.1832	0.1453
08	0.0160	0.0156	0.0166	0.0178	0.0200	0.0202	0.0166	0.0132
09	0.1441	0.1406	0.1496	0.1606	0.1805	0.1817	0.1495	0.1186
10	0.0010	0.0010	0.0011	0.0012	0.0013	0.0013	0.0011	0.0009
11	0.1804	0.1759	0.1873	0.2010	0.2259	0.2274	0.1871	0.1484
12	0.8419	0.8213	0.8741	0.9384	1.0543	1.0617	0.8734	0.6926
13	0.4480	0.4370	0.4651	0.4994	0.5610	0.5649	0.4648	0.3686
14	0.1498	0.1461	0.1555	0.1670	0.1876	0.1889	0.1554	0.1232
15	0.9712	0.9474	1.0083	1.0825	1.2162	1.2247	1.0075	0.7990
16	0.2747	0.2679	0.2852	0.3062	0.3440	0.3464	0.2849	0.2260
17	0.3195	0.3116	0.3317	0.3561	0.4000	0.4028	0.3314	0.2628
18	1.9406	1.8930	2.0148	2.1631	2.4301	2.4471	2.0132	1.5965
19	0.0914	0.0892	0.0949	0.1019	0.1145	0.1153	0.0948	0.0752
20	0.0688	0.0671	0.0715	0.0767	0.0862	0.0868	0.0714	0.0566
21	0.3841	0.3747	0.3988	0.4281	0.4810	0.4843	0.3985	0.3160
22	0.0098	0.0096	0.0102	0.0110	0.0123	0.0124	0.0102	0.0081
23	0.0010	0.0010	0.0011	0.0012	0.0013	0.0013	0.0011	0.0009
24	0.4214	0.4110	0.4375	0.4697	0.5277	0.5313	0.4371	0.3466
25	0.1261	0.1230	0.1309	0.1405	0.1579	0.1590	0.1308	0.1037

Table A.6 Volume of the tanks along the period (1-6 tanks).

States Hours	x'_1	x'_2	x'_3	x'_4	x'_5	x'_6
01h	189.640	511.715	336.207	762.410	14450.000	3100.000
02h	189.640	558.732	304.024	1238.061	14450.000	3100.000
03h	189.640	610.786	426.540	1616.730	14450.000	3100.000
04h	189.640	668.465	585.031	2023.863	14450.000	3100.000
05h	272.284	725.522	742.898	2424.487	14450.000	3100.000
06h	360.372	773.569	891.746	2730.914	14450.000	3100.000
07h	445.000	817.475	1036.448	2994.033	14450.000	3100.000
08h	445.000	851.464	991.222	3250.000	14450.000	3100.000
09h	441.924	793.186	932.914	2426.806	14450.000	3100.000
10h	386.042	726.311	866.000	1513.722	14450.000	3100.000
11h	334.648	664.807	804.462	963.650	14450.000	3100.000
12h	282.479	602.374	741.994	794.048	14450.000	3100.000
13h	233.745	544.054	683.644	762.410	14450.000	3100.000
14h	189.640	491.272	630.838	762.410	14450.000	3100.000
15h	189.640	439.813	579.357	762.410	14450.000	3100.000
16h	199.222	439.813	526.960	762.410	14450.000	3100.000
17h	211.747	469.380	477.306	762.410	14450.000	3100.000
18h	227.708	503.058	585.790	762.410	14450.000	3100.000
19h	244.602	537.851	541.369	762.410	14450.000	3100.000
20h	259.107	569.786	494.087	762.410	14450.000	3100.000
21h	270.706	598.244	443.323	802.375	14450.000	3100.000
22h	277.071	574.596	386.288	784.476	14450.000	3100.000
23h	229.103	517.191	328.854	762.410	14450.000	3100.000
24h	189.640	469.965	281.611	762.410	14450.000	3100.000

Table A.7 Volume of the tanks along the period (7-12 tanks).

States Hours	x_7^t	x_8^t	x_9^t	x_{10}^t	x_{11}^t	x_{12}^t
01h	20808.700	11745.000	1105.830	5994.230	366.593	29901.141
02h	25930.032	11745.000	1360.247	5994.230	366.593	36561.758
03h	32029.942	11745.000	1944.025	6331.372	366.593	44011.268
04h	38835.728	11745.000	3176.249	7825.345	385.618	52341.495
05h	44500.203	11745.000	4407.670	9856.488	876.230	60574.244
06h	56176.836	11745.000	5627.463	12172.141	986.017	67396.249
07h	65200.000	11745.000	6727.628	14341.988	1035.000	73569.657
08h	65200.000	11745.000	7300.000	16000.000	1035.000	78190.170
09h	63809.807	11745.000	6504.785	15356.877	905.130	72733.913
10h	61152.327	11745.000	5698.474	14646.347	547.780	65559.456
11h	59029.142	11745.000	4899.094	13624.146	420.283	60284.633
12h	55684.105	11745.000	4098.515	11897.915	366.593	55213.740
13h	52467.055	11745.000	3303.245	11464.999	366.593	51317.337
14h	49279.507	11745.000	2515.122	12012.627	366.593	48801.209
15h	46249.151	11745.000	1728.707	11986.622	395.814	46614.852
16h	43108.887	11745.000	1210.964	11616.786	366.594	44200.511
17h	40297.845	11745.000	1362.905	10802.396	366.593	42469.076
18h	37948.463	11745.000	1520.153	9379.038	366.593	41636.947
19h	35990.379	11745.000	1678.839	8031.446	366.593	40983.028
20h	33463.934	11745.000	1833.838	6560.026	366.600	39841.929
21h	30479.701	11745.000	1984.348	6312.019	410.384	37834.143
22h	26851.671	11745.000	1720.095	5994.230	400.280	34265.308
23h	23184.562	11745.000	1105.830	5994.230	366.593	30597.156
24h	20808.700	11745.000	1105.830	5994.230	366.593	29465.700

Table A.8 Volume of the tanks along the period (13-17 tanks).

States Hours	x'_{13}	x'_{14}	x'_{15}	x'_{16}	x'_{17}
01h	831.402	8924.850	1545.170	2277.550	176.594
02h	831.402	12741.901	4010.709	2277.550	277.041
03h	831.402	17442.987	5911.361	2310.061	381.487
04h	831.402	22392.930	6998.141	2606.563	490.399
05h	1670.089	26963.725	7299.973	3115.111	598.817
06h	2970.319	30730.420	7115.342	3651.172	700.082
07h	4240.000	34287.846	6905.015	4371.358	798.058
08h	4240.000	37700.000	7300.000	4912.000	888.161
09h	4240.000	37700.000	6891.791	4912.000	841.888
10h	3512.233	34693.878	6394.675	4462.464	788.790
11h	2717.034	31376.444	5865.345	3806.489	739.955
12h	1909.832	28030.236	5228.040	3094.835	690.384
13h	1277.686	24811.479	4566.497	2523.006	644.077
14h	831.402	21764.378	3994.526	2285.813	602.168
15h	831.402	18758.289	3678.177	2277.550	561.310
16h	831.402	17091.847	3386.601	2277.550	519.725
17h	831.402	15510.334	3166.653	2277.550	480.316
18h	1772.840	14056.247	3098.011	2277.550	447.746
19h	2728.697	12904.230	3070.410	2277.551	412.487
20h	3577.283	12095.833	2937.631	2277.550	374.959
21h	2921.228	11681.783	2633.089	2291.082	334.669
22h	2184.187	11406.489	2151.909	2279.264	289.406
23h	1441.993	9960.558	1679.648	2277.550	243.827
24h	831.402	8924.850	1548.299	2277.550	206.330

List of Figures

1.1.	Characteristic regions on model predictive control	4
1.2.	Hierarchical control structure	7
2.1.	Hierarchical control structure of MPC for tracking periodic signals	16
2.2.	Ball and plate system	29
2.3.	Trajectories of z_1, z_2 for the closed loop system (dash-dot blue), the trajectory planner (continuous magenta) and the target reference (discontinuous red). The artificial coupled constraints are shown (yellow) (scenario 1)	31
2.4.	Trajectories of z_1 for the closed loop system (dash-dot blue), the trajectory planner (continuous magenta) and the target reference (discontinuous red) (scenario 1)	31
2.5.	Trajectories of z_2 for the closed loop system (dash-dot blue), the trajectory planner (continuous magenta) and the target reference (discontinuous red) (scenario 1)	32
2.6.	Trajectories of the optimal cost V_N^* (discontinuous blue) and trajectory planner cost V_p^o (discontinuous red) (scenario 1)	32
2.7.	Trajectories of z_1, z_2 for the closed loop system (dash-dot blue), the trajectory planner (continuous magenta) and the target reference (discontinuous red) (scenario 2)	34
2.8.	Trajectories of $\ddot{\theta}_1$ for the closed loop system (blue). The constraints are shown in red (scenario 2)	34
2.9.	Trajectories of $\ddot{\theta}_2$ for the closed loop system (blue). The constraints are shown in red (scenario 2)	35
2.10.	Trajectories of z_1 for the closed loop system (dash-dot blue), the trajectory planner (continuous magenta) and the target reference (discontinuous red) (scenario 2)	35
2.11.	Trajectories of z_2 for the closed loop system (dash-dot blue), the trajectory planner (continuous magenta) and the target reference (discontinuous red) (scenario 2)	36

2.12.	Trajectories of the optimal cost V_N^* (discontinuous blue) and trajectory planner cost V_p^o (discontinuous red) (scenario 1)	36
3.1.	Hierarchical control structure of the economic periodic model predictive control	40
3.2.	Four tank scheme	53
3.3.	Closed-loop (blue), artificial (cyan) and optimal economic (red) trajectories of the level of tank 1 for scenario 1	55
3.4.	Closed-loop (blue), artificial (cyan) and optimal economic (red) trajectories of the level of tank 2 for scenario 1	56
3.5.	Closed-loop (blue), artificial (cyan) and optimal economic (red) trajectories of the level of tank 3 for scenario 1	56
3.6.	Closed-loop (blue), artificial (cyan) and optimal economic (red) trajectories of the level of tank 4 for scenario 1	56
3.7.	Closed-loop (blue), artificial (cyan) and optimal economic (red) trajectories of the water flow a for scenario 1	57
3.8.	Closed-loop (blue), artificial (cyan) and optimal economic (red) trajectories of the water flow b for scenario 1	57
3.9.	Evolution $\frac{1}{T} \mathcal{L}_T(k, \mathbf{x}, \mathbf{u}, \mathbf{p})$	57
3.10.	Closed-loop (blue), artificial (cyan) and optimal economic (red) trajectories of the level of tank 1 for scenario 2	58
3.11.	Closed-loop (blue), artificial (cyan) and optimal economic (red) trajectories of the level of tank 2 for scenario 2	58
3.12.	Closed-loop (blue), artificial (cyan) and optimal economic (red) trajectories of the level of tank 3 for scenario 2	59
3.13.	Closed-loop (blue), artificial (cyan) and optimal economic (red) trajectories of the level of tank 4 for scenario 2	59
3.14.	Closed-loop (blue), artificial (cyan) and optimal economic (red) trajectories of the water flow a for scenario 1	59
3.15.	Closed-loop (blue), artificial (cyan) and optimal economic (red) trajectories of the water flow b for scenario 2	60
3.16.	Evolution of $\frac{1}{T} \mathcal{L}_T(\mathbf{k}, \mathbf{x}, \mathbf{u}, \mathbf{p})$	60
3.17.	Topology of the three-tanks DWN example	61
3.18.	24h demand on points $c125PAL, c70PAL, c110PAP$ and $c10COR$	64
3.19.	Stored volume in the Tank [m^3]	64
3.20.	Optimal periodic (red) and closed-loop (blue) trajectories of valve $VALMA$	65
3.21.	Optimal periodic (red) and closed-loop (blue) trajectories of valve $VALMA45$	65
3.22.	Optimal periodic (red) and closed-loop (blue) trajectories of valve $VALMA47$	66
3.23.	Optimal periodic (red) and closed-loop (blue) trajectories of pump bMS	66
3.24.	Optimal periodic (red) and closed-loop (blue) trajectories of pump $CPIV$	66
3.25.	Optimal periodic (red) and closed-loop (blue) trajectories of pump $CPII$	67
3.26.	Average economic cost of the optimal trajectory during a period (red) and optimal cost of the controller optimization problem (blue) trajectories	67
4.1.	Hierarchical control structure of the application of the previous economic controller to a non-isolated microgrid	71

4.2.	Micro-grid scheme simulated in the test-bed located in the University of Seville.	72
4.3.	Function $\delta_1(x)$, $x = [100, -100]$ and $\alpha=10$.	77
4.4.	(a) Power profiles:(continuous) generation profile, (dash-dot) demand profile, (discontinues) disturbances obtained from generation and demand profile (generation minus demand) and (market continuous) power agreed with the EU; (b) prices profile: prices of intraday market	82
4.5.	(a) Batteries and metal hidride levels, (b) power profiles P_{grid} , P_{H2} and P_{bat} for scenario 1	83
4.6.	Sampling time cost and accumulated cost for scenario 1	84
4.7.	(a) Batteries and metal hidride levels and (b) power profiles P_{grid} , P_{H2} and P_{bat} for scenario 2	85
5.1.	Hierarchical control structure of the robust model predictive control for tracking periodic signals	88
5.2.	Example of shifted state trajectories considering a terminal region and a terminal controller.	96
5.3.	Example of shifted state trajectories considering an equality terminal constraint	98
5.4.	Uncertainty trajectory.	101
5.5.	Trajectories of z_1, z_2 for the closed loop system (dash-dot blue), the trajectory planners (discontinuous green and black), the target reference (discontinuous red) and the limit of the plate (dot black)	102
5.6.	Trajectories of z_1 for the closed loop system (continuous blue), the trajectory planners (discontinuous green and black) and the target reference (discontinuous red)	103
5.7.	Trajectories of z_2 for the closed loop system (continuous blue), the trajectory planners (discontinuous green and black) and the target reference (discontinuous red)	103
5.8.	Trajectories of $\dot{\theta}_1$ for the closed loop system (blue), the trajectory planners (discontinuous green and black) and the constraints are shown in cyan (scenario 2)	104
5.9.	Trajectories of $\dot{\theta}_2$ for the closed loop system (blue), the trajectory planners (discontinuous green and black) and the constraints are shown in cyan (scenario 2)	104
5.10.	Trajectories of the optimal cost V_N^* (discontinuous blue) and trajectory planner cost V_p^o (discontinuous green)	105
6.1.	Hierarchical control structure	108
6.2.	Target trajectories of tanks 10 and 11	111
6.3.	Target trajectories of actuators 15 and 18	112
6.4.	Trajectories of tank number 10 (scenario 1): nominal controller (blue discontinuous), robust controller (blue), robust planner (green discontinuous with circle), level constraints (cyan), target trajectory (red discontinuous)	119
6.5.	Trajectories of tank number 11 (scenario 1): nominal controller (blue discontinuous), robust controller (blue), robust planner (green discontinuous with circle), level constraints (cyan), target trajectory (red discontinuous)	120

6.6.	Trajectories of actuator number 15 (scenario 1): nominal controller (blue discontinuous), robust controller (blue), robust planner (green discontinuous with circle), flow constraints (cyan)	120
6.7.	Trajectories of tank number 10 (scenario 2): nominal controller (black discontinuous with diamond), robust controller (blue), robust planner (green discontinuous with circle), level constraints (cyan), target trajectory (red discontinuous)	121
6.8.	Trajectories of tank number 11 (scenario 2): nominal controller (black discontinuous with diamond), robust controller (blue), robust planner (green discontinuous with circle), level constraints (cyan), target trajectory (red discontinuous)	121
6.9.	Trajectories of actuator number 15 (scenario 2): nominal controller (black discontinuous with diamond), robust controller (blue), robust planner (green discontinuous with circle), flow constraints (cyan)	122
6.10.	Trajectories of tank number 10 (scenario 3): Robust planner for reference 1 (green discontinuous), robust planner for reference 2 (black discontinuous with x), closed-loop trajectories (blue), target reference (red discontinuous) and constraints (cyan)	123
6.11.	Trajectories of actuator number 18 (scenario 3): Robust planner for reference 1 (green discontinuous), robust planner for reference 2 (black discontinuous with x), closed-loop trajectories (blue) and constraints (cyan)	123
6.12.	Trajectory of the optimal cost (scenario 3) of the robust controller (blue discontinuous with circle) and the robust planners for references 1 and 2 (green discontinuous with circle and black discontinuous with x respectively)	124
A.1.	Topology of the seventeen-tanks DWN example	130

List of Tables

3.1.	Parameters of the four tank plant	54
3.2.	Glossary of the topology of the DWN example	61
3.3.	Cost selection	63
4.1.	PEM electrolyzer model parameters	74
4.2.	PEM fuel cell model parameters	74
4.3.	Metal hydride model parameters	75
4.4.	Battery model parameters	75
A.1.	Maximum volumes of the tanks	129
A.2.	Maximum water flows	129
A.3.	Predicted demand from 1h to 8 h	131
A.4.	Predicted demand from 9h to 16h	132
A.5.	Predicted demand from 17h to 24h	133
A.6.	Volume of the tanks along the period (1-6 tanks)	134
A.7.	Volume of the tanks along the period (7-12 tanks)	135
A.8.	Volume of the tanks along the period (13-17 tanks)	136

List of Codes

Bibliography

- Agudelo-Vera, C., Blokker, M.; Vreeburg, J., Bongard, T., Hillegers, S., Van Der Hoek, J., 2014. Robustness of the drinking water distribution network under changing future demand. *Procedia Engineering* 89, 339–346.
- Alvarado, I., 2007. Model predictive control for tracking constrained linear systems. Ph.D. thesis, Univ. de Sevilla.
- Alvarado, I., Limon, D., Muñoz de la Peña, D., Alamo, T., Camacho, E., Sept 2010a. Enhanced iss nominal mpc based on constraint tightening for constrained linear systems. In: *Control 2010, UKACC International Conference on*. pp. 1–6.
- Alvarado, I., Limon, D., noz de la Peña, D. M., Alamo, T., Camacho, E., 2010b. Enhanced iss nominal mpc based on constraint tightening for constrained linear systems. *Control 2010, UKACC International Conference on*, 1 – 6.
- Angeli, D., Amrit, R., Rawlings, J., 2012. On average performance and stability of economic model predictive control. *IEEE Transactions on Automatic Control* 57, 816–820.
- Arefifar, S., Mohamed, Y.-R., El-Fouly, T., Feb 2015. Optimized multiple microgrid-based clustering of active distribution systems considering communication and control requirements. *IEEE Trans. Ind. Electron.* 62 (2), 711–723.
- Barcelli, D., Ocampo-Martinez, C., Puig, V., Bemporad, A., 2010. Decentralised model predictive control of drinking water networks using an automatic subsystem decomposition approach. In *symposium on large scale complex system theory and applications*.
- Becerra, V. M., Roberts, P. D., Griffiths, G. W., 1998. Novel developments in process optimisation using predictive control. *Journal of Process Control* 8, 117–138.
- Bemporad, A., Casavola, A., Mosca, E., 1997. Nonlinear control of constrained linear systems via predictive reference management. *IEEE Transactions on Automatic Control* 42, 340–349.

- Bemporad, A., Morari, M., Dua, V., Pistikopoulos, E., 2002. The explicit linear quadratic regulator for constrained systems. *Automatica* 38, 3–20.
- Boyd, S., Vandenberghe, L., 2004. *Convex Optimization*. Cambridge University Press.
- Camacho, E. F., Bordons, C., 1999. *Model Predictive Control*, 1st Edition. Springer-Verlag.
- Chisci, L., , Mosca, E., 1994. Stabilizing i-o receding horizon control of CARMA plants. *IEEE Transactions on Automatic Control* 39, 614–618.
- Chisci, L., Rossiter, J. A., Zappa, G., 2001. Systems with persistent disturbances: predictive control with restricted constraints. *Automatica* 37, 1019–1028.
- Choi, D.-K., Lee, K.-B., Feb 2015. Dynamic performance improvement of ac/dc converter using model predictive direct power control with finite control set. *IEEE Trans. Ind. Electron.* 62 (2), 757–767.
- D. Limon, I. A., Alamo, T., Camacho, E., 2008. On the design of robust tube-based mpc for tracking. In: 17th IFAC World Congress . Seoul. Korea. pp. 15333–15338.
- Darby, M., Nikolaou, M., Jones, J., Nicholson, D., 2011. Rto: An overview and assessment of current practice. *Journal of Process Control* 21, 874 – 884.
- Engell, S., 2007. Feedback control for optimal process operation. *Journal of Process Control* 17, 203–219.
- Ferramosca, A., Limon, D., Alvarado, I., Alamo, T., Camacho, E. F., 2009. MPC for tracking with optimal closed-loop performance. *Automatica* 45, 1975–1978.
- Ferramosca, A., Rawlings, J., Limon, D., Camacho, E., Dec 2010. Economic mpc for a changing economic criterion. In: *Decision and Control (CDC), 2010 49th IEEE Conference on*. pp. 6131–6136.
- Fiorelli, D., Schutz, G., Meyers, J., 2011. Application of an optimal predictive controller for a small drinking water network in luxembourg. *Urban Water Management: Challenges and Opportunities - 11th International Conference on Computing and Control for the Water Industry, CCWI 2011* 3.
- Garcia, F., Bordons, C., 2013a. Optimal economic dispatch for renewable energy microgrids with hybrid storage using model predictive control. *IEEE 39th Annual Conference - IECON 2013 ,Industrial Electronics Society*, 7932 – 7937.
- Garcia, F., Bordons, C., 2013b. Regulation service for the short-term management of renewable energy microgrids with hybrid storage using model predictive control. *IEEE 39th Annual Conference - IECON 2013 ,Industrial Electronics Society*, 7962 – 7967.
- Gilbert, E., Kolmanovsky, I., Tan, K. T., 1999. Discrete time reference governors and the nonlinear control of systems with state and control constraints. *International Journal of Robust and Nonlinear Control* 5, 487–504.

- Gondhalekar, R., Oldewurtel, F., Jones, C. N., 2013. Least-restrictive robust periodic model predictive control applied to room temperature regulation. *Automatica* 49, 2760–2766.
- Grimm, G., Messina, M. J., Tuna, S. Z., Teel, A. R., 2004. Examples when nonlinear model predictive control is nonrobust. *Automatica* 40, 1729–1738.
- Grosso, J., Ocampo-Martinez, C., Puig, V., 2012. A service reliability model predictive control with dynamic safety stocks and actuators health monitoring for drinking water networks. *Proceedings of the IEEE Conference on Decision and Control CDC 2012*, 4568–4573.
- Grosso, J., Ocampo-Martínez, C., Puig, V., Joseph, B., 2014a. Chance-constrained model predictive control for drinking water networks. *Journal of Process Control* 24, 504–516.
- Grosso, J., Ocampo-Martinez, C., Puig, V., Limon, D., Pereira, M., 2014b. Economic mpc for the management of drinking water networks. *Control Conference (ECC), 2014 European*, 790 – 795.
- Grosso, J. G., Ocampo-Martinez, C., Puig, V., 2013. Learning-based tuning of supervisory model predictive control for drinking water network. *Engineering Applications of Artificial Intelligence* 26 (7), 1741–1750.
- Grüne, L., 2012. NMPC without terminal constraints. *4th IFAC Nonlinear Model Predictive Control Conference* 4, 1–13.
- Grüne, L., 2013. Economic receding horizon control without terminal constraints. *Automatica* 49, 725–733.
- Heidarinejad, M., Liu, J., Christofides, P. D., 2012. Economic model predictive control of nonlinear process systems using Lyapunov techniques. *AIChE Journal* 58, 855–870.
- Heidarinejad, M., Liu, J., Christofides, P. D., 2013a. Algorithms for improved fixed-time performance of Lyapunov-based economic model predictive control of nonlinear systems. *Journal of Process Control* 23, 404–414.
- Heidarinejad, M., Liu, J., Christofides, P. D., 2013b. Economic model predictive control of switched nonlinear systems. *Systems & Control Letters* 62, 77–84.
- Huang, R., Biegler, L., Harinath, E., 2012. Lyapunov stability of economically oriented NMPC for cyclic processes. *Journal of Process Control* 22, 51–59.
- Jiang, Z.-P., Wang, Y., 2001. Input-to-state stability for discrete-time nonlinear systems. *Automatica* 37, 857–869.
- Johansson, K. H., 2000. The quadruple-tank process. *IEEE Trans. Cont. Sys. Techn.* 8, 456–465.
- Keerthi, S. S., Gilbert, E. G., 1988. Optimal infinite-horizon feedback laws for a general class of constrained discrete-time systems: Stability and moving-horizon approximations. *Journal of Optimization Theory and Applications* 37, 265–293.

- Kellett, C. M., Teel, A. R., 2004. Smooth lyapunov functions and robustness of stability for difference inclusions. *Systems & Control Letters* 52 (5), 395 – 405.
URL <http://www.sciencedirect.com/science/article/pii/S0167691104000325>
- Kern, B., Böhm, C., Findeisen, R., Allgöwer, F., 2009. Receding horizon control for linear periodic time-varying systems subject to input constraints. In: Magni, L., Raimondo, D., Allgöwer, F. (Eds.), *Nonlinear Model Predictive Control*. Vol. 384 of *Lecture Notes in Control and Information Sciences*. Springer Berlin Heidelberg, pp. 109–117.
- Lazar, M., de la Peña, D. M., Heemels, W., Alamo, T., 2008. On input-to-state stability of min–max nonlinear model predictive control. *Systems & Control Letters* 57 (1), 39 – 48.
URL <http://www.sciencedirect.com/science/article/pii/S0167691107000837>
- Le Quiniou, M., Mandel, P., Monier, L., 2014. Optimization of drinking water and sewer hydraulic management: Coupling of a genetic algorithm and two network hydraulic tools. *Procedia Engineering* 89, 710–718.
- Lee, J., Natarajan, S., Lee, K., 2001. A model-based predictive control approach to repetitive continuous processes with periodic operations. *Journal of Process Control* 11, 195–207.
- Limon, D., 2002. Control predictivo de sistemas no lineales con restricciones: estabilidad y robustez. Ph.D. thesis, Universidad de Sevilla.
- Limon, D., Alamo, T., Camacho, E., Dec 2002. Input-to-state stable mpc for constrained discrete-time nonlinear systems with bounded additive uncertainties. In: *Decision and Control, 2002, Proceedings of the 41st IEEE Conference on*. Vol. 4. pp. 4619–4624 vol.4.
- Limon, D., Alamo, T., de la Peña, D. M., Zeilinger, M., Jones, C., Pereira, M., 2012. Mpc for tracking periodic reference signals. *NMPC'12*.
- Limon, D., Alamo, T., Raimondo, D. M., de la Peña, D. M., Bravo, J. M., Ferramosca, A., Camacho, E. F., 2009a. Input-to-state stability: a unifying framework for robust model predictive control. In: Magni, L., Raimondo, D. M., Allgöwer, F. (Eds.), *International Workshop on Assessment and Future Direction of Nonlinear Model Predictive Control*. Springer, pp. 1–26.
- Limon, D., Alamo, T., Raimondo, D. M., de la Peña, D. M., Bravo, J. M., Ferramosca, A., Camacho, E. F., 2009b. Input-to-state stability: an unifying framework for robust model predictive control. In: Magni, L., Raimondo, D. M., Allgöwer, F. (Eds.), *International Workshop on Assessment and Future Direction of Nonlinear Model Predictive Control*. Springer, pp. 1–26.
- Limon, D., Alamo, T., Raimondo, D. M., Muñoz de la Peña, D., Bravo, J. M., Camacho, E. F., 2008. Input-to-state stability: an unifying framework for robust model predictive control. In: *Proceedings of the Int. Workshop on Assessment and Future Directions of Nonlinear Model Predictive Control (NMPC08)*. 5-9 Sept. Pavia, Italy.

- Limon, D., Alamo, T., Salas, F., Camacho, E. F., 2006a. Input to state stability of min-max MPC controllers for nonlinear systems with bounded uncertainties. *Automatica* 42, 629–645.
- Limon, D., Alamo, T., Salas, F., Camacho, E. F., 2006b. On the stability of MPC without terminal constraint. *IEEE Transactions on Automatic Control* 42, 832–836.
- Limon, D., Alvarado, I., Alamo, T., Camacho, E. F., 2008. MPC for tracking of piece-wise constant references for constrained linear systems. *Automatica* 44, 2382–2387.
- Limon, D., Pereira, M., Muñoz de la Peña, D., Alamo, T., Grosso, J., 2014. Single-layer economic model predictive control for periodic operation. *Journal of Process Control* 24 (8), 1207–1224.
- Limon, D., Pereira, M., Munoz de la Pena, D., Alamo, T., Jones, C., Zeilinger, M., 2015. Mpc for tracking periodic references. *Automatic Control, IEEE Transactions on PP* (99), 1–1.
- Mäder, U., Morari, M., 2010. Offset-Free Reference Tracking with Model Predictive Control. *Automatica* 46 (9), 1469–1476.
- Magni, L., De Nicolao, G., Scattolini, R., 2001. Output feedback and tracking of nonlinear systems with model predictive control. *Automatica* 37, 1601–1607.
- Manish Gupta, J. H. L., 2006. Period-robust repetitive model predictive control. *Journal of Process Control* 16, 545–555.
- Mayne, D., Langson, W., Nov 2001. Robustifying model predictive control of constrained linear systems. *Electronics Letters* 37 (23), 1422–1423.
- Mayne, D. Q., 2014. Model predictive control: Recent developments and future promise. *Automatica* 50 (12), 2967–2986.
- Mayne, D. Q., Michalska, H., 1990. Robust horizon control of nonlinear systems. *IEEE Transactions on Automatic Control* 35, 814–824.
- Mayne, D. Q., Rawlings, J. B., Rao, C. V., Sokaert, P. O. M., 2000. Constrained model predictive control: Stability and optimality. *Automatica* 36, 789–814.
- Mayne, D. Q., Seron, M. M., Rakovic, S. V., 2005. Robust model predictive control of constrained linear systems with bounded disturbances. *Automatica* 41, 219–224.
- Miland, H., Ulleberg, Ø., 2012. Testing of a small-scale stand-alone power system based on solar energy and hydrogen. *Solar Energy* 86, 666–680.
- Moreno-Armendáriz, M. A., Pérez-Olvera, C. A., Rodríguez, F. O., Rubio, E., 2010. Indirect hierarchical FCMAC control for the ball and plate system. *Neurocomputing* 73, 2454–2463.

- Ocampo-Martínez, C., Barcelli, D., Puig, V., Bemporad, A., 2012. Hierarchical and decentralised model predictive control of drinking water networks: Application to barcelona case study. *IET Control Theory and Applications* 6 (1), 62–71.
- Ocampo-Martínez, C., Puig, V., Bovo, S., 2011. Decentralised mpc based on a graph partitioning approach applied to the barcelona drinking water network. *Proceedings of the 18th IFAC World Congress* 18, 1577–1583.
- Ocampo-Martínez, C., Puig, V., Cembrano, G., Quevedo, J., 2013. Application of predictive control strategies to the management of complex networks in the urban water cycle. Institute of Electrical and Electronics Engineers, *IEEE Control Systems* 33 (1), 15–41. URL <http://hdl.handle.net/10261/96298>
- Ocampo-Martínez, C., Puig, V., Cembrano, G., Quevedo, J., 2013. Application of predictive control strategies to the management of complex networks in the urban water cycle [applications of control]. *IEEE Control Systems Magazine* 33 (1), 15–41.
- Pannocchia, G., 2004. Robust model predictive control with guaranteed setpoint tracking. *Journal of Process Control* 14, 927–937.
- Pannocchia, G., Laacho, N., Rawlings, J. B., 2005. A candidate to replace pid control: Siso-constrained lq control. *AIChE Journal* 51, 1178–1189.
- Pariso, A., Rikos, E., Glielmo, L., 2014a. A model predictive control approach to microgrid operation optimization. *IEEE Transactions on Control Systems Technology*.
- Pariso, A., Rikos, E., Tzamalis, G., Glielmo, L., 2014b. Use of model predictive control for experimental microgrid optimization. *Applied Energy* 115, 37–46.
- Pascual, J., Romera, J., Puig, V., Cembrano, G., Creus, R., Minoves, M., 2013. Operational predictive optimal control of barcelona water transport network. *Control Engineering Practice* 21, 1020–1034.
- Pereira, M., Limon, D., Muñoz de la Peña, D., Valverde, L., Alamo, T., August 2015a. Periodic economic control of a nonisolated microgrid. *IEEE Transactions on industrial electronics* 62 (8), 5247–5255.
- Pereira, M., Muñoz de la Peña, D., Limon, D., Alvarado, I., Alamo, T., 2015b. Robust model predictive controller for tracking periodic signals : Application and validation on different cis. Tech. rep., GEPOC.
- Pinheiro, J. V. ., Lemos, J. M., Vinga, S., 2011. Nonlinear mpc of hiv -1 infection with periodic inputs. *50th IEEE Conference on Decision and Control and European Control Conference (CDC-ECC)*.
- Qi, W., Liu, J., Chen, X., Christofides, P. D., 2011a. Supervisory predictive control of stand-alone wind-solar energy generation systems. *IEEE Trans. Contr. Syst. Techn.* 19, 199–207.

- Qi, W., Liu, J., Christofides, P. D., 2011b. A distributed control framework for smart grid development: Energy/water system optimal operation and electric grid integration. *J. Process Control* 21, 1504–1516.
- Qi, W., Liu, J., Christofides, P. D., 2012. Supervisory predictive control for long-term scheduling of an integrated wind/solar energy generation and water desalination system. *IEEE Trans. Contr. Syst. Techn.* 20, 504–512.
- Quevedo, J., Puig, V., Cembrano, G., Aguilar, J., Isaza, C., Saporta, D., Benito, G., Hedo, M., A., M., 2006. Estimating missing and false data in flow meters of a water distribution network. In *Proceedings of the IFAC SAFEPROCESS, Beijing (China)*.
- Rakovic, S. V., Kerrigan, E. C., Kouramas, K. I., Mayne, D. Q., 2005. Invariant approximations of the minimal robustly positively invariant sets. *IEEE Transactions on Automatic Control* 50, 406–410.
- Rao, C. V., Rawlings, J. B., 1999. Steady states and constraints in model predictive control. *AIChE Journal* 45, 1266–1278.
- Rawlings, J. B., Amrit, R., 2009. Optimizing process economic performance using model predictive control. In: Magni, L., Raimondo, D. M., Allgöwer, F. (Eds.), *International Workshop on Assessment and Future Direction of Nonlinear Model Predictive Control*. Springer, pp. 315–323.
- Rawlings, J., Angeli, D., Bates, C., 2012. Fundamentals of economic model predictive control. In: *Decision and Control (CDC), 2012 IEEE 51st Annual Conference on*. pp. 3851–3861.
- Rawlings, J. B., Mayne, D. Q., 2009. *Model Predictive Control: Theory and Design*, 1st Edition. Nob-Hill Publishing.
- Rockafellar, R. T., 1970. *Convex Analysis*. Princeton University Press.
- Salazar, J., Tadeo, F., Valverde, L., 2013. Predictive control of a renewable energy micro-grid with operational cost optimization. *IEEE 39th Annual Conference - IECON 2013, Industrial Electronics Society*, 7950 – 7955.
- Sampathirao, A. K., Grosso, J. M., Sopasakis, P., Ocampo-Martinez, C., Bemporad, A., Puig, V., 2014. Water demand forecasting for the optimal operation of large-scale drinking water networks: The barcelona case study. *19th IFAC World Congress, Cape Town, South Africa* 19, 10457–10462.
- Tatjewski, P., 2008. Advanced control and on-line process optimization in multilayer structures. *Annual Reviews in Control* 32, 71–85.
- Touretzky, C. R., Baldea, M., 2014. Integrating scheduling and control for economic mpc of buildings with energy storage. *J. Process Control* 24, 1292–1300.

- Valverde, L., Bordons, C., Rosa, F., 2012. Power management using model predictive control in a hydrogen-based microgrid. *IECON Proceedings (Industrial Electronics Conference)*, 5669–5676.
- Valverde, L., Rosa, F., Bordons, C., 2013a. Design, planning and management of a hydrogen-based microgrid. *IEEE Transactions on Industrial Informatics* 9, 1398–1404.
- Valverde, L., Rosa, F., Del Real, A., Arce, A., Bordons, C., 2013b. Modeling, simulation and experimental set-up of a renewable hydrogen-based domestic microgrid. *International Journal of Hydrogen Energy* 38, 11672–11684.
- Vidyasagar, M., 1993. *Nonlinear Systems Theory*, 2nd Edition. Prentice-Hall.
- Wang, P., Jin, C., Zhu, D., Tang, Y., Loh, P. C., Choo, F. H., Feb 2015. Distributed control for autonomous operation of a three-port ac/dc/ds hybrid microgrid. *IEEE Trans. Ind. Electron.* 62 (2), 1279–1290.
- Wang, Y., Sun, M., Wang, Z., Liu, Z., Chen, Z., 2014. A novel disturbance-observer based friction compensation scheme for ball and plate system. *ISA Transactions* 53, 671–678.
- Witsenhausen, H., Feb 1968. A minimax control problem for sampled linear systems. *Automatic Control, IEEE Transactions on* 13 (1), 5–21.
- Wurth, L., R., H., Marquardt, W., 2011. A two-layer architecture for economically optimal process control and operation. *Journal of Process Control* 21, 311 – 321.
- Yu, S., Reble, M., Chen, H., Allgöwer, F., 2014. Inherent robustness properties of quasi-infinite horizon nonlinear model predictive control. *Automatica* 50 (9), 2269 – 2280. URL <http://www.sciencedirect.com/science/article/pii/S0005109814002891>
- Zanin, A. C., de Gouvea, M. T., Odloak, D., 2002. Integrating real time optimization into the model predictive controller of the fcc system. *Control Engineering Practice* 10, 819–831.

Glossary

- CLF** Control Lyapunov Function. 8
- DRTO** Dynamic Real Time Optimizer. 10, 44, 52
- DWN** Drinking Water Network. 60–62, 107–109, 138, 141
- EU** Electric Utility. 70, 71, 78, 83
- ISS** Input to State Stable. 8, 9
- LQR** Linear Quadratic Regulator. 3
- MHL** Metal Hydride Level. 72, 74, 80, 83, 84
- MPC** Model based Predictive Control. IX, XIII, XV, XVI, 2, 3, 5–10, 12, 15, 19, 20, 28, 30, 33, 39, 43, 45, 47, 49, 51, 69, 70, 74, 77, 84, 85, 87, 89, 93, 94, 99, 107, 108, 111–114, 116, 118, 122, 126
- OPC** OLE for Process Control foundation specifications. 73
- PEM** Polymer (or Proton) Electrolyte Membrane. X, 73
- PID** Proporcional Integral Derivative Regulator. IX, 6
- PLC** Programmable Logic Controllers. 6, 73, 127
- PV** PhotoVoltaic panels. 72, 76–78, 81, 83
- RTO** Real Time Optimizer. IX, 6–8, 15
- SOC** Stage Of Charge of the batteries. 72, 74, 76, 80, 83, 84
- SSTO** Steady State Target Optimizer. 7